(3)

PROGRESS REPORT

Study of CO_2 Absorption Spectra Between 15 and 18 Microns

BY

ROBERT P. MADDEN

Work done in part under contract with

E OF NAVAL RESEARCH

Contract Nonr 248 (01)

JOHNS HOPKINS UNIVERSITY

LABORATORY OF ASTROPHYSICS AND PHYSICAL METEOROLOGY

BALTIMORE 18, MARYLAND

FEBRUARY 1, 1957

PROGRESS REPORT

Study of CO_2 Absorption Spectra Between 15 and 18 Microns

BY

ROBERT P. MADDEN

Work done in part under contract with

OFFICE OF NAVAL RESEARCH

Contract Nonr 24[illegible] (01)

THE JOHNS HOPKINS UNIVERSITY

LABORATORY OF ASTROPHYSICS AND PHYSICAL METEOROLOGY

BALTIMORE 18, MARYLAND

FEBRUARY 1, 1957

ABSTRACT

A study has been made of the absorption due to individual lines and Q branches of CO_2 bands in the 15 to 18 μ micron spectral region. The bands occurring in this region are due to transitions between the lower vibrational energy states of the CO_2 molecule -- the strongest band corresponding to the ν_2 fundamental frequency. The strengths and widths of absorption lines in the fundamental band and in the $02^{0}0 - 01^{1}0$ band of $C^{12}O_2^{16}$ have been measured. In the latter band the variation of line strength and width with J has been determined. The strengths of five other bands of $C^{12}O_2^{16}$ have been determined from measurements on their Q branches. In addition, the strengths of the ν_2 fundamental bands of the isotopes $C^{13}O_2^{16}$ and $O^{18}C^{12}O^{16}$ have been estimated.

The accuracy with which these strengths and widths have been determined varies according to the strength of the absorption and the amount of overlap on any one band by others.

In addition to the measurements of strength and width, the ν_2 fundamental band head of the $O^{18}C^{12}O^{16}$ isotope is reported; and the rotational structure of the ν_2 fundamental Q branch for $C^{12}O_2^{16}$ is partially resolved, and the band constants determined.

The spectra were taken on a new Ebert spectrometer which has demonstrated an optical slit width of 0.06 cm^{-1} and a wave number location accuracy of 0.01 cm^{-1} at 17

microns. The 1/6 spectrometer utilizes a 3 in. long slit and a 14 in. x 12 in. grating. The absorption by H_2O and CO_2 in the optical path of the spectrometer is eliminated by the removal of these gases. The present experiments were performed with a slit width of 0.24 mm, corresponding to a spectral slit width of 0.1 cm^{-1}.

ACKNOWLEDGEMENTS

The author wishes to express his indebtedness to Professor Strong who has not only been endlessly available for consultation, and collaborated in solving the more difficult experimental problems in this work, but also has been a source of inspiration throughout the entire program. The author is also much indebted to Dr. William S. Benedict for his guidance in the interpretation and analysis of the spectra, and the interpretation of the results; also for the use of several unpublished tables. The author also wishes to thank Dr. Lewis Kaplan for several helpful suggestions and the use of tables in his possession; and to express his appreciation to Dr. H. W. Babcock of the Mt. Wilson and Palomar Observatories for successfully ruling the large diffraction grating. Finally, thanks are due to the entire staff of the Laboratory of Astrophysics and Physical Meteorology, especially Mr. McClellan and Mr. Brustad, for their generous assistance in carrying out, and completing, this research.

This work was supported in part by Navy Contract Nonr 248(01).

TABLE OF CONTENTS

I. INTRODUCTION

The object of this research has been to advance the knowledge of the intensity distribution of gaseous CO_2 absorption lines in the spectral region 545 to 667 cm^{-1}. Such research is amply justified since this region of CO_2 absorption plays an important role in the heat balance of the earth's atmosphere,[1] and the transmission of infrared radiation through this atmosphere. In addition, a calculation[2] of the emissivity of CO_2 and an understanding of the role of CO_2 in flame emission, both of considerable military interest, require such measurements.

Three basic quantities may be studied in absorption spectroscopy: the wavelength position, the strength and the shape of the absorption. In the following discussion these will be considered in turn.

Wavelength positions of the individual lines are of interest since the molecular constants, and the energy levels for the molecule may be determined from them. Little attention has been given to this phase of the problem in this study since the position of the lines in the important bands in this region have recently been studied with good resolution by Blau, etc.,[3] and an evaluation of this and other studies has been made by Benedict.[4]

Table 1 is a list of the lower vibrational states of CO_2, including the upper and lower levels of all the important transitions of CO_2 occurring at normal temperature in the 545 to 667 cm^{-1} region. Table 2 contains the

band constants which are most useful in the present study.

The only wavelength measurement in these experiments is the band head determination of the 01'0 - 000 band of the $O^{18}C^{12}O^{16}$ isotope. Also relative positions of the Q branch lines for the 01'0 - 000 transition of the $C^{12}O_2^{16}$ isotope were made to determine the band constants for the Q branch. These measurements have not previously been recorded.

The second basic quantity of interest is the strength of absorption, from which transition moments may be calculated. The strength of absorption for a whole band, or the band strength, may be determined by adding the strengths of all the lines in the band. This method requires that all the individual line strengths be observable, but has the advantage of yielding the distribution of strength within the band. The evaluation of strengths of whole CO_2 bands has not been made by adding the strengths of individual lines since no spectrometer has been available with sufficient resolution to resolve the overlapping bands. Methods have been developed[5,6,7] for determining whole band strengths from measurements on unresolved bands. Difficulties arise however, if several bands overlap, for it is impossible to be sure of the separate contributions of each.

The first investigation of the 15 to 18 micron spectral region in which the CO_2 rotational structure was resolved was made by Martin and Barker.[8] The resolution

attained, however, was insufficient for individual line strength determinations and no intensity analysis was made. Although several investigators[9,10,11,12,13,14] have measured the total absorption by CO_2 in the 13 to 18 micron region, they were unable to apportion the proper share of the total intensity to the separate bands. Recently, Kostkowski[15] determined the strengths at elevated temperatures of the bands on the high frequency side of the ν_2 fundamental at 15 microns. The most recent and perhaps the best attack on the room temperature intensities of the bands on the high frequency side of the fundamental, and the fundamental itself, has been made by Kaplan and Eggers.[16] They have made total band measurements using a low resolving power.

Calculations of expected intensities in the fundamental and several other bands, based on available experimental evidence, and assumptions of a molecular model, have been made by Kaplan[1,17] and more recently by Benedict.[18] A discussion of the agreement between the present experimental values and Benedict's predicted values will be given.

The third basic quantity to be studied in absorption spectroscopy is the shape of absorption lines, from which molecular interaction forces and other broadening influences may be determined. The width of an absorption line is a measure of the strength of the broadening influence.

Unfortunately, it is difficult to study the shape of individual lines at any distance from the line center in such a crowded spectrum as occurs in the 15 to 18 micron region of CO_2 absorption. In these experiments, only the width of the absorption lines was determinable.

Absorption lines are broadened predominantly by three mechanisms: the natural width, the Doppler effect, and collision broadening. For CO_2 in the infrared, the natural width is negligible compared with that due to the other two mechanisms. The Doppler effect can be important at elevated temperatures. At room temperature, however, the Doppler width for CO_2 is only .0011 cm^{-1}, while the width due to collision broadening is about 0.2 cm^{-1} at one atmosphere pressure. Since the Doppler width is independent of the pressure, while the collision width is proportional to the pressure, the Doppler effect can be neglected in these measurements for pressures greater than .01 atmos. The range of pressures used in these experiments was from 0.025 atmosphere to 1 atmosphere.

The collision width of absorption lines cannot be calculated from Kinetic Theory since the collision diameter for optical interaction is different from the collision diameter determined from viscosity and conductivity measurements. Therefore, the collision width must be determined directly from the spectra.

Adel[19] studied the ν_2 fundamental of CO_2 under high resolution using a grazing incidence grating spectrometer.

He determined what he considered an upper limit of 0.12 cm^{-1} for the average half-width of the lines in the fundamental band. The average half-width for the 2077 cm^{-1} band of CO_2 was determined by Benedict and Silverman[20] to be .075 cm^{-1}. Kostkowski[15] determined the average half-width for the peak of the R branch of the 961 cm^{-1} band to be 0.084 cm^{-1}.

High resolution is necessary to make measurements of strength and width on individual absorption lines, and thus determine the variation of strength and width with J. In addition, the use of high resolution reduces the uncertainty in band strength determinations caused by the overlap of different bands. The spectrometer used in the present experiments has available the highest resolution yet attained in the 15 to 25 micron spectral region, and measurements on strengths and widths of individual absorption lines were possible in many cases.

II. METHODS OF DETERMINING STRENGTHS AND WIDTHS FROM ABSORPTION SPECTRA

A study was made of the methods available to reduce the spectra in order to determine the experimental conditions which yield measurements containing the most accessible information. The desired quantities are line and band strengths and line half-widths. These quantities are defined below.

A. Definitions

The transmission of the gas at frequency ν is defined as $T_\nu = \frac{I_\nu}{I_\nu^\circ}$. Here I_ν° is the intensity of light of frequency ν incident on the gas sample; and I_ν is the intensity of light of frequency ν transmitted by it.

The absorption of the gas at frequency ν is defined as $A_\nu = 1 - T_\nu$.

The absorption coefficient at frequency ν, k_ν, is now defined by the Lambert's Law relation: $T_\nu = e^{-k_\nu \ell}$ where ℓ is the length of path through the gas sample over which the light travels, and k_ν has the dimensions cm^{-1}. It is assumed that the gas has a uniform density throughout this path. (If this condition is not satisfied, the quantity $dI_\nu = -I_\nu^\circ k_\nu d\ell$ must be integrated over the whole path.)

The integrated absorption coefficient for an absorption line is defined as: $S = \int_0^\infty k_\nu \, d\nu$ where k_ν is the absorption coefficient for that line alone, and S has the dimensions cm^{-2}.

The line strength is basically defined as the integrated absorption coefficient per molecule, S/N_o, where N_o is the molecular density of the gas. However, since the ideal gas law holds for all pressures used in these experiments, and since all measurements were taken at one temperature, it is much more useful experimentally to define the line strength per atmosphere, S^o, at 300°K by;

$$S^o = S/P$$

where P is the gas pressure in atmospheres, and S^o has the dimensions $cm^{-2}/atmos$.

The band strength $S_{v''}^{v'}$, is then given by:

$$S_{v''}^{v'} = \sum_i S_i^o$$

where the sum is over all lines in the band, and S_i^o is the line strength of the i^{th} line. $S_{v''}^{v'}$ is a most important quantity since it has been shown[11] to be directly related to the vibration transition moment by the relation:

$$S_{v''}^{v'} = \frac{8\pi^3 N_o \nu_o \left(1 - e^{-\frac{h\nu_o}{kT}}\right) \left|R_{v''}^{v'}\right|^2 G \; e^{-\frac{E_{v''}}{kT}}}{3hc\, Q_v} \qquad (1)$$

where $R_{v''}^{v'}$ is the vibrational transition moment

N_o = molecular density at 1 atmosphere pressure and 300°K

G is 1 for all bands observed in these experiments

$$Q_v = \sum_{v''} g_{v''} e^{-\frac{E_{v''}}{kT}}$$

$$g_{v''} = \begin{cases} 1 \text{ for } \Sigma \text{ states} \\ \\ 2 \text{ for all other states} \end{cases}$$

The half-width, γ , of an absorption line is defined as one-half the width of the absorption coefficient curve measured at a height equal to one-half of the maximum value of the absorption coefficient for that line. Kinetic Theory, the collision broadening theory of Lorentz,[21] and considerable experimental evidence leads to the conclusion that the half-width of a collision-broadened absorption line is proportional to pressure over a wide range of pressures -- and certainly over the pressure range of these experiments. Accordingly, we define γ^o , the half-width corrected to atmospheric pressure at 300°K, by

$$\gamma^o = \frac{\gamma}{P}$$

where P is the pressure in atmospheres of the gas at 300°K.

B. Direct Determination

From the observed spectra we wish to determine the physical quantities S_i^o, $S_{v''}^{v'}$, and γ^o . This determination is a straightforward procedure if the resolving power of the spectrometer is high enough, and the pressure of the gas is adjusted so that: a) No given line

is overlapped by its neighbors, and b) the width of the line is large compared with the spectrometer optical slit width. In this case there would be no distortion of the true transmission curve by the spectrometer, and by dividing the logarithm of the transmission by the path length one would obtain the true absorption coefficient. Since by assumption there is no overlap, the line width could be measured directly and the strength could be determined by integrating the absorption coefficient over the wavelength interval.

Since the experimental conditions necessary to use such a direct method are seldom realized, it is necessary to consider other methods which are made possible by simplifying assumptions. These are listed below in order of the increasing number of assumptions necessary for their use. The listing is not intended to be exhaustive, but it contains the techniques which are appropriate for interpreting the present observations.

C. Direct Determination Using Slit Function Corrections

For cases where the requirements for use of direct determinations can not be met exactly, but can be met approximately (i.e., conditions require that the line width be of the same order of magnitude as the optical slit function of the spectrometer), the above method can still be used if a correction is made for the "smearing out" effect of the spectrometer on the spectra. Such corrections depend on a good knowledge of the slit function,

defined as:

$$\sigma(\nu_o, \nu) = \frac{\text{intensity of light of frequency } \nu \text{ passed by the slit}}{\text{intensity of light of frequency } \nu_o \text{ passed by the slit}}$$

where ν_o is the frequency setting of the spectrometer, and ν is the frequency in the spectrum.

This slit function is primarily dependent only on the variable $(\nu-\nu_o)$, and its dependence on this variable must be known to make the correction mentioned above.

Kostkowski and Bass[22] have calculated the appropriate corrections to be used in obtaining true S, δ, and peak absorption from the observed spectrum assuming a Gaussian slit function. The corrections were calculated for many values of the ratio of line width to optical slit width. These corrections are particularly appropriate for use in this study, since it has been experimentally confirmed recently by Von Planta,[23] that a Gaussian slit function is a good approximation in an Ebert type spectrometer for the slit widths used here. Figures 1 and 2 show the corrections to be applied to the observed S and δ' (calculated from curves of log $T_{obs.}$) in order to determine the true S and δ. It should be noted that the correction for δ is much greater than the correction for S under identical experimental circumstances.

D. <u>S^o Determination for Weak Absorption</u>

When the line width is smaller than the optical slit width, which is the case if low pressures are required to

separate the spectral structure, it is necessary to turn to even more indirect methods of determining S^o and δ^o. Of prime importance in these methods is the quantity called "equivalent width," or W, defined by:

$$W = \int A_{\nu\,obs.}\, d\nu$$

Here the range of integration must begin and end in regions of zero absorption if the definition is to have meaning, and it is assumed that there is no overlapping of lines. The importance of this quantity centers about the fact that it is independent of the slit width (so long as the slit function is symmetrical). The integral may extend over any desired interval if the restrictions mentioned above are satisfied -- $A_{\nu obs.}$ being the observed absorption in that interval. Since W is independent of the slit function it follows that:

$$W = \int A_{\nu\,obs.}\, d\nu \quad = \int A_\nu\, d\nu \qquad (2)$$

i.e. the integrated observed absorption over any interval beginning and ending in a region of zero absorption is equal to the integral of the true absorption over that interval.

Since $A_\nu = 1 - T_\nu = 1 - e^{-k_\nu \ell}$

we have $W = \int (1 - e^{-k_\nu \ell})\, d\nu$

Now let $k_\nu \ell \to 0$. Then:

$$\lim_{\text{as } k_\nu \ell \to 0} W = \ell \int k_\nu \, d\nu = \ell S = \ell P S^\circ \qquad (3)$$

Thus if W is measured for a given spectral interval at many path lengths, and the quantity $\frac{W}{\ell P}$ is extrapolated to $\ell = 0$, S° is obtained. This S° may be the strength of one line, or the aggregate strength of many lines, depending on the spectral interval over which the absorption was integrated.

This method has two limitations. Firstly, since the most important measurements to be made are those when the observed absorption is extremely small, it is difficult experimentally to obtain accurate measurements. Secondly, there is no way of determining δ° from such a treatment.

E. "Curve of Growth" Method

In order to determine δ° under the condition that the line width is not large compared to the spectrometer slit width, and so that measurements on lines of stronger absorption will be of some help in determining S°, another method has been developed called the "Curve of Growth" method. The important assumption made in the use of this method is that the shape of the absorption coefficient curve for any given line is the symmetrical shape calculated by Lorentz[21] for collision broadening. Lorentz predicted a Cauchy shaped line given by:

$$k_\nu = \frac{1}{\pi} \frac{S\delta}{(\nu - \nu_0)^2 + \delta^2} \qquad (4)$$

where S and γ have been defined, and ν_o is the central frequency of the line.

While there is some question remaining as to whether or not the Lorentz shape is correct for frequencies far from the line center, there is general agreement that the Lorentz formula predicts the correct shape near the center of the line. In particular Benedict[18] has reported that the Lorentz formula predicts the correct value of the absorption coefficient at a distance of 1 cm^{-1} away from the line center for CO_2 absorption lines in the 4.7 micron band. Because the absorption measured under all experimental conditions of this study is negligible at a distance of 1 cm^{-1} away from the line center, the assumption of the Lorentz shape for this work seems justified.

With this assumption the following argument is made:

$$W = \int_0^\infty A_\nu \, d\nu = \int_0^\infty (1 - e^{-k_\nu \ell}) \, d\nu$$

If the entire contribution to W is due to a single line,

$$W = \int_0^\infty \left(1 - \exp\left[\frac{1}{\pi} \frac{S\gamma\ell}{(\nu - \nu_o)^2 + \gamma^2} \right] \right) d\nu$$

This integral has been solved[5] by Ladenburg and Reiche and the result is:

$$W = 2\pi\gamma \times e^{-X} \left[J_o(iX) - i J_1(iX) \right] \qquad (5)$$

$$\text{where} \quad X = \frac{S\ell}{2\pi\gamma} \qquad (6)$$

J_o, J_1 are Bessel functions of the 0 and 1 order. For simplicity this equation may be written:

$$W = 2\pi\gamma\, F(x)$$

where $$F(x) = x\, e^{-x}\left[J_o(ix) - i\, J_1(ix)\right]$$

The function F(x) has been tabulated by Stover.[24] Figure 1 is a plot of F(x) vs. x. This function is called the Ladenburg-Reiche Function.

For the limiting case of $x \to o$, $\lim_{\text{as } x \to o} F(x) = x$ (linear region). Then:

$$W = 2\pi\gamma \cdot \frac{S\ell}{2\pi\gamma} = S\ell \qquad (x \to o) \qquad (7)$$

which agrees with the result of the previous discussion.

For large x,

$$F(x) \approx \sqrt{\frac{2x}{\pi}} \qquad \text{(square-root region)}$$

In this case,

$$W = 2\pi\gamma\sqrt{\frac{2S\ell}{2\pi^2\gamma}} = 2\sqrt{S\gamma\ell} \qquad (x \gg o) \qquad (8)$$

It is noteworthy that x is independent of pressure. This can be shown if we set:

$$S = S^\circ P$$

$$\gamma = \gamma^\circ P$$

Substituting in (6) we have:

$$x = \frac{S^\circ \ell}{2\pi\gamma^\circ} \tag{9}$$

Also noteworthy is the fact that W is proportional to P since we may now write:

$$W = 2\pi\gamma^\circ P F\left(\frac{S^\circ \ell}{2\pi\gamma^\circ}\right) \tag{10}$$

It is, therefore, convenient to define a quantity, W°, by $W^\circ = \frac{W}{P}$, which is called the equivalent width corrected to atmospheric pressure at 300°K. Finally, the pressure independent equation for W° is:

$$W^\circ = 2\pi\gamma^\circ F(x) \tag{11}$$

In this equation W° and ℓ are the experimentally determined data, F(x) is the tabulated Ladenburg-Reiche Function, and S°, γ° are the unknowns to be determined. Mathematically, a measurement of W° for two absorption path lengths would be sufficient to determine S° and γ°. In practice, it is found desirable to obtain W° as a function of ℓ over a wide range of x in order to best obtain the numerical values of S° and γ°. For example, if only two values of x were measured, and x was large in both cases, W° for both cases would be nearly given by $W^\circ = 2\sqrt{S^\circ\gamma^\circ\ell}$ and only the product of $S^\circ\gamma^\circ$ could be determined with any accuracy. If, on the other hand, both choices of x were quite small, W° in both cases would

be very nearly given by $W^{\circ} = S^{\circ}\ell$ and the solution would be very insensitive to γ° . Thus, in the "Curve of Growth" Method, for each line studied it is desirable to make measurements of W° with path lengths appropriate to have x values extending from the linear region into the square-root region of the Ladenburg-Reiche Function.

If the spectral interval of absorption of the line being studied is overlapped by neighboring lines, simple corrections can be made to W° only if the overlap contribution is not too large.

F. Method of Wilson and Wells

The previous methods have required that the individual lines being studied be reasonably free from overlap. A method has been developed by Wilson and Wells[6] which yields the total band strength when the structure of the band is completely "smeared out." "Smeared out" means that the individual line widths are larger than the spacing of the lines. For CO_2 this condition is met at reasonable pressures in the $\perp$ band Q branches where the line spacing is quite small.

With this "smeared out" condition fulfilled, and with a sufficiently narrow spectrometer slit function so that the transmission suffers little distortion by the spectrometer; the observed transmission $T^{obs.}$ is very nearly the true transmission, T. Under this condition,

$$T_{\nu} = e^{-\sum_j k_j(\nu)\,\ell}$$

$$\text{and} \int_0^\infty (-\ln T)\, d\nu = \ell \int_0^\infty \left(\sum_J k_J(\nu)\right) d\nu$$

If the integration above is performed over all the frequencies at which there is measurable absorption for a given band, or branch,

$$\int_0^\infty \left(\sum_J k_J(\nu)\right) d\nu = \sum_J \int_0^\infty k_J(\nu)\, d\nu = \sum_J S_J$$

$$S_J = P S_J^\circ$$

and finally

$$\int_0^\infty (-\ln T)\, d\nu = \ell P \sum_J S_J^\circ \qquad (12)$$

$\sum_J S_J^\circ$ represents the strength of the band, or branch, over which the integration has been performed. If the integration has been over the entire band, $S_{v''}^{v'}$ is obtained. If the integration was performed over a Q branch, the theoretical ratio of Q branch strength to total band strength may be used to find $S_{v''}^{v'}$.

Wilson and Wells show that an extrapolation procedure yields the best results, since in most cases the resolution available is not sufficient to leave the transmission completely undistorted by the spectrometer slit function. Such an extrapolation yields:

$$\lim_{\text{as } \ell \to 0} \int_0^\infty (-\ln T)\, d\nu = \ell P \sum_J S_J^\circ$$

G. Elsasser Band Method

A final method must be mentioned which can sometimes be used when conditions for the above methods can not be met - namely - when the lines of a band are not wide compared to their spacing, and yet where the spectral slit width of the spectrometer is wide enough so that several lines pass through the slit simultaneously. In order to use this method, however, it is necessary to assume that the band is of the idealized type considered by Elsasser. An Elsasser band is one containing an infinite number of equally spaced Lorentz-shaped lines of equal strength and width. Elsasser has shown[7] that the total absorption averaged over an interval of the line spacing of such an idealized band is given by:

$$A = \sinh\beta \int_0^\infty \exp[-Y \cosh\beta]\, J_0(iY)\, dY \qquad (13)$$

where $$Y = \frac{S\ell}{D \sinh\beta}$$

$$\beta = \frac{2\pi\delta}{D}$$

D = spectral range between lines

Kaplan[25] has tabulated this function, giving A as a function of Y and β .

III. EXPERIMENTAL DISCUSSION

A. Spectrometer

It is well recognized that the princi barrier to obtaining spectra with high resolving power in the thermal detection infrared lies in the difficulty in getting a sufficiently high signal/noise ratio with narrow slits. In 1950, the Laboratory of Astrophysics and Physical Meteorology of The Johns Hopkins University began the design* of a spectrometer transmitting a large light flux -- sufficient to enable the use of much higher resolution than was possible before. The construction of this spectrometer has been completed, and its performance tested. The instrument has demonstrated[26] an optical slit width of 0.06 cm^{-1} at 600 cm^{-1}, which is only 15% greater than the theoretical width. In addition a wavelength accuracy of 0.01 cm^{-1} at 600 cm^{-1} has been achieved. The essential features of this spectrometer are described below:

(1) Optics

Figure 5 shows schematically the optics of the instrument. It is of the Ebert type,[27] the Ebert mirror being 30" in diameter and of 90" focal length. The grating is 14" wide and 12" high ruled 1000 lines to the inch.

---

*The principles upon which this design was based were described by John Strong in a paper discussing high resolving power in the infrared, presented at the 1950 meeting of the Ohio State Symposium on Molecular Structure and Spectroscopy.

The slits are 3" long and are curved on a 15" diameter circle. Either a Globar or a carbon arc[28,29] can be used as a source. In the present work a Globar was used. The light is chopped at the source with a mica chopper, travels through the Ebert system, and coming through the long exit slit it is sliced and condensed onto a Golay cell pneumatic detector. Figure 6 shows the operation of the image slicer. In effect, it slices the 3" long exit slit into three 1" long segments, and causes these segments to be imaged adjacent to one another on the detector. A similar arrangement is used with the carbon arc on the entrance side of the spectrometer to enable the crater of the carbon arc to fill the long entrance slit.

The elimination of overlapping grating orders is effected by 3 or 4 reflections of the light from MgO crystals in conjunction with the mica chopper. Since the 0.003" thick mica chopper transmits well out to 9 microns and only the a.c. component of the signal incident on the detector is amplified, higher order light is considerably reduced. Figure 7 shows the reststrahlen reflection from a typical MgO crystal. After four such reflections, the first order of the grating from 14 to 25 microns is obtained completely free of higher order light even when a carbon arc is used.

(2) Grating

The 14" x 12" grating was ruled in a 13-micron thick silver film evaporated on a glass blank with

excellent uniformity using a new technique[30] which was developed here. The ruling was done by Dr. H. W. Babcock on the large ruling engine of Mt. Wilson and Palomar Observatories.

Before the ruling of the large blank, many small gratings were ruled in similar silver films by Mr. Wilbur Perry of the Johns Hopkins Gratings Laboratory. These gratings, all blazed for the 20-micron region, were ruled with different groove forms and their blazes studied, in order to determine the optimum specifications for the groove of the large grating.

Figure 8 shows some of the data taken for a small grating having a groove form similar to that specified for the large grating. The specifications decided upon were a groove spacing of 25 microns and a facet angle of 25°. These specifications have the effect of shifting the maximum of the curve in Figure 8 to somewhat longer wavelengths.

Figure 9 is a photograph of the grating in its mounting on a table, adjustable with respect to its axis of rotation. The detailed reflection indicates the sharpness of the blaze.

(3) Drive and Rotation

Figure 10 is a closeup photograph showing the drive mechanism incorporated to rotate the grating. The screw adapted for the drive of this spectrometer was originally made to test new methods of making ruling engine screws.[37]

It is driven in fixed bearings so that the nut moves when the screw is rotated. A sapphire flat mounted on the moving nut pushes on a steel ball fixed at the end of the grating table arm to cause the rotation. This type of drive yields a cosine variation in angular velocity of grating rotation which just compensates for the cosine dependence of grating dispersion. As a result, when the screw is driven by a synchronous motor, the variation of wavelength on the exit slit of the spectrometer is remarkably linear in time.

The rotation axis of the grating is located by four highest precision Fafnir ball bearings. These bearings are mounted in pairs spaced two feet apart. The pairs are made up of matched bearings arranged so that the errors in one are compensated by those of the other. The pairs are preloaded by a small force directed along the axis of rotation. This force eliminates any bearing "slop."

(4) Alignment Instrument

To obtain the maximum available resolution from the spectrometer, critical alignment of its components is necessary. Figure 11 shows the schematic operation, and Figure 12 is a photograph of an instrument devised which greatly facilitates the alignment of the spectrometer. Its operation is described in the caption for Figure 11.

(5) CO_2 and H_2O Removal

The spectral region of operation of this spectrometer

contains strong atmospheric CO_2 and H_2O absorption. Thus, if these gases are to be studied under controlled conditions, or if other gases are to be studied with which the CO_2 or H_2O interfere, the residual CO_2 and H_2O must be removed from the spectrometer. In the present case one would expect this to be a particularly difficult task since high resolution is available, and the optical path of the spectrometer is about 15 meters. However the following procedure was remarkably successful.

The spectrometer is completely enclosed in a copper housing, and can be operated entirely from without. All wires to the interior run through hermetic seals, and a copper-lined door can be sealed into place during operation. The CO_2 is removed from the interior atmosphere by circulating the air through KOH pellets. After 4 to 6 hours, a desiccant is added to the path of circulation by remote control. The highly effective desiccant used is Linde Air Products Molecular Sieve. Several more hours of continued circulation removes all trace of the CO_2 and H_2O from the spectrometer path. Figure 13 demonstrates the success, showing the complete disappearance of the CO_2 fundamental Q branch, and the double H_2O line at 592 cm^{-1}, which affords the strongest H_2O absorption between 15 and 19 microns.

(6) Calibration

The spectrometer was calibrated using the wavelength determinations of Plyler, Blaine, and Conner[31] on CO in

the 4.7 micron band. Their measurements were taken with interferometer fringes superimposed on the spectrum for calibration. Here, the rotational structure of the 4.7 micron CO band was observed in the 3d, 4th, and 5th orders to establish the calibration of this spectrometer. The resulting calibration curve deviates from absolute linearity in wavelength by only 5 Å from 14.5 to 24 microns. The deviation of the calibration points from a linear equation is shown in Figure 14. The average deviation of the calibration points from the best uniform curve is about 3 Å, which represents an accuracy of better than 0.01 cm^{-1} at 20 microns.

The remaining inaccuracy is not at all random, however, there being a very consistent correlation with the temperature of the spectrometer, which at present, varies about 2 degrees C in a day. Since the temperature dependence is roughly 2 Å per degree C, a temperature control to 0.2 degrees C could conceivably yield a factor of 4 or 5 in wavelength accuracy, or plus or minus several thousands of a wave number at 20 microns.

A useful filter for isolating the 4.7 micron CO band was made by evaporating a $\lambda/2$ (at 4.7 microns) film of Tellurium onto 0.027" thick mica. The mica plus the 6.3 micron H_2O absorption causes the long wavelength cut-off, and the Tellurium cut-off plus the 2.7 micron H_2O absorption eliminates the shorter wavelengths. The filter transmits 75% at 4.7 microns. Figure 15 is a transmission curve of this filter.

(7) Resolution

The available resolution of the instrument was determined by observing the widths of absorption lines of N_2O in the 17-micron band. The spectrometer slits were set equal to the theoretical Rayleigh resolution limit as calculated for the 14" wide grating and $\lambda = 17$ microns. The carbon arc was used as a source to supply the maximum possible signal/noise ratio. N_2O at 35 mm pressure was introduced to a 25 cm absorption cell. Figure 16 shows the $R_{(4)}$ and $R_{(5)}$ lines of the N_2O 17-micron band with hot band satellite lines completely resolved 0.2 cm^{-1} away. The observed width of absorption of the lines is about 0.08 cm^{-1}. Under these conditions, the effective optical slit width of the spectrometer would be about 0.06 cm^{-1}. The broader appearance is due to the influence of the width of absorption of the line itself -- as would be observed with infinite resolution. This represents 70% of theoretical resolution for the grating used at the angle corresponding to 17 microns, which compares favorably with 80% calculated theoretically by Jacquinot[32] for the use of slits equal to the diffraction width.

As can be seen from Figure 16, the signal/noise ratio is just about the minimum necessary to do effective work, and so it would appear that this spectrometer has reached the diffraction limit to resolution and the energy limit to resolution simultaneously.

(8) Electronics

The electrical signal generated by the Golay pneumatic detector is amplified with an a.c. amplifier. The amplified signal is rectified synchronously with the chopping frequency by a mechanical rectifier, after which it is fed through an RC filter network with an adjustable time constant. The signal is then displayed on a Leeds and Northrup pen recorder.

B. Experimental Set-Up for the Study of CO_2

The first problem to which the spectrometer, described above, has been turned is the present study of the CO_2 intensities in the 545 - 667 cm^{-1} spectral region. For this work the Globar was used as a source. The entire 3" of slit was used in conjunction with the exit slit image slicer. The slit width used for all measurements was 0.24 mm, and corresponds to an optical slit width of about 0.1 cm^{-1}.

Three absorption cells, of lengths 1.133, 5.08, and 25.17 cm were constructed to fit into the exit beam of the spectrometer. (From here on these cells will be referred to as the 1, 5, and 25 cm cells.) The cells were made of brass and had KBr windows. The windows were sealed by means of neoprene o-ring seals. The absorption cell in use was connected to the exterior of the spectrometer housing by copper tubing so that the gas content could be controlled from the outside. A one-liter glass bottle was connected to the system on the outside as a ballast

volume, which was especially useful in maintaining a constant pressure over a long period of time when the 1 cm cell was being used. Two Hg manometers were used to read the pressure in the absorption cell. The entire system to be isolated was of metal or glass, except for the o-ring seals at the cell windows and the connections to the copper tubing -- which were of plastic hose. The system could be isolated for many hours with no detectable change in pressure. The cells were filled to a prescribed pressure with pure CO_2. The brand used was blue banded Southern Oxygen Co. CO_2, and the purity of this brand has been checked in the past to be better than 99.7%.

A constant check of the temperature of the absorption cell was kept by reading the voltage of a thermocouple attached to the absorption cell.

For all runs the spectrometer housing was sealed up and all CO_2 and H_2O were removed from the spectrometer path before beginning any measurements. From the recorder a record was obtained of the gas transmission as a function of wavelength for several pressures in each cell. Repeats were often made.

The wave number locations of the CO_2 absorption lines of interest in this study were taken from the work of Blau, etc.,[3] and appear in the tables. The use of their accurate measurements avoids the necessity of dealing with the temperature dependent error of this spectrometer [see A(6)].

The amplifier was quite stable and maintained a steady zero signal over many hours. The 100% transmission curve was checked at frequent intervals by recording the signal after pumping out the absorption cell. The amount of scattered radiation could be determined by observing the depth of absorption for the strong Q branches, and in most cases unwanted radiation was negligible. A small scattering correction was introduced in the region below 618 cm^{-1}.

IV. DATA

A. Spectra

CO_2 absorption spectra were observed from 545 to 674 cm^{-1} under a variety of pressures in each of the 1, 5, and 25 cm absorption cells. It is impractical to include all this data here. The tables include the results from all measurements, but only representative spectra are shown. Figures 17 and 18 are spectra of the entire range of study in these experiments, using the 25 cm absorption cell with the pressures indicated. Each vibrational transition is indicated at the band head, and the P and R branch lines are labeled according to the J quantum number of the lower state and the following convention:

for $C^{12}O_2^{16}$	A,a :	R,P branch	$01^{1}0 - 000$
	B,b :	" "	$02^{2}0 - 01^{1}0$
	C,c :	" "	$02^{0}0 - 01^{1}0$
	K,k :	" "	$C_{}^{1}0 - 02^{0}0$
	F,f :	" "	$03^{1}0 - 02^{2}0$
for $C^{13}O_2^{16}$	✱,∝ :	" "	$01^{1}0 - 000$

The spectra shown here were taken with a spectral slit width of $\sim$ 0.1 cm^{-1}, which is the highest resolution with which the CO_2 spectrum in this region has ever been recorded. Thus more lines are visible and a better identification of satellites is possible than heretofore.

Figure 19 is a scan of the $01^{1}0 - 000$ Q branch with higher dispersion. The Q branch line positions are marked.

The frequencies of the clearly observed Q branch lines together with the constant ($B''-B'$) they define are given in Table 3.

From Figures 17 and 18 it is obvious that a considerable portion of the spectral range is crowded to the extent that measurements on individual lines would be difficult. Therefore measurements were not made on all lines. Three regions were selected for concentrated study: 661 - 666 cm^{-1}, 624.5 - 629 cm^{-1}, and 598 - 613 cm^{-1}. These regions were selected for the following reasons: a) The principal lines in these regions are nearly free from overlap; b) lines of low, medium, and high J occur; and c) the strength of the lines occurring in this region allow convenient-sized absorption cells to be used.

Spectra in the first region, 661 - 666 cm^{-1}, are shown in Figure 20 with high dispersion. A scan with each of the 1, 5, and 25 cm absorption cells is represented. Lines a2, a4, and a8 of the ν_2 fundamental P branch were studied, as well as lines b8 and b9 of the 1st harmonic P branch. Also an estimate was made of the strength of the $O^{18}C^{12}O^{16}$ isotope fundamental Q branch.

Spectra occurring in the second region of study 624.5 - 629 cm^{-1} are shown in Figure 21, with scans using the 1, 5, and 25 cm absorption cells. The lines studied here were a50, 52, 54, and 56 of the fundamental, and C9, 11, and 13 of the R branch of the $02^{\circ}0 - 01'0$ transition. The third series of "apparent" lines in Figure 21

are blends of k and α lines and therefore not suitable for an intensity study.

In these bands alternate J lines are missing. This is because in each transition a Σ state is involved, which for CO_2 contains only levels of even J.*

The third region of detailed study was 598 - 613 cm^{-1} as shown in Figure 22. Here P branch lines c7 through c25 of the $02^{0}0$ - $01'0$ band are found quite free from overlap or background. (The F band lines occurring here have only a two or three percent contribution which may be easily taken into account.) For this reason the most accurate measurements were made in this region.

In addition to a concentrated study in these three spectral regions, a measurement of the total Q branch strength was made for the $02^{0}0$ - $01'0$ band at 618 cm^{-1}, the $03'0$ - $02^{2}0$ band at 597 cm^{-1}, and the $03'0$ - 100 band at 544.5 cm^{-1}.

The Q branches for the $03'0$ - $02^{0}0$ band and the fundamental of the $C^{13}O_2^{16}$ and $O^{18}C^{12}O^{16}$ isotopes are nearly hidden under P branch lines of the $C^{12}O_2^{16}$ fundamental (see Figure 17). However, rough estimates were possible of the strengths of these bands. Figure 23 shows the spectral region 646 - 649 cm^{-1} taken with lower pressure in the 25 cm absorption cell where the $03'0$ - $02^{0}0$ band of $C^{12}O_2^{16}$ and the $01'0$ - 000 band of $C^{13}O_2^{16}$ occur. The $O^{18}C^{12}O^{16}$

*The oxygen nuclei being identical and of zero spin, the antisymmetric (odd J) levels of Σ_g^+ states are absent.

fundamental Q branch can be seen with high dispersion in Figure 20.

B. Analysis of the Spectra

The methods used to determine the line widths and strengths from the observed spectra are described in Section II. In the case of the P branch lines of the C band it was possible to use several methods, and the results could be cross-checked. The most frequently used method is the "Curve of Growth" method described in Section II-E. A further remark is made here with regard to the application of this method to the present study.

The important result of the "Curve of Growth" treatment is stated in Equation 11. To repeat,

$$W^\circ = 2\pi\gamma^\circ F\left(\frac{S^\circ \ell}{2\pi\gamma^\circ}\right) \qquad (11)$$

If the value of W° for a line is known at two absorption path lengths, S° and γ° can be calculated for that line. This procedure is cumbersome, however, since $F(x)$ is in tabular form. Instead of this, a graphical procedure has been used which yields results more readily. This is as follows: The data are plotted as log W° versus log ℓ . A curve of log F versus log x is then superimposed on the data curve and positioned so that the best fit is made with the experimental points. (These curves are most conveniently obtained by the use of log log graph paper.) A simple argument then shows that S° is equal to the value of W° at the intersection of the

Ladenburg-Reiche curve "linear region" asymptote $(F(x) = x)$ and the line $\log \ell = 0$ (ℓ = 1 cm). Further, it may be shown that the value of W° at the intersection of the "linear region" asymptote and the "square root region" asymptote $\left(F(x) = \sqrt{\frac{2x}{\pi}}\right)$ is given by $W^\circ = 4\,\gamma^\circ$. Thus S° and γ° may be determined quite simply when the data are put in this graphical form.

In the discussion to follow concerning the reduction of the data, the three spectral regions in which a concentrated effort was made will be considered in turn, followed by a discussion of the treatment of the various Q branches observed.

(1) 661 - 666 cm^{-1} Region

The lines occurring in the first region of interest, 661 - 666 cm^{-1}, are strong, and low pressures are required to eliminate overlap and keep down the background. As a result the lines are narrower than the optical slit width and direct measurements are impractical even with slit function corrections. Also, the lines are too strong to use the "Weak Absorption" method. Therefore the "Curve of Growth" technique was attempted for the analysis of this region. The average W° of a2, 4, 8 determined from several runs at various pressures for each of the 1, 5, and 25 cm cells is given in Table 4. The pressures used for each cell length are indicated in Table 5. The data were plotted graphically as discussed above. Figure 24 shows the result for the line a4. As can be seen from the

graph, the experimental points fit the logarithmic Ladenburg-Reiche curve (abbreviated L-R curve in further discussion) almost entirely in the "square-root" region. Therefore the data can not yield S° and γ° with any accuracy, but will determine the product $S^\circ \gamma^\circ$ to the accuracy of the measurements. For the "square-root" region it has been stated in II-E that

$$W = 2\sqrt{S\gamma\ell} \tag{8}$$

or $$W^\circ = 2\sqrt{S^\circ \gamma^\circ \ell} \tag{16}$$

In a region close to the "square-root" region, a better approximation is:

$$W^\circ = 2\sqrt{S^\circ \gamma^\circ \ell}\left(1 - \frac{1}{8x}\right) \tag{17}$$

Since x is necessarily large for this approximation, a rough value of x is all that is required. The $S^\circ \gamma^\circ$ products were determined for a2, a4, and a8 for each W°. These results are shown in Table 8.

The value of W° for the lines b8 and b9 was determined from the spectra taken with the 25 cm absorption cell. Equation 17 was used to determine $S^\circ \gamma^\circ$ for b8 and b9. If the assumption is made that γ° for b8 and b9 is equal to γ° for a8, the ratio of S° for b8 and b9 to S° for a8 may be determined. In a similar manner, the strength of b34 plus b35 (see Figure 17) was determined

relative to the strength of a34. These results are tabulated in Table 9. (In Table 9, the strength of b34 + b35 is divided into a contribution from each line assuming a Boltzmann distribution.)

The strength of the Q branch of the $O^{18}C^{12}O^{16}$ band was estimated using the "Elsasser band" method. A description of this case will be included in a later discussion of several Q branch strength determinations by this method.

(2) 624.5 - 629 cm^{-1} Region

The second region studied, from 624.5 to 629 cm^{-1}, contains many closely spaced lines. P branch lines of the A, K, and A bands and R branch lines of the C band occur predominantly. Also P branch lines of the B band and R branch lines of the F band occur weakly. This region is of interest since it is the only region in which measurements on R branch lines of the C band and high J lines of the A band can be attempted.

The equivalent widths of a50, 52, 54, 56 and C9, 11, 13, were measured at various pressures (Table 5), and an average W^o calculated for each line for each absorption cell length. These are shown in Table 4. The measurement of equivalent width of a line requires that an integration be made over all absorption due to the line. It can be seen in Figure 21 that the absorption due to each line is overlapped by that due to others for the 1 cm path length measurements. This difficulty may be overcome

by a simple approximation which holds well when the overlap absorption is small and the lines do not differ greatly in peak absorption. First the absorption is divided into regions by drawing vertical lines between the absorption lines, dividing their spacing into components of length having the same ratio as their peak absorption. The equivalent width of a line is then measured by integrating the absorption over the block containing the line. The assumption is that the integrated absorption lost by cutting off the wings of the line being measured is compensated for by including the wings of the neighboring lines when the cutoff is made in the manner prescribed above.

It was necessary to make background corrections to the W^{o} values for the a50, 52, 54, 56 lines. A theoretical spectrum was calculated using values of band strength and line width that have been estimated by Benedict.[34] The contribution of the background lines to the equivalent width measured was then calculated for each condition of pressure and path length used. The appropriate corrections were made to the observations. These corrections, averaging only a few percent and the largest of which is 8%, have been used on the values of W^{o} occurring in Table 4.

Due to the weak absorption, and overlap and background corrections necessary, the values of W^{o} for lines in this region obtained with the 1 and 5 cm path lengths have considerable uncertainty. To increase the accuracy

obtained by the graphical "Curve of Growth" method, the data for a50, 52, 54, and 56 were plotted together for a single comparison to the L-R curve. Two assumptions are necessary for this step. The first is that the value of γ^{o} is the same for all four lines. The second is that the ratios of the line strengths are the theoretical ratios predicted for a Boltzmann distribution -- i.e. ratios of the factor:

$$\left(\frac{J''-1}{2}\right) e^{-\frac{E_{J''}}{kT}} \quad \frac{\nu}{\nu_0} \frac{\left(1-e^{-\frac{h\nu}{kT}}\right)}{\left(1-e^{-\frac{h\nu_0}{kT}}\right)} \qquad \text{for each line.}$$

For a few adjacent high J lines these assumptions are expected to be quite good. The data are now plotted as log W^{o} versus log $S^{o}\ell$ where S^{o} for each line is given in units of $S^{o}50$. Thus many points instead of three determine the fit of the data curve to the L-R curve. This is shown in Figure 25. From the curve is obtained γ^{o} for all lines, and the value of S^{o} for a50. S^{o} for the other lines is determined by the theoretical ratios.

This method was also used to plot data for the lines C9, 11, and 13, as is shown in Figure 26. Here the assumptions regarding γ^{o} and the ratio of the S^{o}'s seem valid if one considers the expected values estimated from measurements of γ^{o} and S^{o} in the P branch of the C band.

The values of S^{o} and γ^{o} determined for the lines in this region are given in Table 10.

(3) 598 - 613 cm^{-1} Region

The only strong lines in this region are the c7 - c25 lines of the $02^{0}0 - 01^{1}0$ band P branch. Here pressures up to an atmosphere do not cause serious overlap, and S° and δ° were determined for these lines by direct measurement as well as by the "Curve of Growth" method.

Direct measurements were possible with only small slit function corrections, since the width of the absorption coefficient curve at a pressure of 1 atmosphere is over twice the width of the spectrometer slit function. The logarithm of the transmission curve was calculated for 4 runs with the 1 cm and 5 cm absorption cells where the pressure was between 0.8 atmos. and 1.0 atmos. Then $\delta^{\circ}_{obs.}$ was measured directly, and $S^{\circ}_{obs.}$ was obtained by integration of the log T curve for each line -- as discussed in II-B. These observed values were corrected for the effect of the slit by the amounts indicated in Figures 1, 2, and 3. The resulting S° and δ° for each line is given in Table 6.

The equivalent width of each line c7 - c25 was measured for the 1, 5, and 25 cm path lengths for several runs under a variety of pressures -- as indicated in Table 5. The value of W° for each line at each path length is given in Table 4. These values of W° were smoothed by plotting W° versus J for each path length and drawing a smooth curve through the experimental

points. This is shown ir Figure 27. Log W° (smoothed) was plotted against log ℓ , and S° and δ° for each line determined by the graphical "Curve of Growth" method. An average example of the fit of the data to the L-R curve is shown for line c17 in Figure 28. The resulting values of S° and δ° are given in Table 6 where they may be compared with the results of the corrected direct measurements.

(4) Q Branch Measurements

The Q branch strength of six bands was determined. In the discussion below, they will be grouped according to the method used to reduce the data.

The Q branch of the 03'0 - 100 band at 544.26 cm^{-1} is weak and is free from overlap with other bands. The "Weak Absorption" method was used to determine the strength of this Q branch. The integrated absorption was averaged for four scans over the Q branch, and the strength determined as outlined in II-D. The value obtained is given in Table 11.

The Q branch strength of the $02^{0}0$ - 01'0 transition (C band) and the 03'0 - $02^{2}0$ transition (F band) were determined by the method of Wilson and Wells. For each band, $\int(-\ln T)d\nu$ was evaluated at several conditions of path length and pressure (see Table 7), and S° determined by the extrapolation procedure outlined in II-F. For the C band Q branch the strength of the Q branch + line c1 was determined, since this first P line is well

surrounded by Q branch structure. After a minor background correction for overlapping "a" and " α " lines, the C band strength was determined from the measured S^{o} by the ratio of the C Q branch + c1 line to total band strength calculated assuming a Boltzmann distribution in the P branch. The extrapolation is shown in Figure 30, and the C Q branch strength is included in Table VII.

The F band Q branch measurement was a much more approximate procedure. Before the method of Wilson and Wells could be applied, the effect of the line c27 had to be removed from the absorption due to the F Q branch. This was done by carefully reconstructing the c27 line as it would appear in the absence of the F Q branch. It was assumed that the absorption due to c27 was equal to the average value of absorption for the lines c25 and c29 which could be clearly observed. After constructing the c27 line the difference between the constructed and observed absorption was assumed to be due to the F Q branch, and the method of Wilson and Wells was pursued. The extrapolation for the F Q branch strength is shown in Figure 29. The resulting Q branch strength is included in Table 11.

The remaining three Q branches are nearly buried beneath P branch lines of the A band, and are also overlapped with lines of the B and C bands. An accurate determination of their strengths cannot be made by direct measurements; however a rough value was obtained using the following technique: First an estimate was made of

the absorption due to the Q branch as a function of ν. From the band constants, separations of the Q branch lines were calculated at frequency intervals greater than the spectrometer slit function width. The "Elsasser Band" method, II-G, was then applied for each frequency at which the line separation was calculated. From Equation 13 the S^o of the average strength line being passed by the spectrometer when set at that frequency was determined. A δ^o of 0.11 cm^{-1} was assumed for the calculation. For each of the line strengths thus determined, a Q branch strength may be calculated if a Boltzmann distribution is assumed for the Q branch. The Q branch strengths for the K band and the isotopic A band were determined in this manner, and the results are given in Table 11. The Q branch strength of the $01^{1}0 - 000$ transition of the $O^{18}C^{12}O^{16}$ isotope was also estimated by this method. This Q branch has two series of lines as a result of ℓ-doubling. Since the even J series diverges more rapidly, it makes the major contribution to the absorption in the wing of the Q branch. The measurements were made in the wing of the Q branch, and the effect of the odd J series was ignored in the reduction. The contribution to the observed strength due to this second series is estimated roughly as 30%. Making this correction to the observed S^o, the value of Q branch strength found in Table 11 represents a "most probable" choice.

V. DISCUSSION OF RESULTS

The primary results of this study are the values of S^o and δ^o determined for the lines listed in Table 10, and the Q branch strengths listed in Table 11. An estimate of the uncertainty in these results is listed for each value in the table -- the most important source of uncertainty being the lack of reproducibility of the quantities derived directly from the spectra due to the noise fluctuations.

The band strength determinations are considered secondary results since an assumed band intensity distribution must be used in the calculation of these quantities.

In the discussion below, the results of this study are compared with the results of other experimental and theoretical investigations. A discussion of strengths will be given first, followed by a discussion of line widths.

A. Line and Band Strengths

The line strengths for the P branch of the C band obtained from the corrected direct determination and the "Curve of Growth" methods are plotted as a function of J in Figure 31. This curve establishes the experimental variation of strength with J. In a first attempt to compare these results with theory, the rotational distribution was calculated assuming a Boltzmann distribution. It has been shown[33,11] that this distribution for CO_2

is given by:

$$S_J^o = \frac{S_{v''}^{v'} F(J'')}{Q_J} \cdot \frac{\nu\left(1-e^{-\frac{h\nu}{kT}}\right)}{\nu_o\left(1-e^{-\frac{h\nu_o}{kT}}\right)} \cdot e^{-\frac{E_{J''}}{kT}} \qquad (14)$$

where S_J^o, $S_{v''}^{v'}$ have been defined,

$F_{(J'')}$ is a function of J'' which differs for the P, Q and R branches and depends on the vibrational transition. For the P branch of the C band, $F(J'') = \frac{J''+1}{2}$

ν_o is the frequency of the band head.

$\left(1-e^{-\frac{h\nu}{kT}}\right)$ is the induced emission term.

$e^{-\frac{E_{J''}}{kT}}$ is the Boltzmann factor.

$Q_J = \sum_{J''}(2J''+1)e^{-\frac{E_{J''}}{kT}}$ is the rotational partition function.

The value of $S_{v''}^{v'}$ was adjusted to give the most favorable fit of this distribution to the data, and for $S_{v''}^{v'}$ = 3.84 cm^{-2} atmos.$^{-1}$ the results are shown in Figure 32. The experimental points show a consistent deviation from the calculated distribution suggesting a refinement of the theoretical distribution. Benedict[18] has shown that a consideration of the Coriolis vibration-rotation interaction leads to a formula for the rotational intensity distribution given by Equation 14 multiplied by the following

term:

$$(1+\zeta m)^2 \qquad (15)$$

where m is the ordinal number of the line, and ζ is a parameter depending on the strength of the Coriolis interaction and the vibrational transition involved. No theoretical estimates have been made of the value of ζ for the C band, although $\zeta = +.0016$ has been estimated[18] for the A band.

Using Equation 14 with the addition of the term (15) and adjusting the parameters $S^{v'}_{v''}$ and ζ, a most satisfactory fit to the experimental data is obtained. This is shown in Figure 33 for $S^{v'}_{v''} = 4.27$ cm^{-2} atmos.$^{-1}$ and $\zeta = +.0035$.

The effect of a positive ζ is to decrease the intensity of the P branch and increase the intensity of the R branch. The parameters were adjusted so that almost perfect agreement with experiment is obtained at c11 -- the value of S^o for c11 being 0.0685 cm^{-2} atmos.$^{-1}$. For the R branch, the predicted value of S^o for C11 is 0.0736 cm^{-2} atmos.$^{-1}$ while the experimental value is 0.070 cm^{-2} atmos.$^{-1}$. This agreement is well within the estimate of reliability for the measurement of S^o for C11.

The determination of $S^{v'}_{v''}$ for the C band from the C Q branch measurement must be considered as a check on the value obtained from the other measurements. The value obtained is $S^{v'}_{v''} = 3.72$ cm^{-2} atmos.$^{-1}$ which is 13% lower

than the value determined above from the P branch measurements. The uncertainty in the value obtained from the Q branch measurement is considerably greater than that for the determination from the P branch measurements however, due to the abundance of data in the latter case. It should also be mentioned that a consideration of the effects due to the Fermi resonance between the $02^{0}0$ state (upper state for the C band), and the 100 state yields the conclusion that the observed strength of the C Q branch should give too low a value of $S_{v}^{v'}$ if the effects are neglected, as they were here. The magnitude of this effect, however, has been estimated[34] as less than 5%.

The distribution of line strengths in the fundamental, or A, band can not be determined from measurements made in this study since the strength has been determined at only one place in the band. If a distribution is assumed however, the band strength can be determined from the measurement of the line strengths for a50 - a56 given in Table 10. The distribution assumed is that given in Equation 14 multiplied by the Coriolis term (15), where $F(J'') = \frac{J''-1}{2}$ for the P branch of the A band. This calculation has been carried out for three values of ζ : $\zeta = 0$ corresponding to no Coriolis interaction; $\zeta = +.0016$ which is the value calculated[18] theoretically for this band; and $\zeta = +.0035$ which is the value obtained in this study for the C band. Benedict points out[34] that the magnitude of the ζ parameter

for the C band is expected to be somewhat greater than that of the A band. For these three values of ζ , the values of $S_{v''}^{v'}$ for the A band are:

ζ	$S_{v''}^{v'}$ (cm^{-2} atmos.$^{-1}$)
0	196
+ .0016	235
+ .0035	290

The result of Kaplan and Eggers[16] measurement on the ν_2 fundamental by a low resolution "Curve of Growth" method is $S_{v''}^{v'}$ = 214 cm^{-2} atmos.$^{-1}$. The strength of a50 observed in this study can be obtained from their value of $S_{v''}^{v'}$ if a ζ of +.00084 is assumed. No final conclusion can be drawn as to the value of $S_{v''}^{v'}$ for the A band, but in light of all available evidence, the most reasonable value is perhaps 235 cm^{-2} atmos.$^{-1}$ with a ζ = +.0016.

The strength of the first harmonic, or B band has only been determined relative to the A band, and is therefore equally ambiguous.

Vibrational transition moments were calculated by Equation 1 for all the bands studied. The results appear in Table 12 where they are compared with the transition moments that have been calculated by Benedict[18] on the basis of a theoretical model. The available parameters in the dipole expansion for this model have been adjusted to best fit the CO_2 intensity data known previous to the

present study, and no attempt was made to further adjust the parameters in light of the present results. Three values of transition moment have been calculated for the A and B bands corresponding to a value of ζ for the A band of 0, +.0016 and +.0035.

The agreement of other investigations (740 - 864 cm^{-1} region) with the predictions of the model is included for comparison.

B. Line-Widths

The values of δ° for c7 - c25 determined from corrected direct measurements and the "Curve of Growth" method are included in Table 6. In addition δ° values have been determined from "square-root region" measurements of $S^\circ \delta^\circ$ in the 25 cm cell and from the best values of line strength determined by all methods. The results of these three methods of obtaining δ° are shown graphically in Figure 34. Included also is the value of δ° obtained from Kinetic Theory assuming a collision diameter, d = 3.3 x 10^{-8} cm, given by viscosity and conductivity measurements.* δ° has the almost constant value of 0.103 cm^{-1} from c9 to c23. There is a slight indication of higher values of δ° at lower J" and lower values at higher J". The δ° determined from R branch measurements on C9, 11, 13 has the value 0.11 cm^{-1}.

δ° was determined for the P branch of the fundamental (A band) to be δ° = 0.060 cm^{-1} at a50 - 56. The value of δ° for a2, 4, 8 could be determined from

*Handbook of Chemistry and Physics, 30th edition, 2627 (1947), Chemical Rubber Publishing Co., Cleveland

the $S^{\circ}\ \gamma^{\circ}$ products of Table 8 if the band strength and intensity distribution were known. Three values of A band strength were calculated in the previous section for ζ = 0, +.0016, and +.0035. The values of γ° for a2, 4, and 8 calculated from the $S^{\circ}\ \gamma^{\circ}$ products for these three cases are:

ζ	$S_{v'}^{v''}$ $cm^{-2}atm^{-1}$	$\gamma^{\circ}(a2)$ $cm^{-1}atm^{-1}$	$\gamma^{\circ}(a4)$ $cm^{-1}atm^{-1}$	$\gamma^{\circ}(a8)$ $cm^{-1}atm^{-1}$	
0	196	.129	.116	.095	~ 10% uncertainty in all values
+.0016	235	.108	.098	.08	
+.0035	290	.088	.079	.065	

For any reasonable choice of ζ it would appear that the γ° at low J" is considerably higher than the γ° at J" = 50. This result fits well with the observed trend of γ° versus J" in the C band. It is proposed therefore that in the A and C bands of CO_2, γ° is high at low J, becomes nearly constant at a somewhat lower value over intermediate J, and drops off at higher J to approach the Kinetic Theory value. This proposition is quite compatible with theoretical expectation. It has been shown[35,36] that molecules with a strong dipole moment have a maximum value of γ° at a J" value near the peak of the Boltzmann distribution, since a molecule making a transition at such a J" finds a greater number of perturbing molecules with which it may resonate. However this effect is very weak for molecules with a small dipole moment. Smith, Lackner, and Volkov[36] have measured γ°

for OCS in the microwave region and measure only a 7% increase in δ° from $J'' = 1$ to $J'' = 5$. They have also calculated the expected widths using Anderson's Theory[35] of collision broadening extended to include the effects of near-resonant interactions and conclude that the expected increase in δ° is only 4% from $J'' = 1$ to $J'' = 5$ for OCS.

CO is another molecule with a weak dipole which has been investigated. Measurements of δ° for the CO fundamental have been reported by Benedict.[18] The results, reproduced graphically in Figure 35, show a variation with J not inconsistent with the results of this study for CO_2. The observed increase in δ° at low J can be explained by the following argument: In the case of a very weak dipole-dipole interaction, or for a quadrupole-quadrupole interaction (which must be the principal cause of collision diameters greater than the Kinetic Theory diameter in a non-polar molecule such as CO_2), the collisions in which exact resonance occur are relatively less important than those in which a moderate degree of near-resonance takes place. Since the low J levels are more closely spaced, a molecule radiating from a low J quantum state will have significant near-resonant collisions with a greater number of molecules, causing an increased line width.

VI. CONCLUSIONS

The distribution of line strength and the variation of line width with J has been determined for intermediate

J in the P branch of the $02^{0}0 - 01'0$ absorption band of CO_2. The observed intensity distribution can be completely explained if the Coriolis vibration-rotation interaction is introduced. The line width is quite constant from $J'' = 9$ to $J'' = 23$, with some indication of being larger for lower J and smaller for higher J. The strength and line width of the J50 to 56 lines in the P branch of the $01'0 - 000$ band have been measured; however, the band intensity is indeterminate since the magnitude of the Coriolis interaction parameter is not known for this band. A value has been obtained for the strength of all the absorption bands of CO_2 prominent at room temperature in the spectral region 545 - 667 cm^{-1} -- with varying reliability.

It is suggested that measurements be made with long absorption paths on higher J lines in the P branch of the $02^{0}0 - 01'0$ band to determine the further variation of line width with J, and to establish the value of the Coriolis interaction parameter with greater certainty. It is suggested also, that a further study of the low J lines in the $01'0 - 000$ band be made with shorter path lengths, to determine the strengths of these lines -- for in this way the magnitude of the Coriolis interaction parameter for this band could be established, the band strength determined, and a comparison of line widths be made for low and high J.

BIBLIOGRAPHY

1. L. D. Kaplan, Jour. Chem. Phys. 18, 186 (1950)
2. S. S. Penner, Jour. Appl. Phys. 23, 1283 (1952)
3. Blau, Dalby, Lakshmi, Nielsen, Rao, Infrared Spectroscopy of Molecules, Contract DA-33-019-ORD-1507, Ohio State University (1955)
4. To appear in Table of Solar Spectrum Wavelengths, 2.8 - 23 Microns, by Migeotte, Neven and Swanson, Proc. of Royal Society of Liège
5. R. Ladenburg and F. Reiche, Annalen der Physik 421, 181 (1911)
6. E. B. Wilson, Jr. and A. J. Wells, Jour. Chem. Phys. 14, 578 (1946)
7. W. M. Elsasser, Phys. Rev. 54, 126 (1938)
8. P. Martin and E. F. Barker, Phys. Rev. 41, 291 (1932)
9. A. M. Thorndike, Jour. Chem. Phys. 13, 868 (1947)
10. H. Rubens and E. Ladenburg, Verh.d.D. Phys. Ges. 7, 179 (1905)
11. D. F. Eggers, Jr. and B. L. Crawford, Jr., Jour. Chem. Phys. 19, 1554 (1951)
12. Howard, Burch, and Williams, Near Infrared Transmission Through Synthetic Atmospheres, Report No. 1, Contract AF19(604)-516, Ohio State University (1954)
13. W. Peters, Dissertation, The Johns Hopkins University (1949)
14. W. H. Cloud, The 15 Micron Band of CO_2, Progress Report Contract Nonr 248(01), The Johns Hopkins University (1952)

15. H. J. Kostkowski, Dissertation, The Johns Hopkins University (1955)

16. L. D. Kaplan and D. F. Eggers, Jr., Intensity and Line-Width of the 15 Micron CO_2 Band Determined by a Curve of Growth Method, presented at Ohio State Symposium on Mol. Struct. and Spectros. (1955)

17. L. D. Kaplan, Jour. Chem. Phys. 15, 809 (1947)

18. W. S. Benedict, Theoretical Studies of Infrared Spectra of Atmospheric Gases, Final Report, Contract No. AF19(604)-1001, (1956)

19. A. Adel, Phys. Rev. 52, 53 (1953)

20. W. S. Benedict and S. Silverman, Line Shapes in the Infrared, paper given at Meeting of Am. Phys. Soc., (January 1954)

21. H. A. Lorentz, Proc. Roy. Acad. (Ams..) 8, 591 (1906)

22. H. J. Kostkowski and A. M. Bass, Slit Function Effects in the Direct Measurement of Line Widths and Intensities, presented before the Opt. Soc. of Am. (October 1955)

23. P. C. von Planta, private communication

24. L. H. Stover, Table to be published as part of a paper by L. D. Kaplan and D. F. Eggers, entitled Intensity and Line-Width of the 15 Micron CO_2 Band Determined by a Curve-of-Growth Method

25. L. D. Kaplan, Jour. of Meteorology 10, 100-104 (1953)

26. R. P. Madden, A High Resolution Spectrometer for the 20 Micron Region, paper presented at the Ohio State Symposium on Mol. Struct. and Spectros. (June 1956)

27. W. G. Fastie, Jour. Opt. Soc. Am. 42, 641 (1952)

28. C. S. Rupert and J. Strong, Jour. Opt. Soc. Am. 40, 455 (1950)

29. J. H. Taylor, Dissertation, The Johns Hopkins University (1952)

30. R. P. Madden, 10-15 Micron Thick Silver Films for Infrared Gratings, paper presented before the Opt. Soc. of Am. (March 1955)

31. Plyler, Blaine, and Conner, Jour. Opt. Soc. Am. 45, 102 (1955)

32. P. Jacquinot, private communication

33. B. L. Crawford, Jr. and H. L. Dinsmore, Jour. Chem. Phys. 18, 983 (1950)

34. W. S. Benedict, private communication

35. P. W. Anderson, Phys. Rev. 76, 647 (1949)

36. W. V. Smith, H. A. Lackner, A. B. Volkov, Jour. Chem. Phys. 23, 389 (1955)

37. J. Strong, Jour. Opt. Soc. Am. 41, 3 (1951)

Table 1

Vibrational Levels of $C^{12}O_2^{16}$**

v_1	v_2^l	v_3	Sym	J	G_v cm^{-1}	B cm^{-1}	D 10^{-7} cm^{-1}	
0	0^o	0	Σ_g^+	e	0.00	0.39021	1.3	
0	1'	0	Π_u	o	667.40	.39062	1.3	
				e		.39123	1.3	
0	2^o	0	Σ_g^+	e	1285.43	.39046	1.475	
1	0^o	0	Σ_g^+	e	1388.19	.39018	1.125	
0	2^2	0	Δ_g	e,o	1335.16	.39164	1.3	
0	3'	0	Π_u	o	1932.45	.39076	1.40	
				e		.39174	1.46	
1	1'	0	Π_u	o	2077.86	.39039	1.20	
				e		.39125	1.14	
0	3^3	0	Φ_u	o,e	2003.28	.39236	1.3	
0	4^o	0	Σ_g^+	e	2548.51	.39096	1.5	
1	2^o	0	Σ_g^+	e	2670.5	.3899	1.3	*
2	0^o	0	Σ_g^+	e	2797.19	.39059	1.1	
0	4^2	0	Δ_g	e,o	2585.1	.39199	1.38	*
1	2^2	0	Δ_g	e,o	2760.75	.39152	1.22	
0	44	0	Γ_g	e,o	2674.76	.39307	1.3	*

*Constants determined indirectly; levels not observed with high resolution.

**Prepared by W. S. Benedict

Table 2

CO_2 Band Constants Useful in this Study

Isotope	Upper Level	Lower Level	ν_o (cm^{-1})	J"	B'+B" (cm^{-1})	B'-B" ($10^{-4} cm^{-1}$)	2(D'+D") ($10^{-7} cm^{-1}$)	D'-D" ($10^{-8} cm^{-1}$)
$C^{12}O_2^{16}$	03'0	100	4[illegible].26	e	.78094	5.8	5.05	2.75
"	03'0	02^20	597.29	e	.78240	-8.8	5.4	1.0
				o	.78338	1.0	5.52	1.6
"	02^00	01'0	618.03	o	.78108	-1.6	5.55	1.75
"	03'0	02^00	647.02	e	.78122	3.0	5.75	- .075
				o	.78220	12.8	5.87	- .015
"	01'0	000	667.40	e	.78083	4.10	5.2	0
"	02^20	01'0	667.76	e	.78287	4.10	5.2	0
				o	.78226	10.24	5.2	0
$C^{13}O_2^{16}$	01'0	000	648.52	e	.78088	4.0	5.2	0

Table 3

Line Positions and Band Constants

Determined for the Q Branch of the

01'0 - 000 Transition of $C^{12}O_2^{16}$

Line	ν Observed* cm^{-1}
Q38	668.91
40	669.07
42	669.27
54	670.46
56	670.68

These line positions have been fitted by the following equation:

$$\nu = 667.40 + (B'-B'')J(J+1) + (D'-D'')J^2(J+1)^2$$

The resulting band constants are:

$$B'-B'' = (10.17 \pm .10) \times 10^{-4} \text{ cm}^{-1}$$

$$D'-D'' = (.32 \pm .30) \times 10^{-8} \text{ cm}^{-1}$$

*These frequencies were determined relative to the position of R branch lines $J'' = 2,4$ as determined by Blau, etc.[3]

Table 4

Equivalent Widths of All Lines Measured

		ℓ = 1.133 cm T = 300°K			ℓ = 5.08 cm T = 300°K			ℓ = 25.17 cm T = 300°K		
Line	ν(cm^{-1})	No. of Runs	Corrected W^o (cm^{-1} atm^{-1})	Est. Uncer-tainty	No. of Runs	Corrected W^o (cm^{-1} atm^{-1})	Est. Uncer-tainty	No. of Runs	Corrected W^o (cm^{-1} atm^{-1})	Est. Uncer-tainty
a2	665.84	4	.284	10%	5	.929	8%	3	1.95	7%
a4	664.29	4	.602	6%	5	1.57	6%	3	3.25	5%
b8	661.52							2	.845	10%
a8	661.18	4	.834	5%	3	2.12	6%	1	4.20	7%
b9	660.81							2	1.03	10%
b34 ++b35	641.65							1	1.34	15%
a34	641.35							1	2.89	15%
a50	629.46	1	.119	10%	1	.406	4%			
c13	628.91	1	.0677	10%	1	.310	5%	4	.761	3%
a52	627.99	2	.0984	6%	1	.326	5%	4	.754	3%

Table 4 Contd.

		ℓ = 1.133 cm T = 300°K			ℓ = 5.08 cm T = 300°K			ℓ = 25.17 cm T = 300°K		
Line	$\nu(cm^{-1})$	No. of Runs	Corrected W^o (cm^{-1} atm^{-1})	Est. Uncer-tainty	No. of Runs	Corrected W^o (cm^{-1} atm^{-1})	Est. Uncer-tainty	No. of Runs	Corrected W^o (cm^{-1} atm^{-1})	Est. Uncer-tainty
c11	627.38	2	.0634	9%	1	.294	7%	4	.748	3%
a54	626.51	2	.0728	7%	1	.281	5%	4	.631	4%
c9	625.83	2	.0626	9%	1	.283	7%	4	.747	3%
a56	625.05	2	.0525	9%	1	.205	10%	4	.487	4%
c7	612.56				2	.238	8%	3	.746	4%
c9	611.00				2	.262	7%	3	.771	4%
c11	609.42	3	.0735	9%	2	.276	7%	4	.756	5%
c13	607.84	3	.0743	9%	2	.280	7%	4	.784	5%
c15	606.27	3	.0726	9%	2	.295	7%	4	.822	6%
c17	604.70	3	.0680	9%	2	.282	7%	4	.789	6%
c19	603.13	3	.0619	9%	2	.277	7%	4	.765	6%
c21	601.56	3	.0583	9%	2	.259	7%	5	.747	5%
c23	599.98	3	.0626	9%	2	.258	7%	5	.681	4%
c25	598.40	3	.0568	9%	2	.224	7%	4	.572	5%

Table 5

Pressures and Path Lengths Used in Study of CO_2

P (atmos) ↓	1.133	5.08	25.17 ← ℓ(cm)
.198	1		
.135	1		
.129	1		
.06	1		
.1322		1	
.0658		1	
.0255			1
.99	2		
.197		2	
.068			2
.053			2
.997	3		
1.00		3	
.790		3	
1.00			3
.285			3
.198			3

Region 1: 661 - 666 cm^{-1}

" 2: 624.5 - 629 cm^{-1}

" 3: 598 - 613 cm^{-1}

Table 6

Results of Corrected Direct Measurements and "Curve of Growth" Method for the 598 - 613 cm^{-1} Region

		Corrected Direct Measurements					"Curve of Growth" Method				
Line	$\nu(cm^{-1})$	No. of Runs	S^o (cm^{-2} atm^{-1})	Est. Uncer-tainty	γ^o (cm^{-1} atm^{-1})	Est. Uncer-tainty	No. of Runs	S^o (cm^{-2} atm^{-1})	Est. Uncer-tainty	γ^o (cm^{-1} atm^{-1})	Est. Uncer-tainty
c7	612.56	2	.0572	12%	.118	25%	5	.0559	6%	.117	17%
c9	611.00	2	.0612	12%	.108	25%	5	.0651	6%	.100	17%
c11	609.42	5	.0663	10%	.119	20%	9	.0702	5%	.097	15%
c13	607.84	5	.0677	10%	.112	20%	9	.0726	5%	.099	15%
c15	606.27	5	.0698	10%	.115	20%	9	.0735	5%	.100	15%
c17	604.70	5	.0681	10%	.113	20%	9	.0702	5%	.100	15%
c19	603.13	5	.0632	10%	.107	20%	9	.0665	5%	.100	15%
c21	601.56	5	.0583	10%	.108	20%	10	.0634	5%	.097	17%
c23	599.98	5	.0602	10%	.116	20%	10	.0588	5%	.097	17%
c25	598.40	5	.0515	10%	.115	20%	9	.0530	5%	.095	17%

Table 7

Data Obtained from Wilson and Wells Method on Q Branches

Q Branch	ν cm^{-1}	P atmos.	ℓ cm	$\frac{\sum(-\ln T_i)\Delta\nu_i}{P\ell}$	Estimated Uncertainty
FQ	597.29	1.000	5.08	.0673	10%
		.790	5.08	.0682	10%
		.997	1.133	.0715	10%
CQ + line c1	618.03	.998	1.133	1.63	5%
		.995	1.133	1.57	5%
		.528	1.133	1.74	5%

Table 8

$S^{o}\gamma^{o}$ Products Determined for Lines a2, 4 and 8

Line	ν cm^{-1}	$S^{o}\gamma^{o}$ (cm^{-3} atm^{-2})	Estimated Uncertainty
a2	665.84	.042	10%
a4	664.29	.110	10%
a3	661.18	.187	15%

Table 9

Ratios of "b" Line Strengths to "a" Line Strengths

"b" line	S^{o} b line / S^{o} a8	S^{o} b line / S^{o} a34	Estimated Uncertainty
b8	.0475		15%
b9	.0623		15%
b34		.085	20%
b35		.077	20%

Table 10

S^{o} and γ^{o} for Individual Lines Determined in this Study

Line	$\nu(cm^{-1})$	S^{o} in $cm^{-2}atm^{-1}$ at 300°K	Est. of Uncer-tainty	γ^{o} in $cm^{-1}atm^{-1}$ at 300°K	Est. of Uncer-tainty
a50	629.46	.143	7%	.06	9%
c13	628.91	.0750	7%	.11	9%
a52	627.99	.101	7%	.06	9%
c11	627.38	.0695	7%	.11	9%
a54	626.51	.0704	7%	.06	9%
c9	625.83	.0613	7%	.11	9%
a56	625.05	.0481	7%	.06	9%
c7	612.56	.0565	3%	.111	15%
c9	611.00	.0627	3%	.108	15%
c11	609.42	.0682	3%	.105	12%
c13	607.84	.0712	3%	.104	10%
c15	606.27	.0715	3%	.103	10%
c17	604.70	.0692	3%	.103	10%
c19	603.13	.0656	3%	.103	10%
c21	601.56	.0614	3%	.102	10%
c23	599.98	.0568	3%	.101	12%
c25	598.40	.0522	3%	.099	15%

Table 11

Measured Values of Q Branch Strength

Isotope	Transition	Letter Notation	ν cm^{-1}	S^o of Q Branch (cm^{-2} atm^{-1}) Weak Absorption Method	Wilson and Wells Method	Elsasser Band Method	Est. of Uncertainty
$O^{18}C^{12}O^{16}$	01'0 - 000		662.39			0.50	35%
$C^{13}O_2^{16}$	01'0 - 000	A	648.52			1.07	25%
$C^{12}O_2^{16}$	03'0 - 02°0	K	647.02			0.52	30%
$C^{12}O_2^{16}$	02°0 - 01'0	C	618.03		$(1.90 - S_{c1}^{o})$		7%
$C^{12}O_2^{16}$	03'0 - 02²0	F	597.29		.0725		12%
$C^{12}O_2^{16}$	03'0 - 100	G	544.26	.050			10%

Table 12

Band Strengths and Vibrational Transition Probabilities

Isotope	Transition	Letter Notation	ν cm^{-1}	Choice of ζ	$S_{\nu'}^{\nu''}$(300°K) (cm^{-2} atm^{-1})	Est. of Uncertainty	|R| in Debyes: Present Study	|R| in Debyes: Benedict's Calc. Values	|R| in Debyes: Other Investigations
$C^{12}O_2^{16}$	$01'0-000$	A	667.40	0	196	7%	.181	.1794	.189 **
"	" "	A	"	+.0016	234	7%	.216	"	
"	" "	A	"	+.0035	289	7%	.266	"	
"	$02^00-01'0$	C	618.03	+.0035	4.27	3%	.138	.1394	
"	$02^20-01'0$	B	667.76	0 (for A band)	16.3	16%	.26	.2496	
"	" "	B	"	+.0016 (for A band)	19.4	16%	.31	"	
"	" "	B	"	+.0035 (for A band)	24.0	16%	.38	"	
"	$03'0-02^20$	F	597.29		.143	12%	.128	.1425	
"	$03'0-02^00$	K	647.02		1.03	30%	.291	.2229	
"	$03'0-100$	G	544.26		.0040	10%	.026	.0428	
$C^{13}O_2^{16}$	$01'0-000$	*	648.52		2.13	25%	.184		
$O^{18}C^{12}O^{16}$	$01'0-000$		662.39		1.00	35%	.29		

Table 12 Contd.

Isotope	Transition	Letter Notation	ν cm^{-1}	Choice of J	$S^{v'}_{v''}(300°K)$ $(cm^{-2}\ atm^{-1})$	Est. of Uncertainty	|R| in Debyes: Present Study	Benedict's Calc. Values	Other Investigations
$C^{12}O_2^{16}$	$11'0-02^20$		741.7					.1039	.108 **
"	12^20-03^30		756.9					.1000	.111 **
"	$11'0-02^00$		791.5					.0281	.0370*
"	$12^20-03'0$		828					.0190	.0255*
"	13^30-04^20		857					.00889	.0241*
"	14^40-05^30		864					.00620	.0146*

** L. D. Kaplan and D. F. Eggers

* H. J. Kostkowski

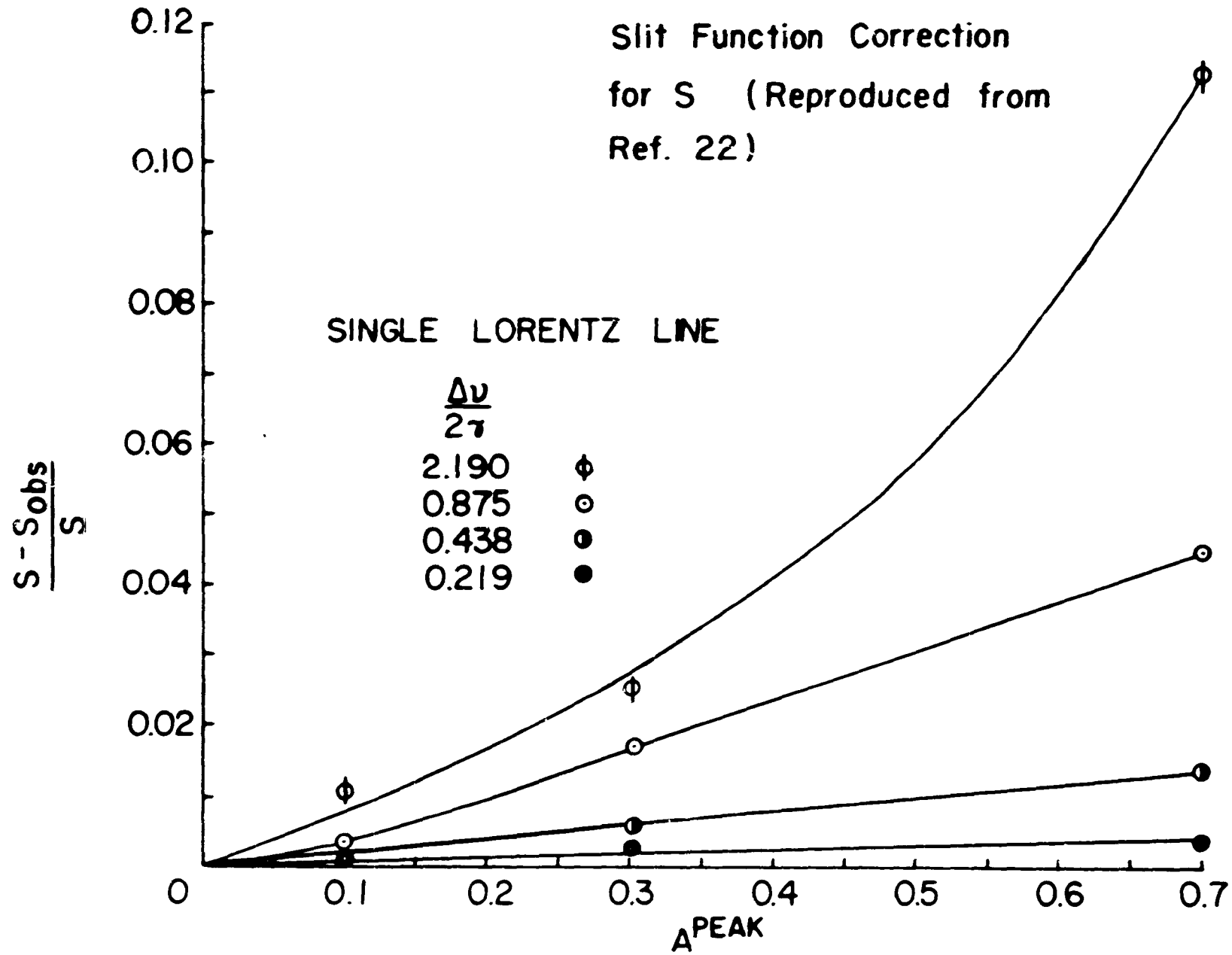
Slit Function Correction for S (Reproduced from Ref. 22)
SINGLE LORENTZ LINE
$\frac{\Delta\nu}{2\pi}$
2.190 ϕ
0.875 ⊙
0.438 ◐
0.219 ●
$\frac{S - S_{obs}}{S}$
0.12
0.10
0.08
0.06
0.04
0.02
0
0.1
0.2
0.3
0.4
0.5
0.6
0.7
A^{PEAK}

FIG. 1

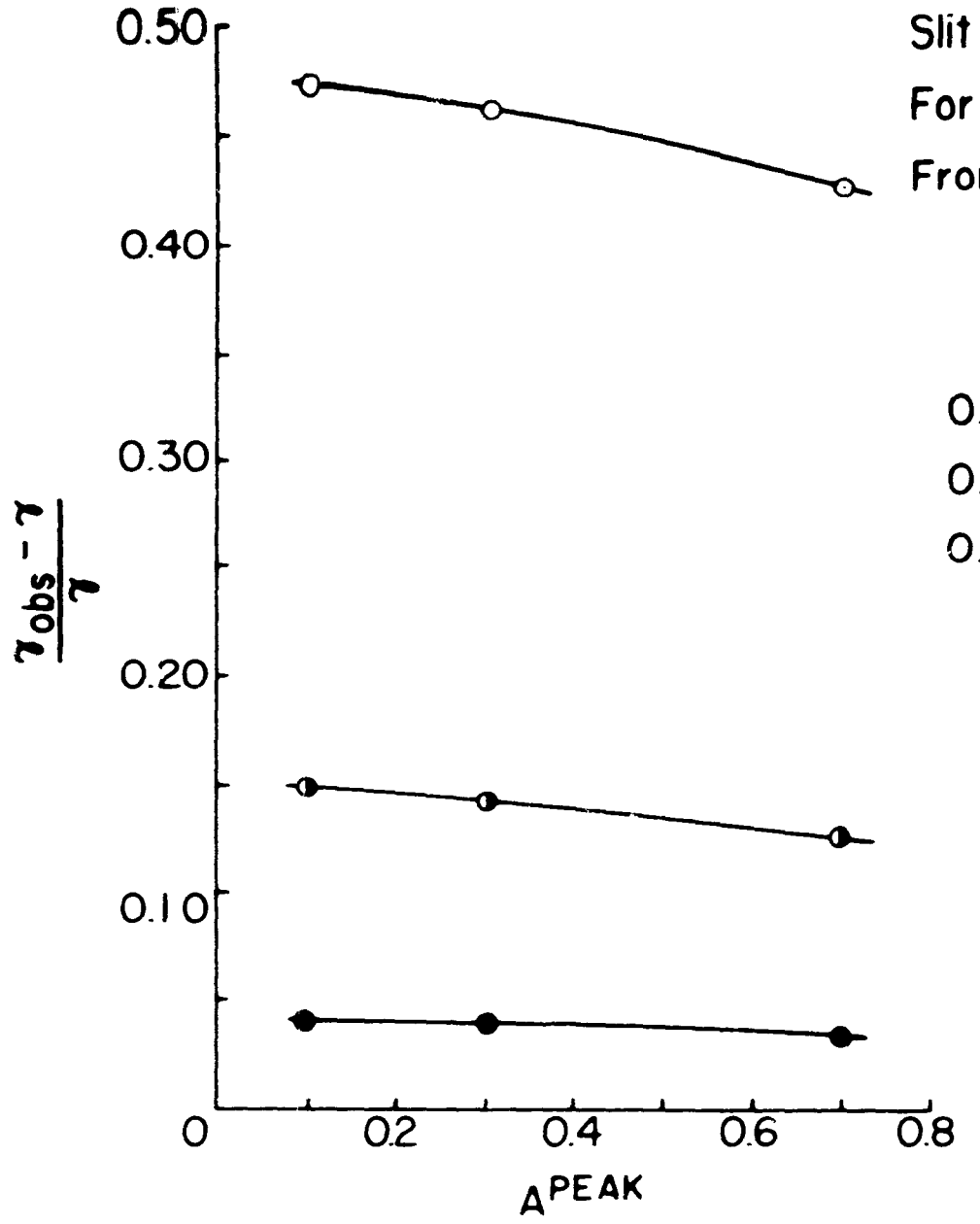
0.50
0.40
0.30
0.20
0.10
0
0.2
0.4
0.6
0.8
$\frac{\gamma_{obs} - \gamma}{\gamma}$
A^{PEAK}
Slit Function Correction
For γ (Reproduced
From Ref. 22)
$\frac{\Delta\nu}{2\gamma}$
0.875
0.438
0.219

FIG. 2

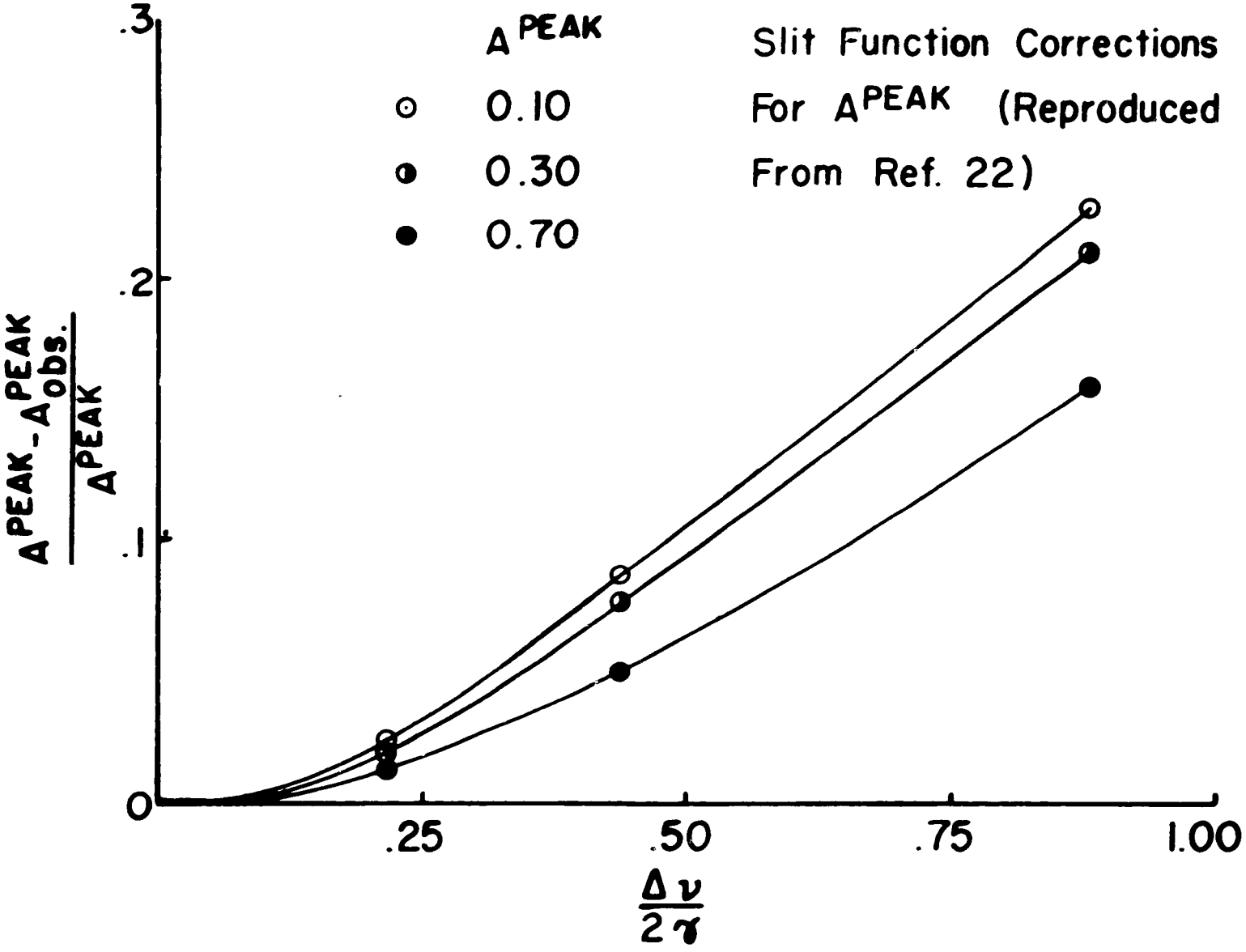
A^{PEAK}
0.10
0.30
0.70
Slit Function Corrections For A^{PEAK} (Reproduced From Ref. 22)
$\frac{A^{PEAK} - A^{PEAK}_{obs.}}{A^{PEAK}}$
.3
.2
.1
0
.25
.50
.75
1.00
$\frac{\Delta\nu}{2\gamma}$

FIG. 3

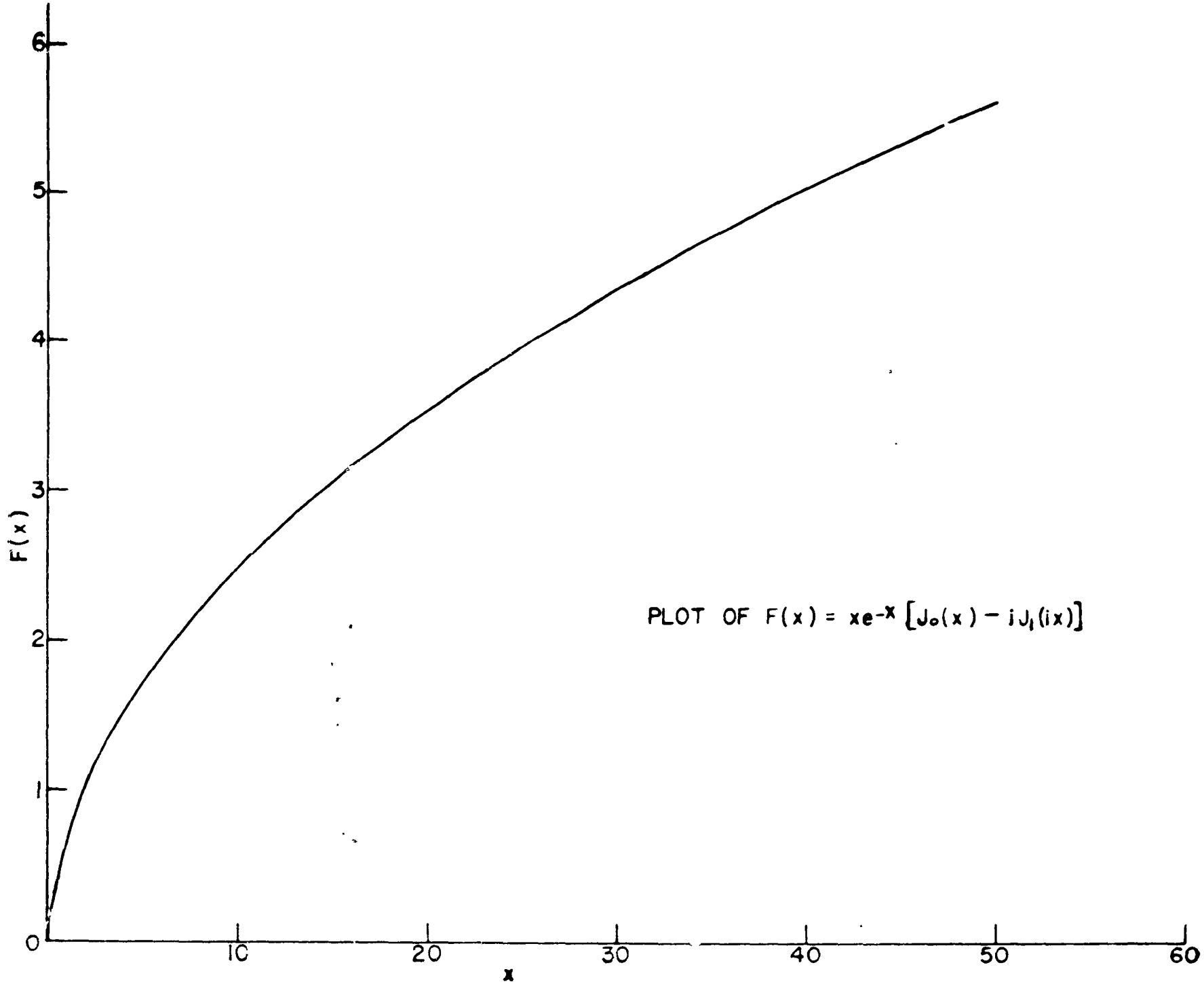

PLOT OF $F(x) = xe^{-x}\left[J_0(x) - iJ_1(ix)\right]$

FIG 4

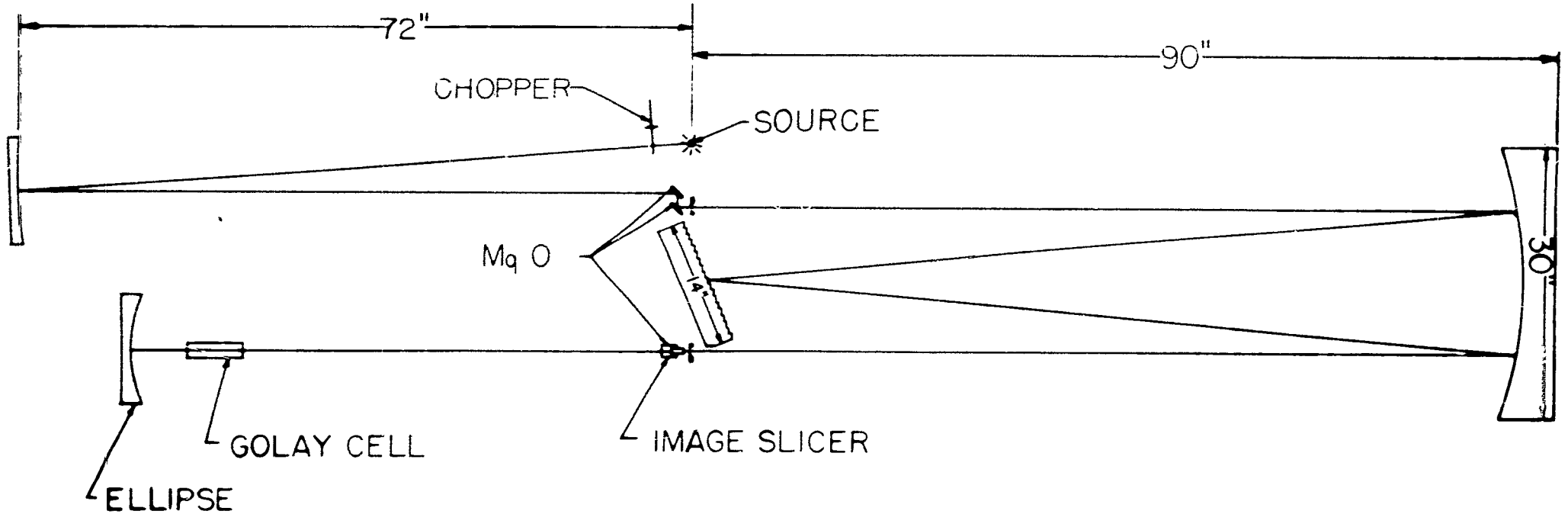
72"
90"
CHOPPER
SOURCE
Mq O
14"
30"
GOLAY CELL
IMAGE SLICER
ELLIPSE

FIG. 5

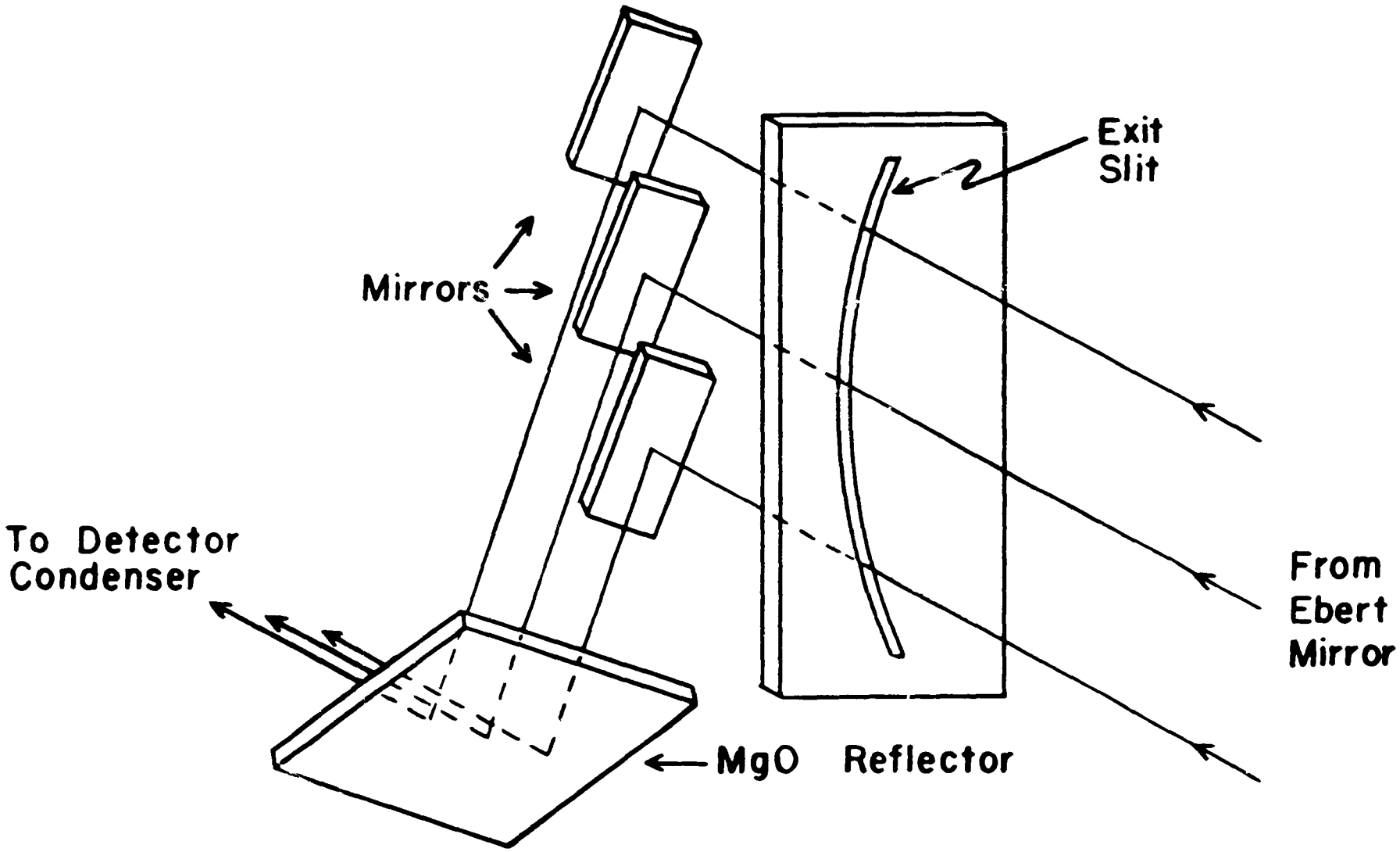

EXIT SLIT IMAGE SLICER
FIG. 6

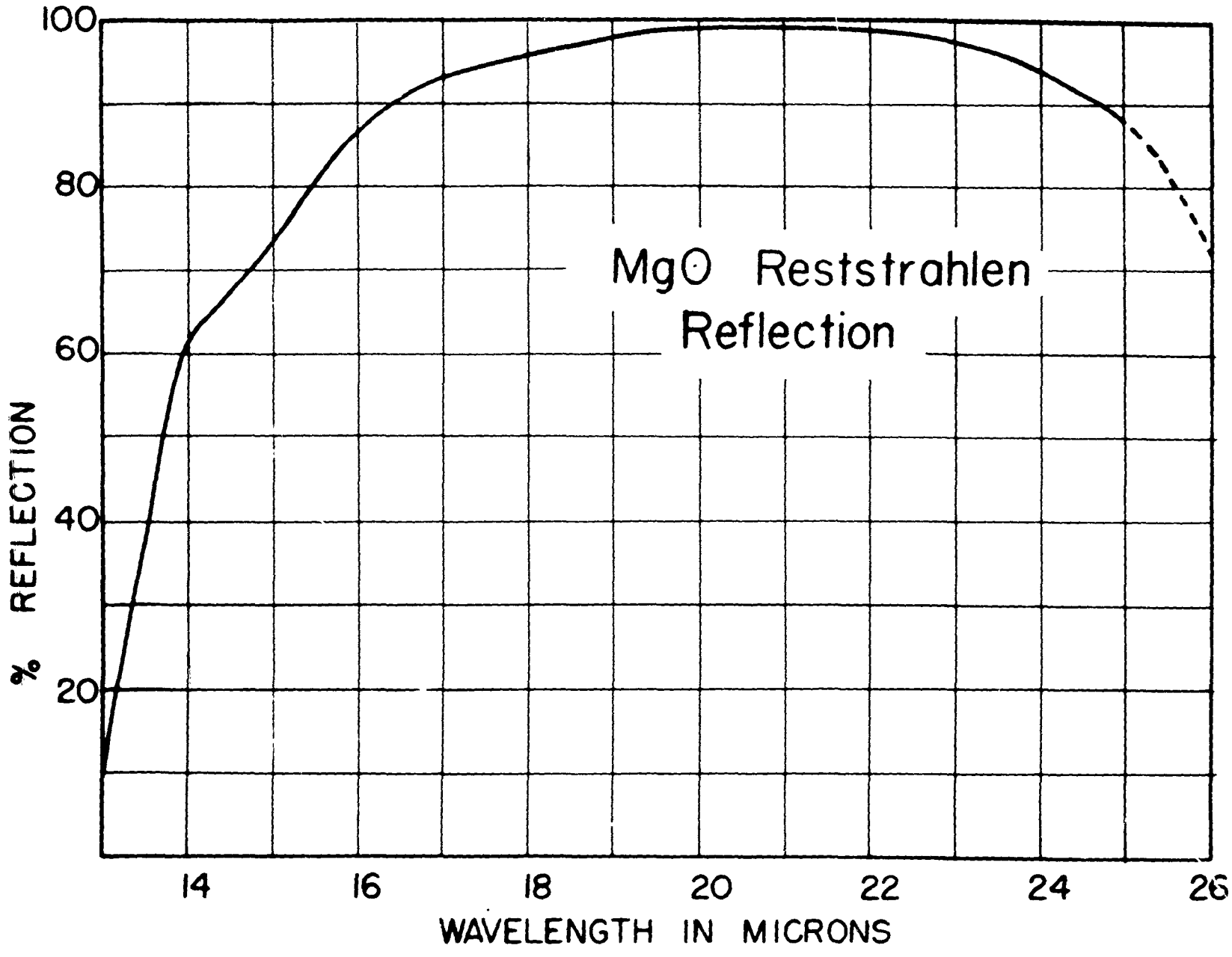
100
80
60
40
20
% REFLECTION
MgO Reststrahlen
Reflection
14
16
18
20
22
24
26
WAVELENGTH IN MICRONS

FIG. 7

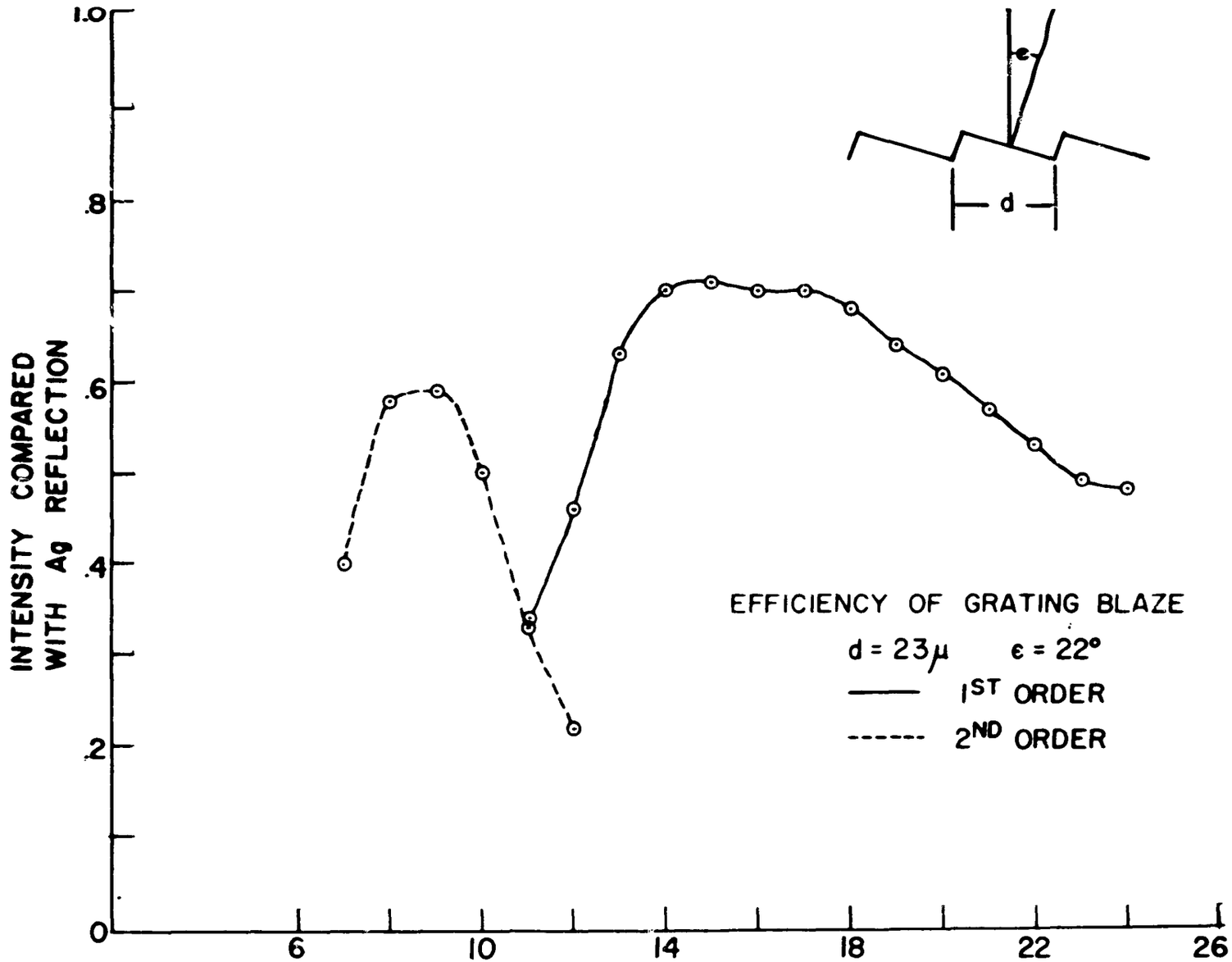
1.0
.8
.6
.4
.2
0
INTENSITY COMPARED WITH Ag REFLECTION
6
10
14
18
22
26
WAVELENGTH IN MICRONS
ε
d
EFFICIENCY OF GRATING BLAZE
d = 23μ ε = 22°
1ST ORDER
2ND ORDER

FIG. 8

Figure 9

Figure 10

Caption for Figure 11

This instrument is used to facilitate the alignment of the Ebert system as follows:

A plane mirror with a central hole is mounted on a hollow cylinder. An eight-point suspension restricts this cylinder to rotational freedom alone. (The bearings are indicated in Figure 11 by "cross" marks.) As a preliminary step the plane mirror is made perpendicular (by autocollimation) to the axis of rotation of the cylinder and the instrument is then positioned in the Ebert optical system as shown in the figure. Cross hairs mounted inside the cylinder are illuminated from the side arm, and, when viewed as indicated in Figure 11, the planes of the object and image cross hairs are brought into coincidence by moving the cross hairs forward or back from the Ebert mirror until they lie in the focal plane of the Ebert mirror. The rotation axis of the alignment instrument is then made parallel to the optic axis of the Ebert mirror by adjusting either the Ebert mirror or the position of the alignment instrument until there is no relative motion between the cross hairs and their image when the cylinder is rotated. A microscope mounted on an arm fixed to the cylinder may then be used to critically adjust the position, curvature and focus of the slit jaws.

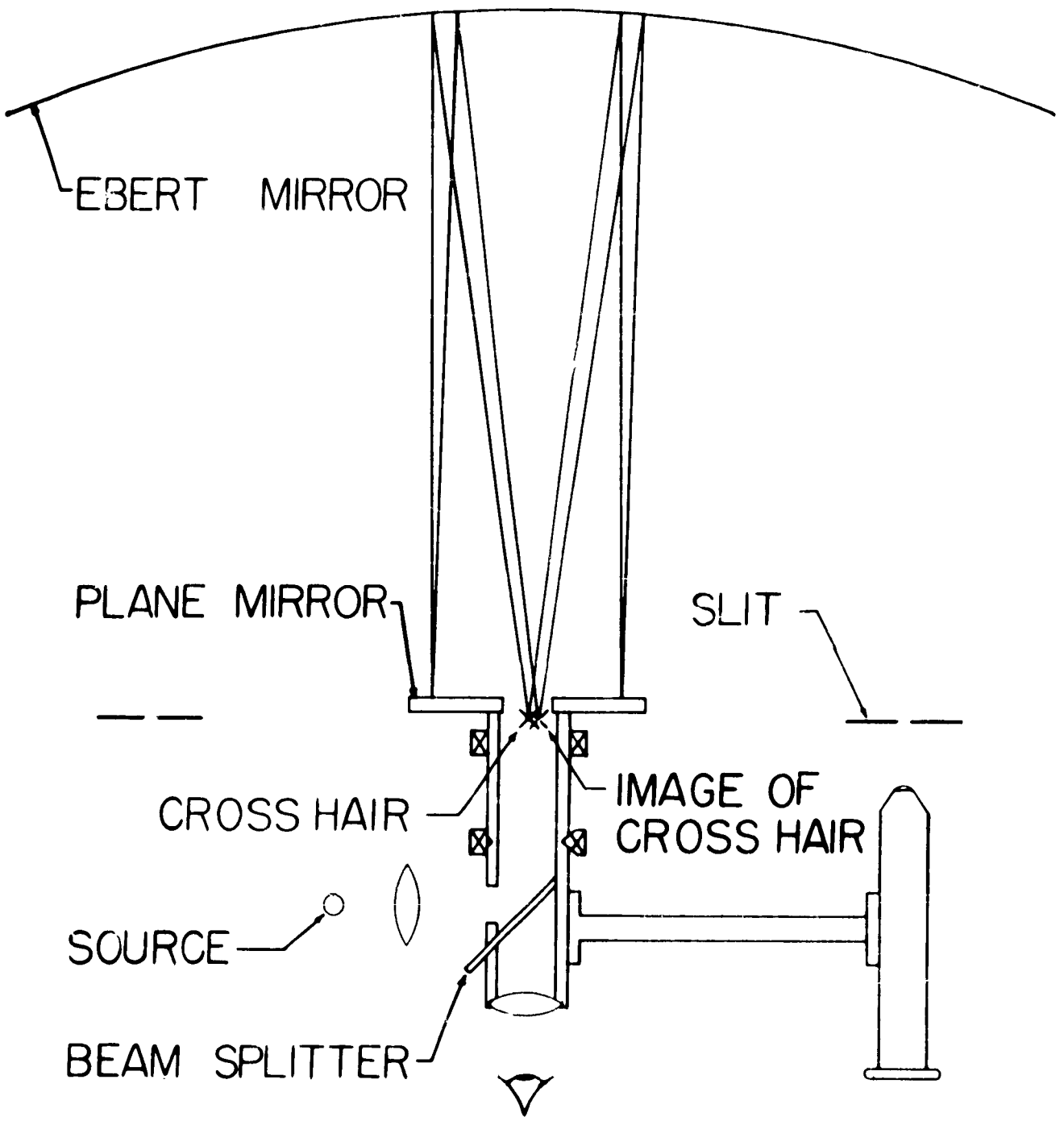

SLIT ALIGNMENT INSTRUMENT

FIG. 11

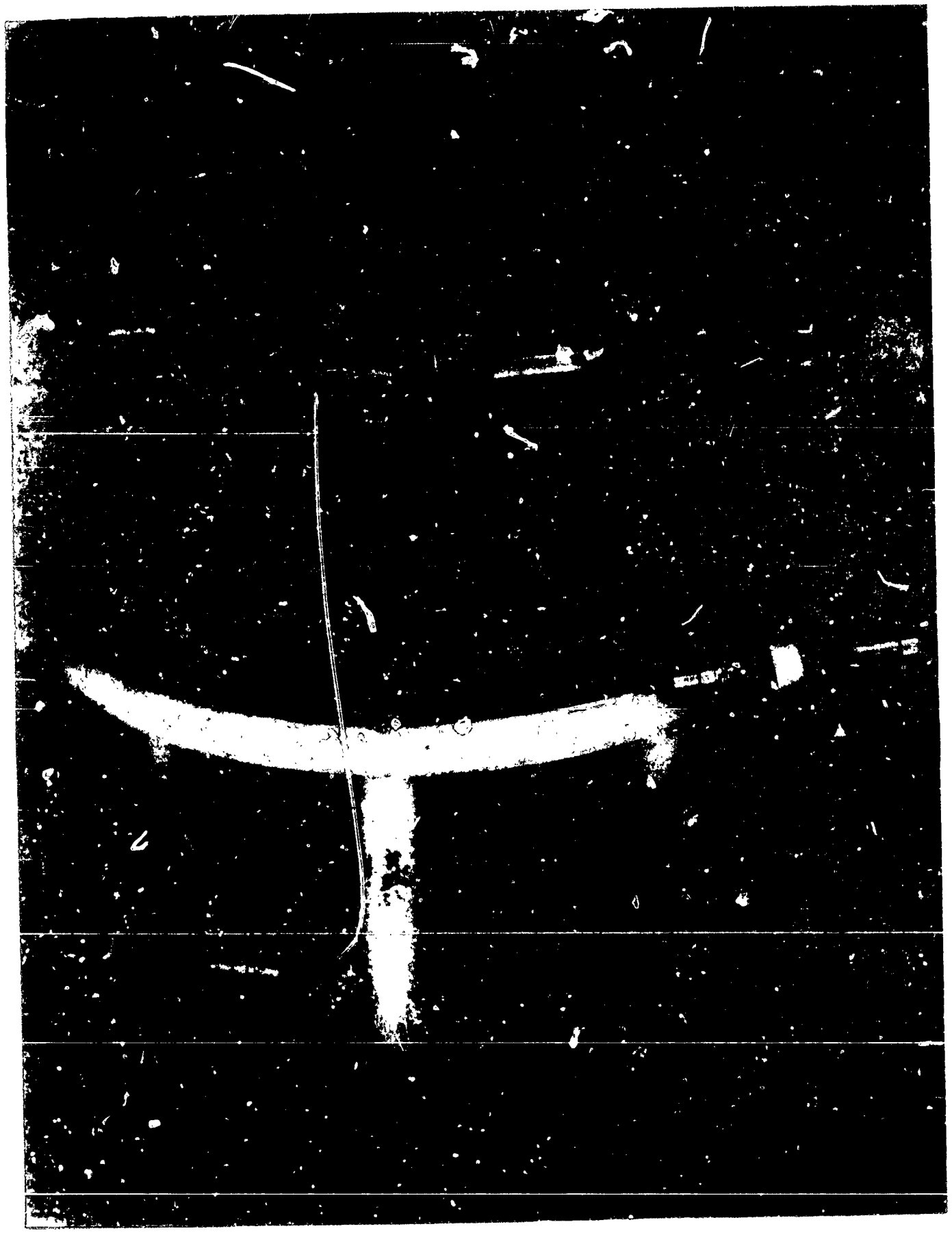

Figure 12

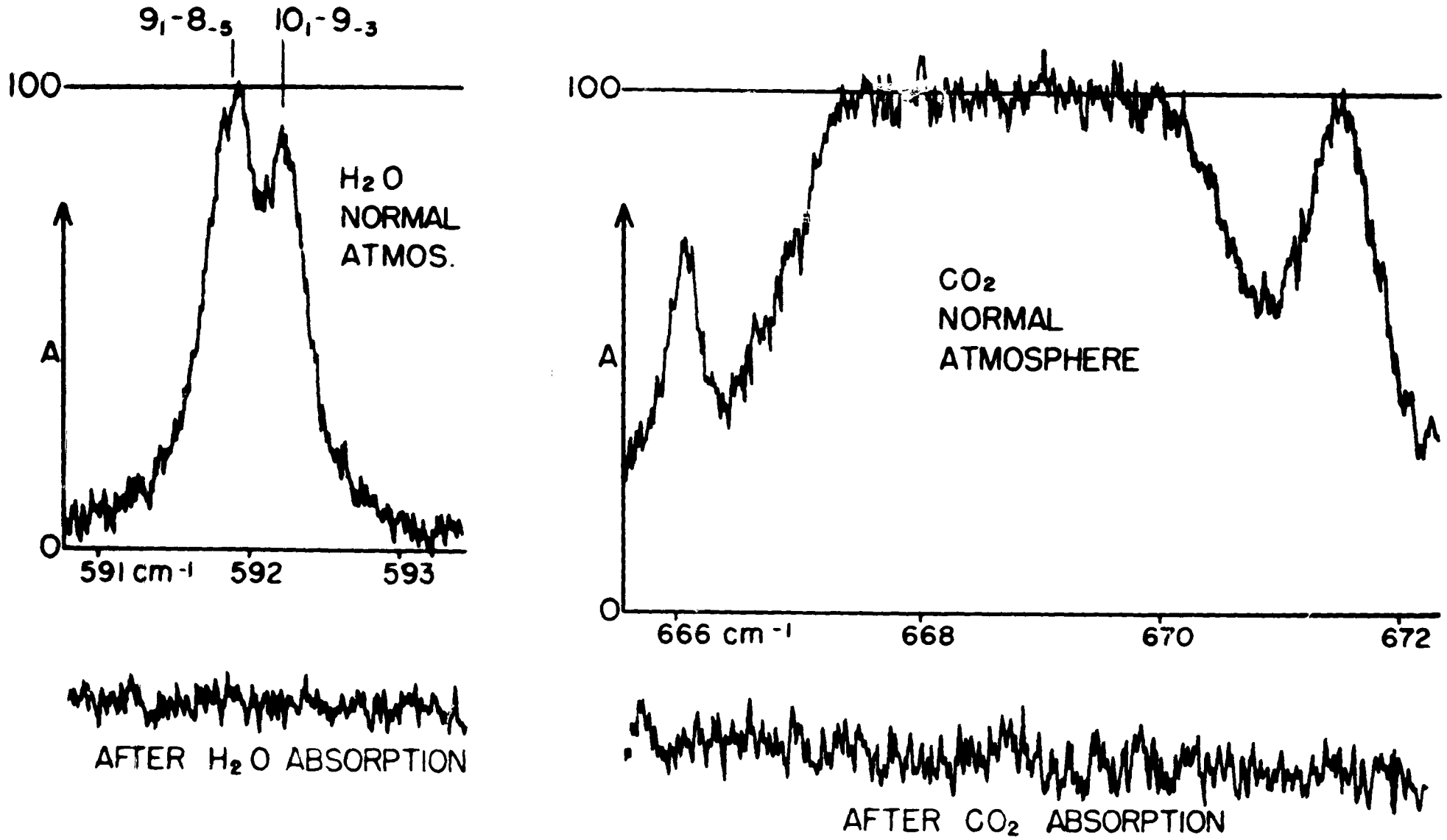
9₁-8₋₅
10₁-9₋₃
100
H₂O
NORMAL
ATMOS.
A
0
591 cm⁻¹
592
593
AFTER H₂O ABSORPTION
100
CO₂
NORMAL
ATMOSPHERE
A
0
666 cm⁻¹
668
670
672
AFTER CO₂ ABSORPTION

FIG. 13

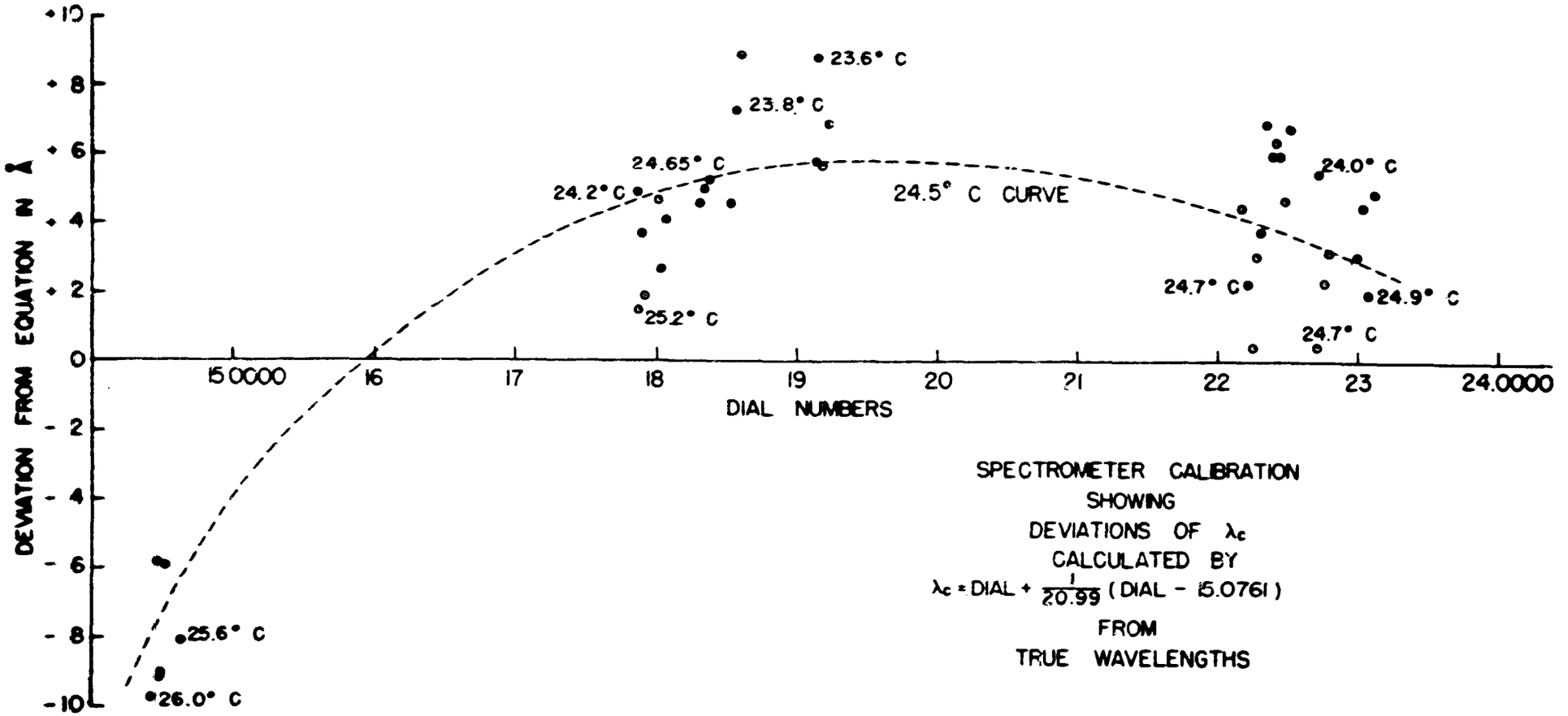
DEVIATION FROM EQUATION IN Å
+10
+8
+6
+4
+2
0
-2
-4
-6
-8
-10
15.0000
16
17
18
19
20
21
22
23
24.0000
DIAL NUMBERS
23.6° C
23.8° C
24.65° C
24.2° C
24.5° C CURVE
24.0° C
24.7° C
24.9° C
25.2° C
24.7° C
25.6° C
26.0° C
SPECTROMETER CALIBRATION
SHOWING
DEVIATIONS OF λc
CALCULATED BY
λc = DIAL + 1/20.99 (DIAL - 15.0761)
FROM
TRUE WAVELENGTHS

FIG. 14

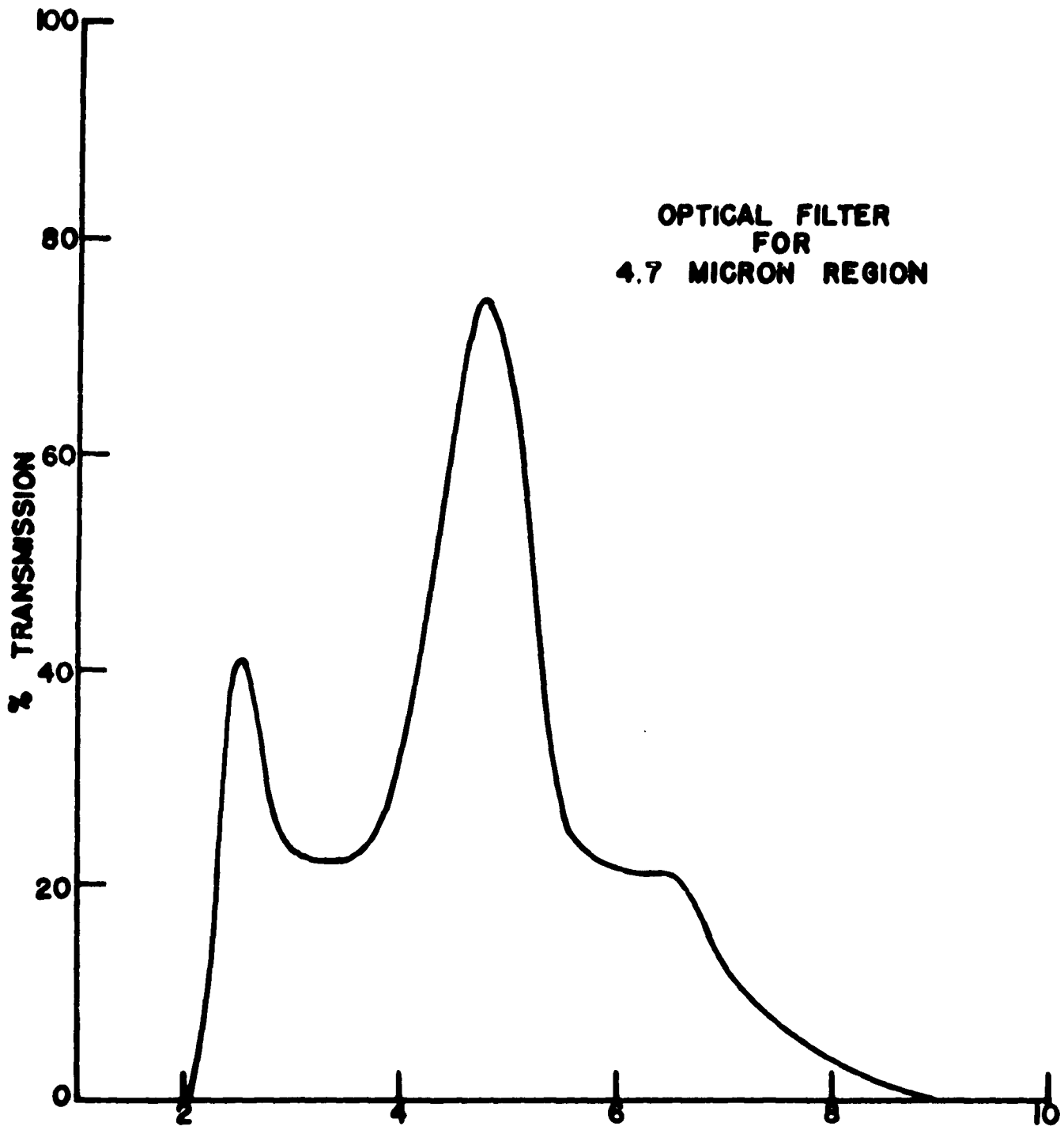
OPTICAL FILTER
FOR
4.7 MICRON REGION
100
80
60
40
20
0
% TRANSMISSION
2
4
6
8
10
WAVELENGTH IN MICRONS

FIG. 15

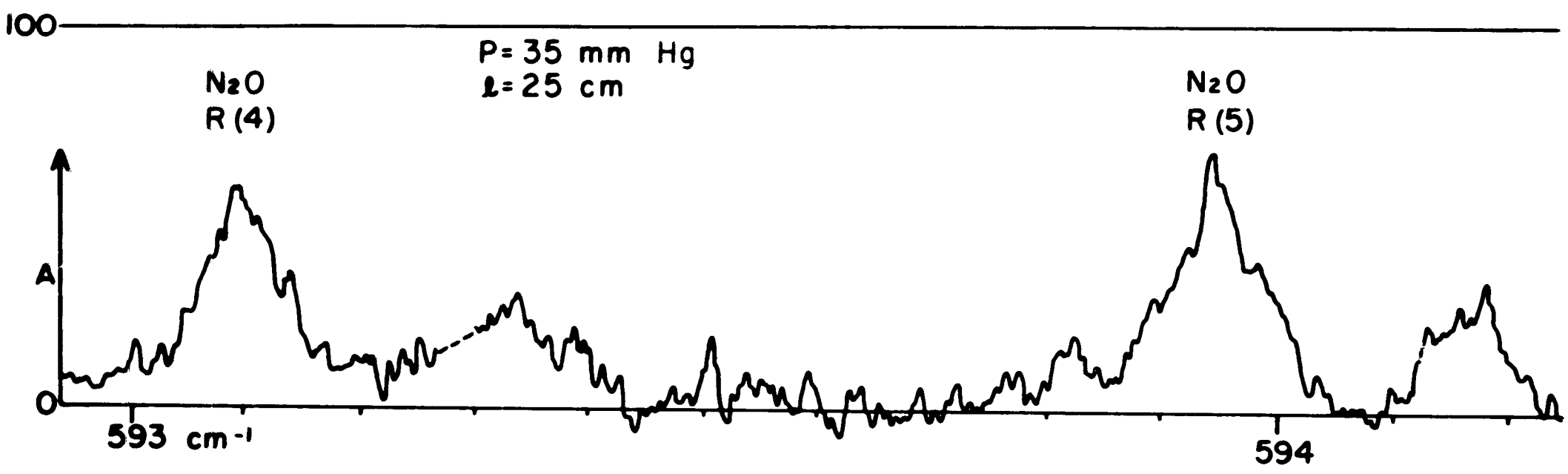

FIG. 16

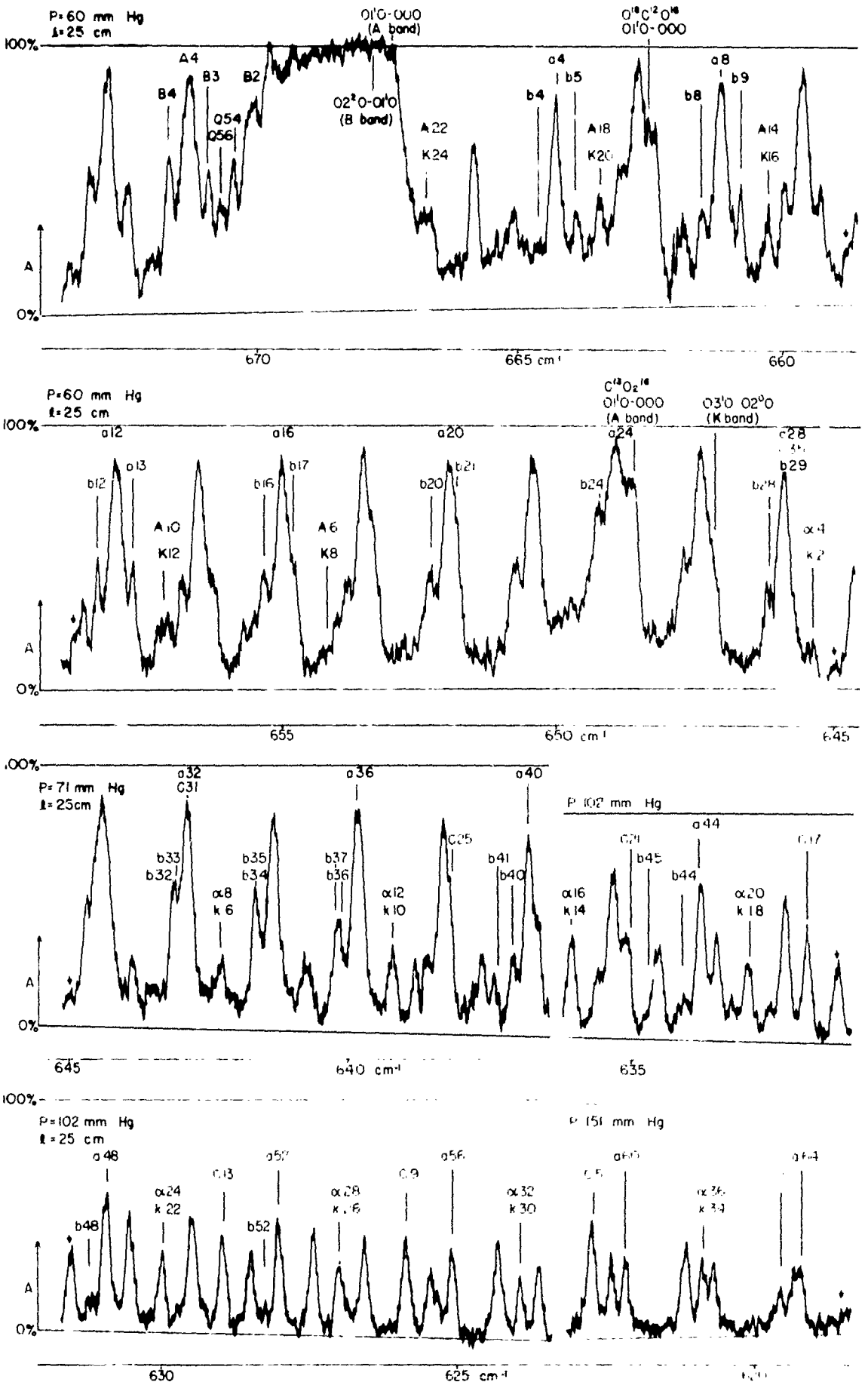
P=60 mm Hg
ℓ=25 cm
100%
0%
A
01'0-000
(A band)
$0^{18}C^{12}O^{16}$
01'0-000
$02^{2}0-01^{1}0$
(B band)
B4
A4
B3
B2
Q54
Q56
A22
K24
b4
a4
b5
A18
K20
b8
a8
b9
A14
K16
670
665 cm⁻¹
660
P=60 mm Hg
ℓ=25 cm
$C^{13}O_2{}^{16}$
01'0-000
(A band)
03'0 02⁰0
(K band)
a12
a16
a20
a24
a28
b12
a13
b16
b17
b20
b21
b24
b29
A10
K12
A6
K8
α4
K2
655
650 cm⁻¹
645
P=71 mm Hg
ℓ=25cm
a32
Q31
a36
a40
b33
b32
b35
b34
b37
b36
Q25
b41
b40
α8
k 6
α12
k 10
645
640 cm⁻¹
P 102 mm Hg
a44
Q29
b45
b44
Q17
α16
k 14
α20
k 18
635
P=102 mm Hg
ℓ=25 cm
a48
α24
k 22
Q13
a52
α28
Q9
a56
α32
k 30
b48
b52
630
625 cm⁻¹
P 151 mm Hg
Q5
α36
k 34

FIG. 17

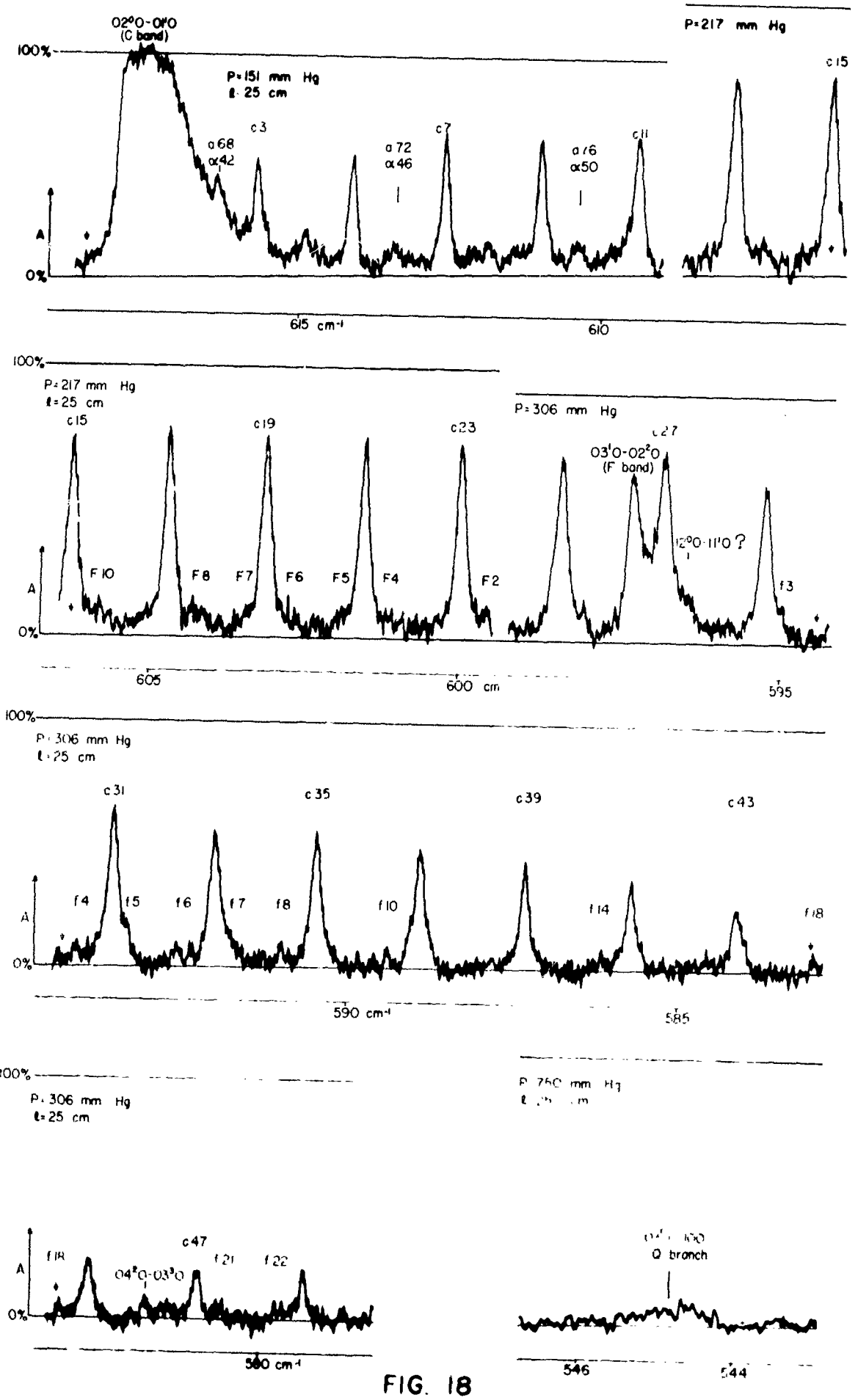
02°0-01'0
(C band)
100%
P=151 mm Hg
ℓ=25 cm
c3
c7
c11
c15
α68
α42
α72
α46
α76
α50
A
0%
615 cm-1
610
P=217 mm Hg
100%
P=217 mm Hg
ℓ=25 cm
c15
c19
c23
F10
F8
F7
F6
F5
F4
F2
A
0%
605
600 cm
P=306 mm Hg
c27
03'0-02°0
(F band)
12°0-11'0 ?
f3
595
100%
P=306 mm Hg
ℓ=25 cm
c31
c35
c39
c43
f4
f5
f6
f7
f8
f10
f14
f18
A
0%
590 cm-1
585
100%
P=306 mm Hg
ℓ=25 cm
f18
c47
f21
f22
04°0-03°0
A
0%
580 cm-1
Q branch
546
544

FIG. 18

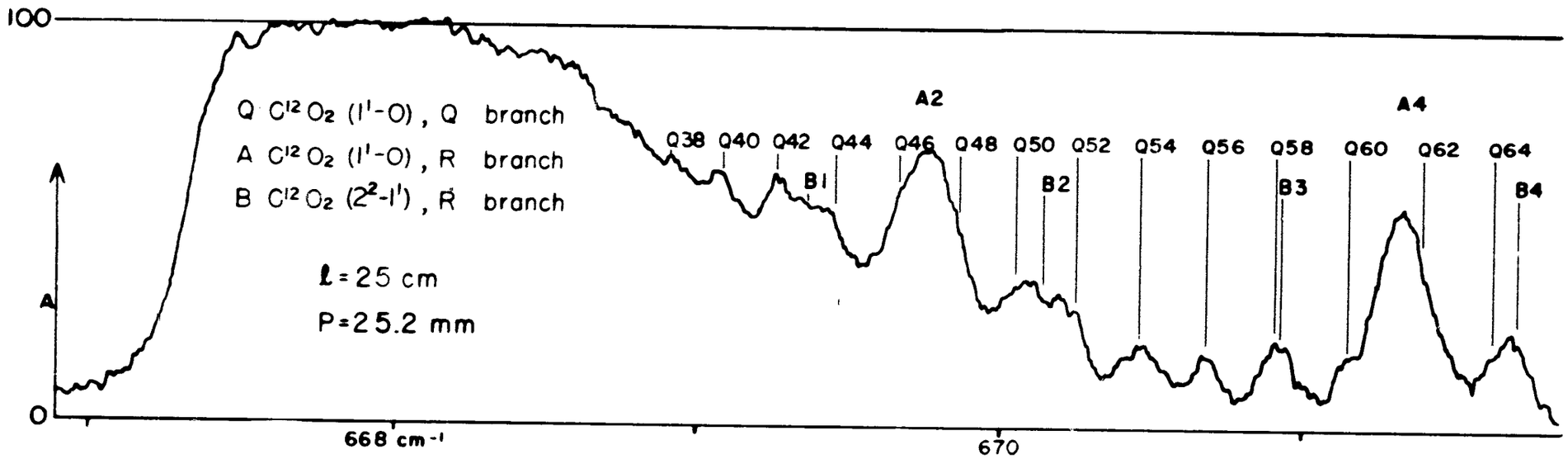
100
0
A
Q $C^{12}O_2$ (1^1-0) , Q branch
A $C^{12}O_2$ (1^1-0) , R branch
B $C^{12}O_2$ (2^2-1^1) , R branch
ℓ = 25 cm
P = 25.2 mm
Q38 Q40 Q42 Q44 Q46 Q48 Q50 Q52 Q54 Q56 Q58 Q60 Q62 Q64
B1
B2
B3
B4
A2
A4
668 cm-1
670

FIG. 19

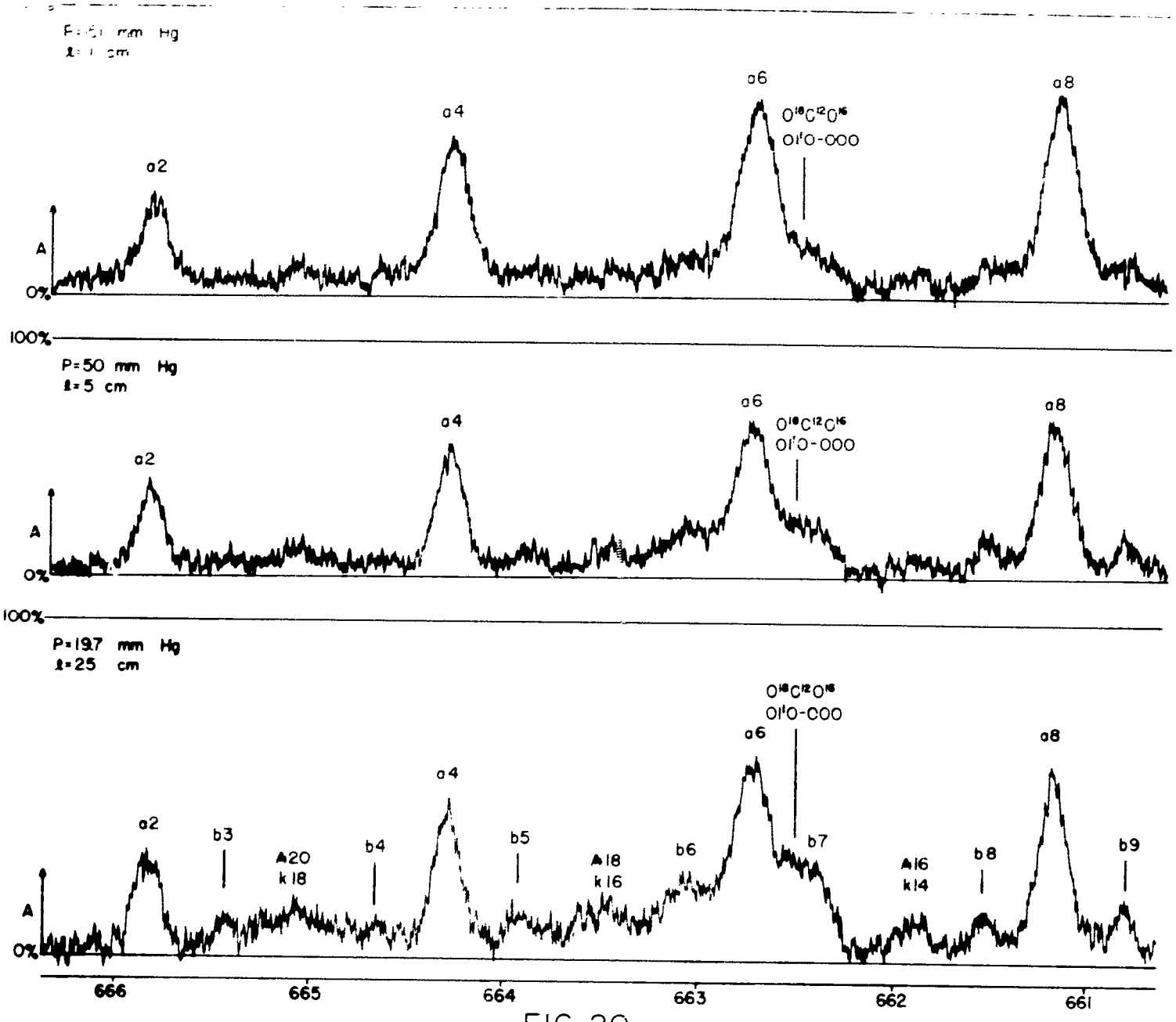
P=[illegible] mm Hg
ℓ=[illegible] cm
a2
a4
a6
a8
$O^{16}C^{12}O^{16}$
$01^{1}0-000$
A
0%
100%
P=50 mm Hg
ℓ=5 cm
a2
a4
a6
a8
$O^{16}C^{12}O^{16}$
$01^{1}0-000$
A
0%
100%
P=19.7 mm Hg
ℓ=25 cm
a2
b3
A20
k18
b4
a4
b5
A18
k16
b6
a6
$O^{16}C^{12}O^{16}$
$01^{1}0-000$
b7
A16
k14
b8
a8
b9
A
0%
666
665
664
663
662
661

FIG. 20

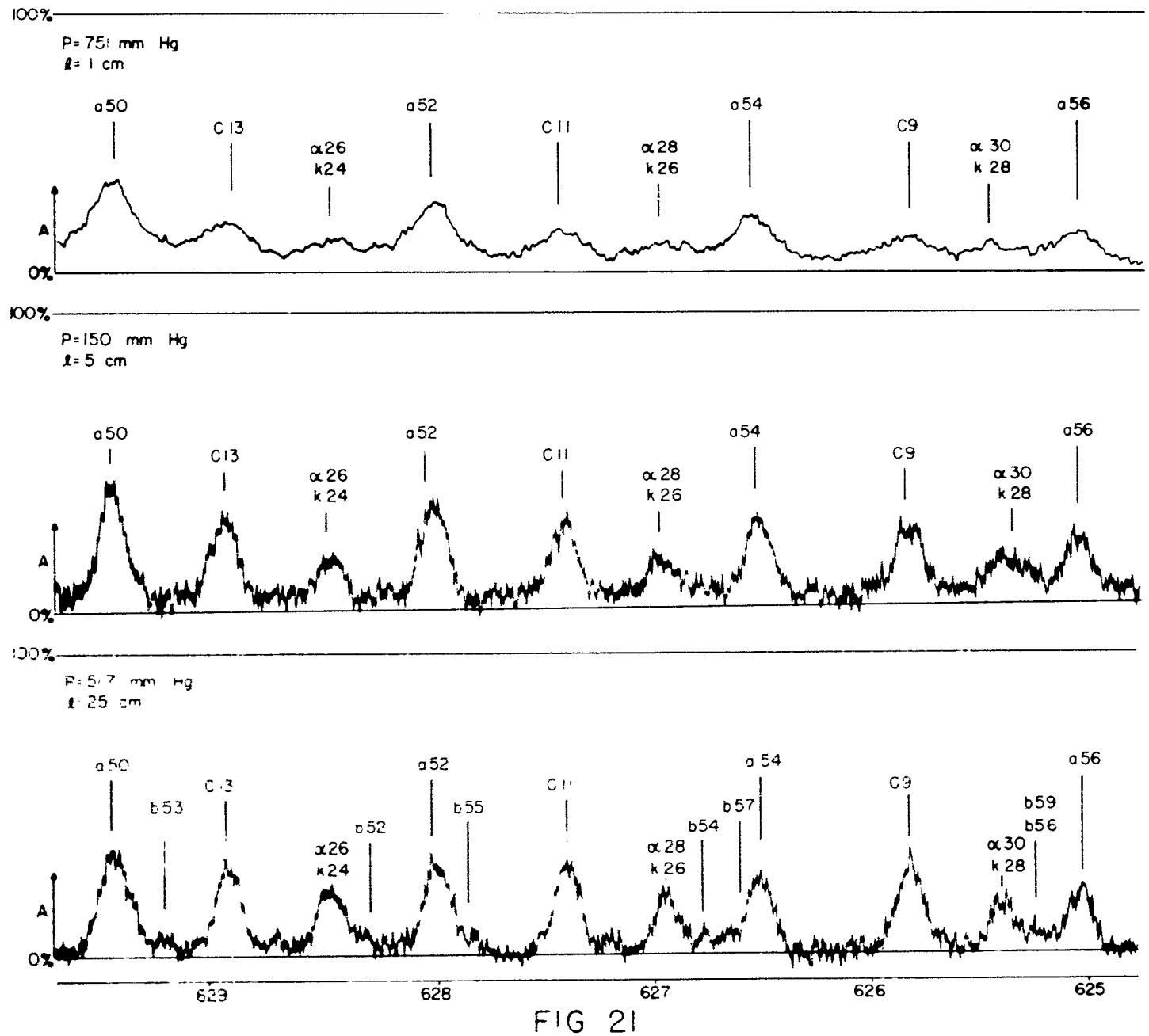
100%
P= 75 mm Hg
ℓ= 1 cm
α50
C13
α26
k24
α52
C11
α28
k26
α54
C9
α30
k28
α56
A
0%
100%
P=150 mm Hg
ℓ= 5 cm
α50
C13
α26
k24
α52
C11
α28
k26
α54
C9
α30
k28
α56
A
0%
100%
P= 5/7 mm Hg
ℓ= 25 cm
α50
b53
C13
α26
k24
b52
α52
b55
C11
α28
k26
b54
α54
b57
C9
b59
b56
α30
k28
α56
A
0%
629
628
627
626
625

FIG 21

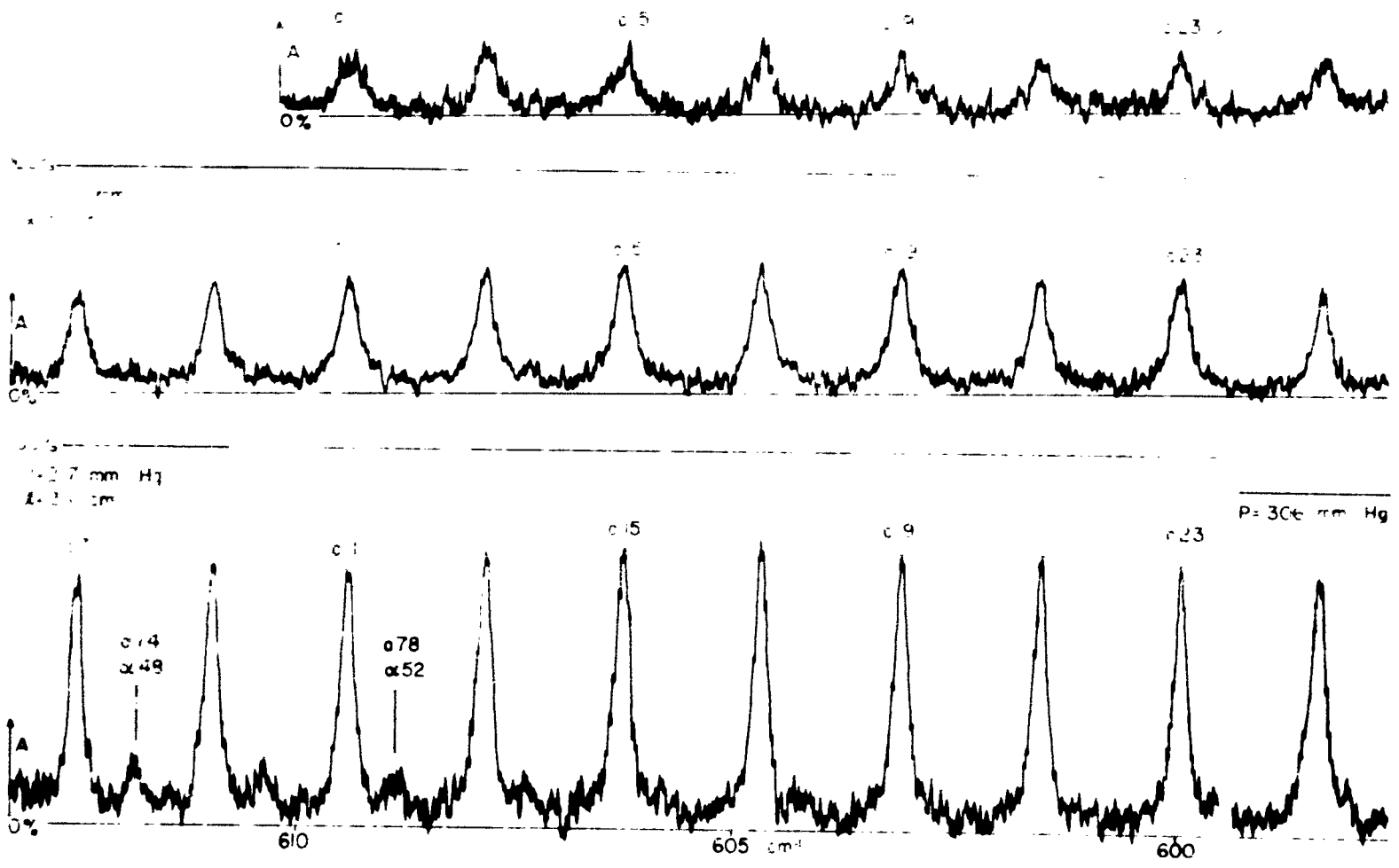

FIG 22

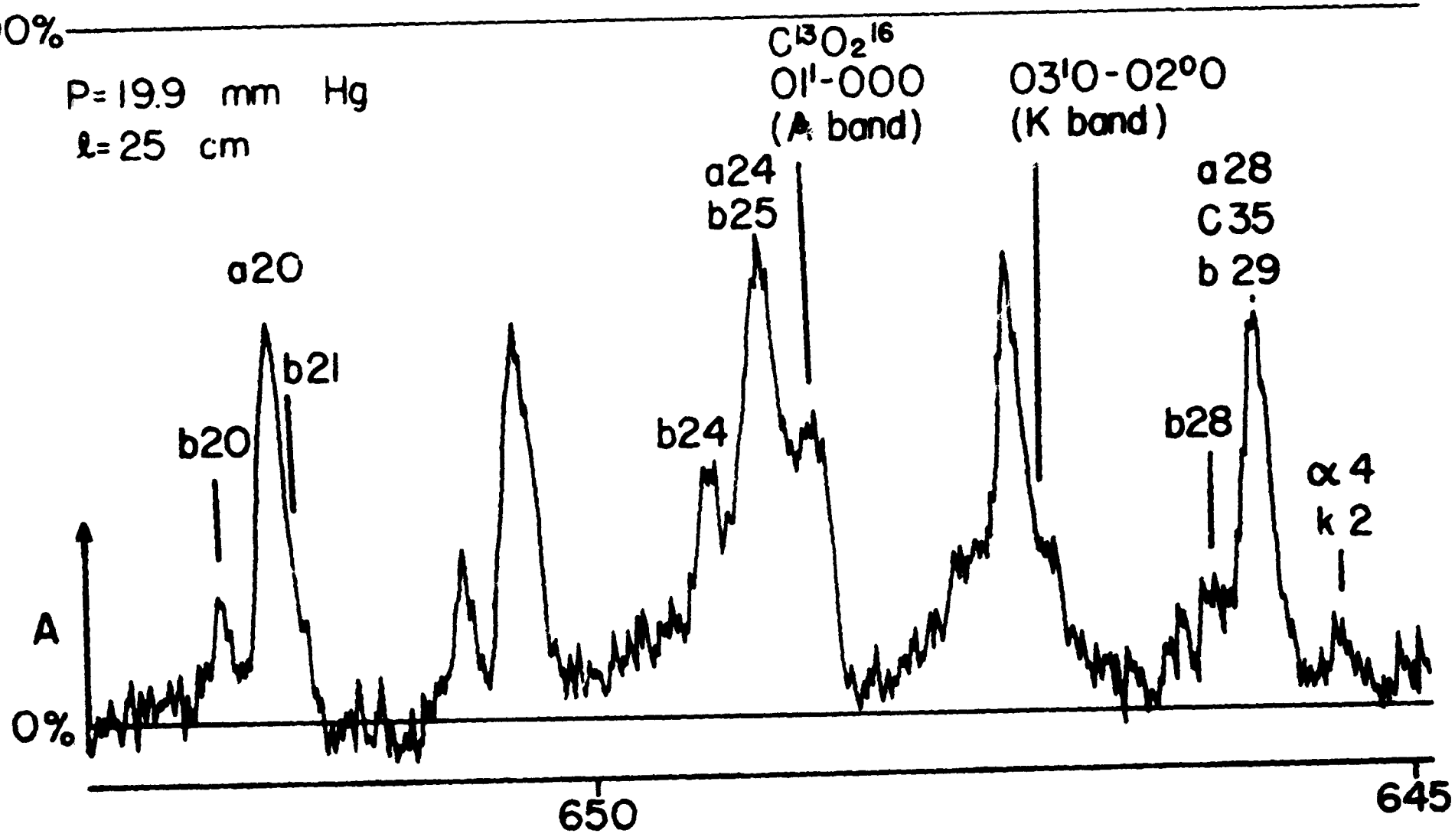
100%
P=19.9 mm Hg
ℓ=25 cm
$C^{13}O_2^{16}$
01¹-000
(A band)
03¹0-02⁰0
(K band)
a20
b21
b20
b24
a24
b25
a28
C35
b 29
b28
α 4
k 2
A
0%
650
645

FIG. 23

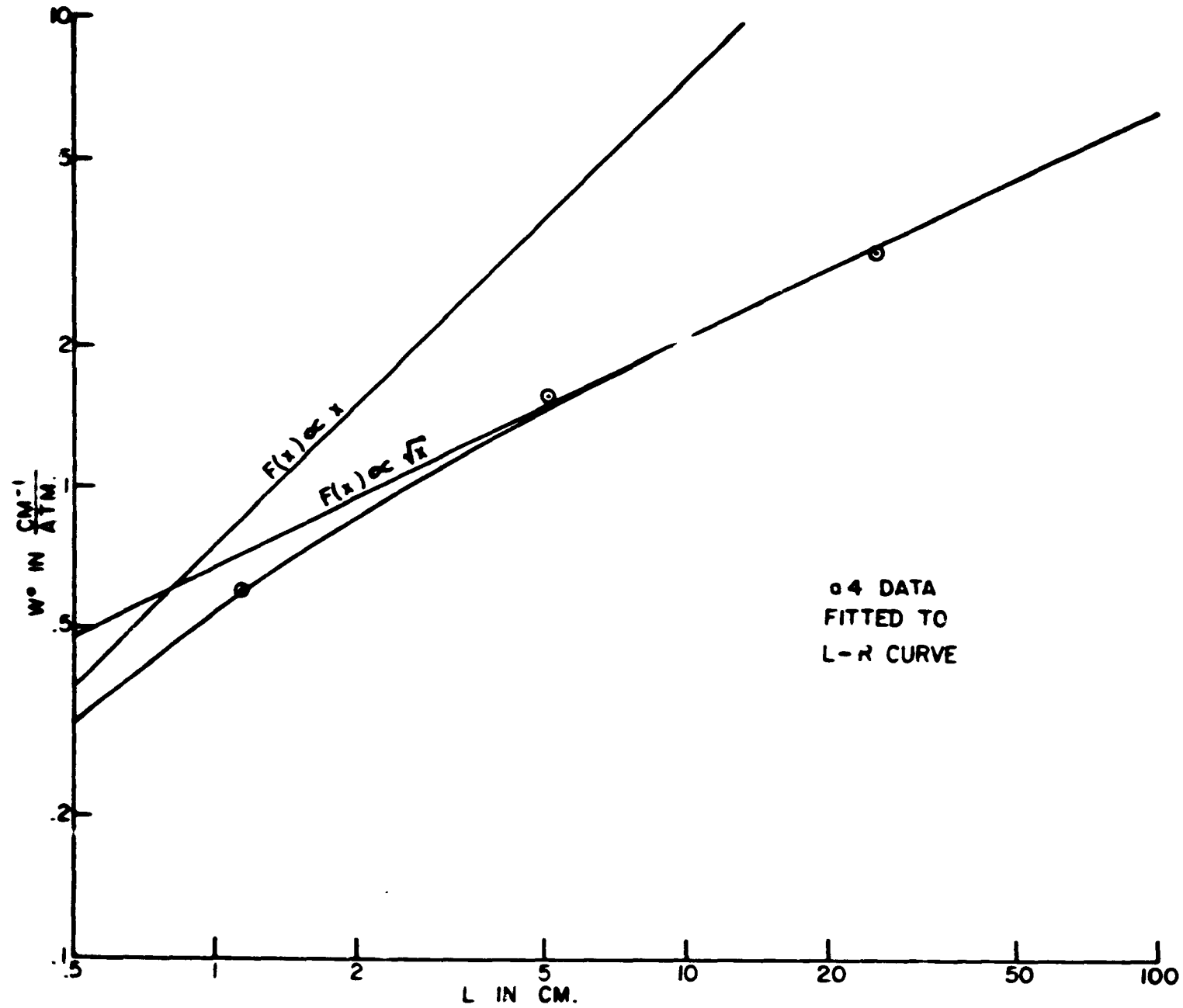
10
5
2
1
.5
.2
.1
W* IN CM⁻¹/ATM.
F(x)∝x
F(x)∝√x
α4 DATA
FITTED TO
L-R CURVE
.5
1
2
5
10
20
50
100
L IN CM.

FIG. 24

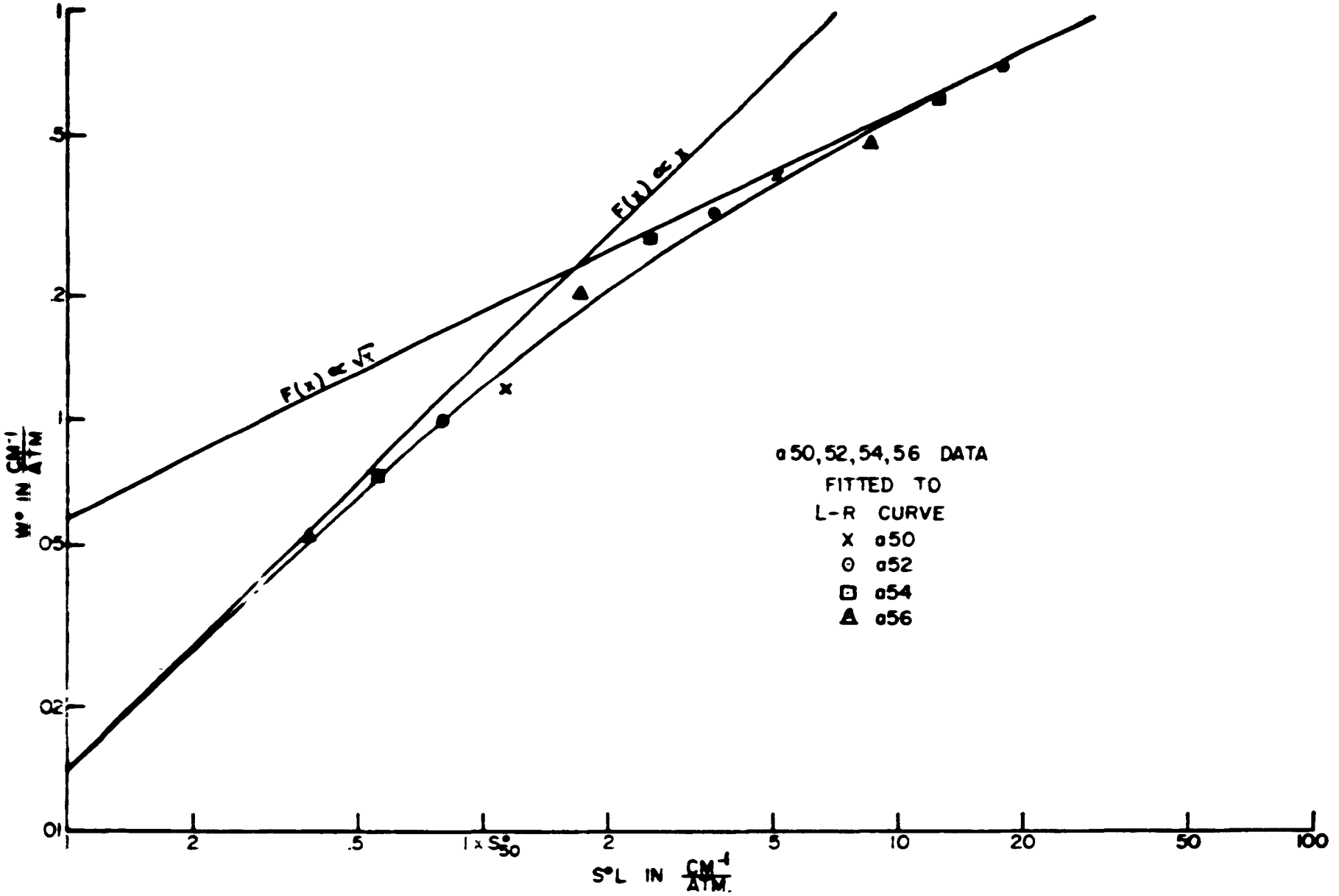
1
5
2
1
05
02
01
W° IN $\frac{CM^{-1}}{ATM}$
F(x) ∝ √x
F(x) ∝ x
1
2
.5
1 x S°50
2
5
10
20
50
100
S°L IN $\frac{CM^{-1}}{ATM.}$
a50,52,54,56 DATA
FITTED TO
L-R CURVE
X a50
⊙ a52
⊡ a54
▲ a56

FIG. 25

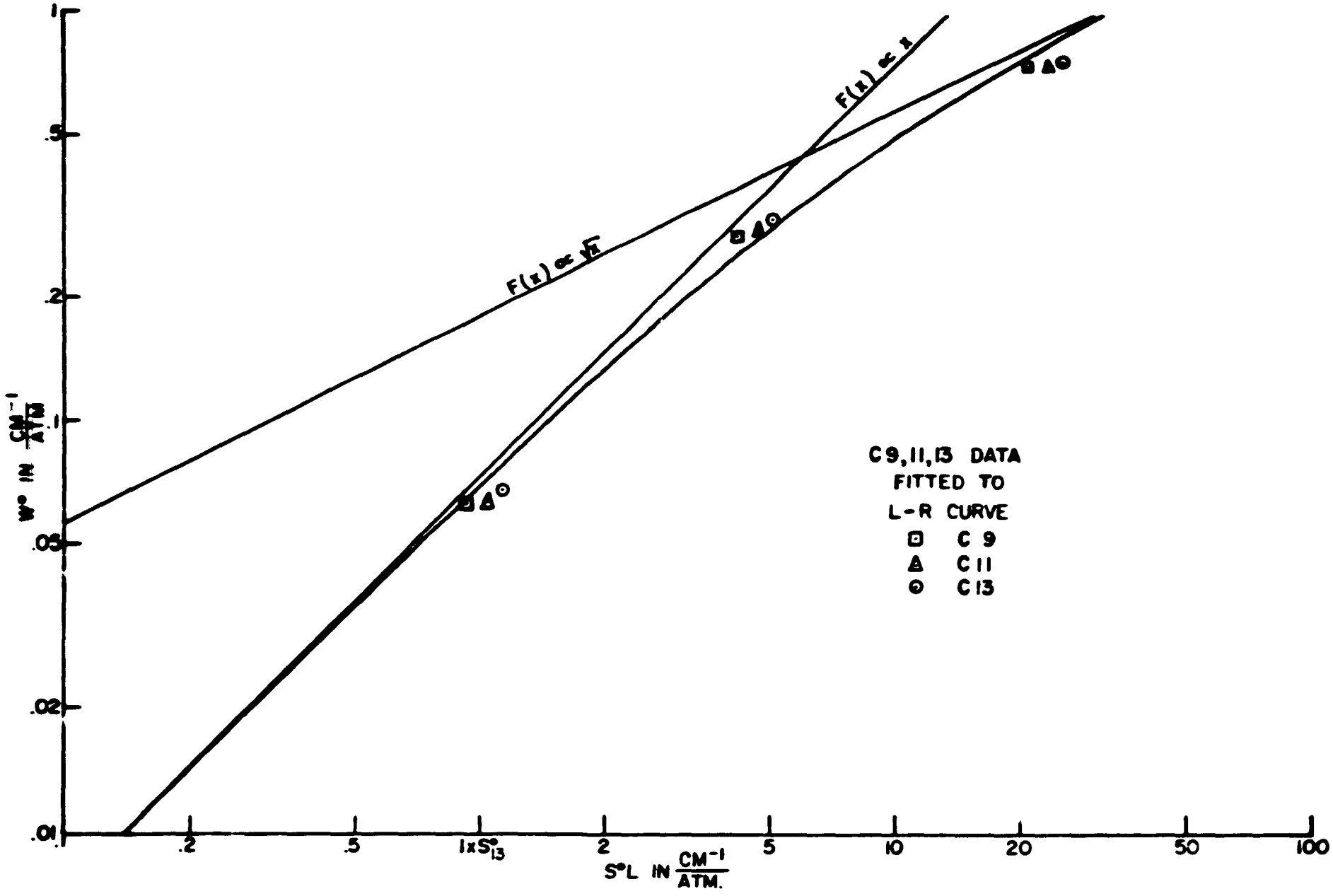
1
.5
.2
.1
.05
.02
.01
$\frac{1}{M^*}$ IN $\frac{CM^{-1}}{ATM}$
$F(x) \propto \sqrt{x}$
$F(x) \propto x$
□ ▲ ⊙
.2
.5
1xS°13
2
5
10
20
50
100
S°L IN $\frac{CM^{-1}}{ATM.}$
C9,11,13 DATA
FITTED TO
L-R CURVE
□ C 9
▲ C 11
⊙ C 13

FIG. 26

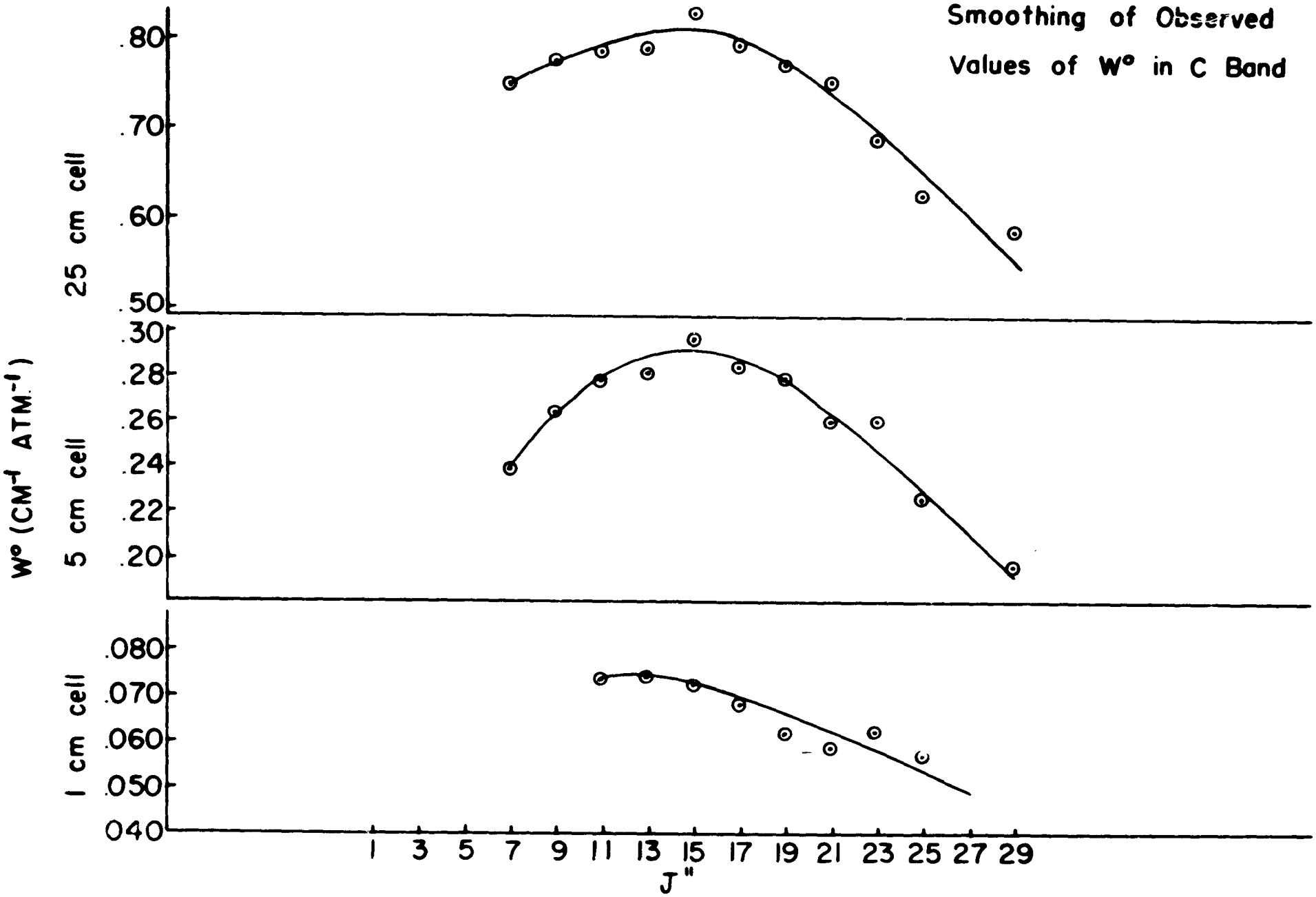
Smoothing of Observed
Values of W° in C Band
W° (CM⁻¹ ATM⁻¹)
25 cm cell
.80
.70
.60
.50
5 cm cell
.30
.28
.26
.24
.22
.20
1 cm cell
.080
.070
.060
.050
040
1 3 5 7 9 11 13 15 17 19 21 23 25 27 29
J"

FIG. 27

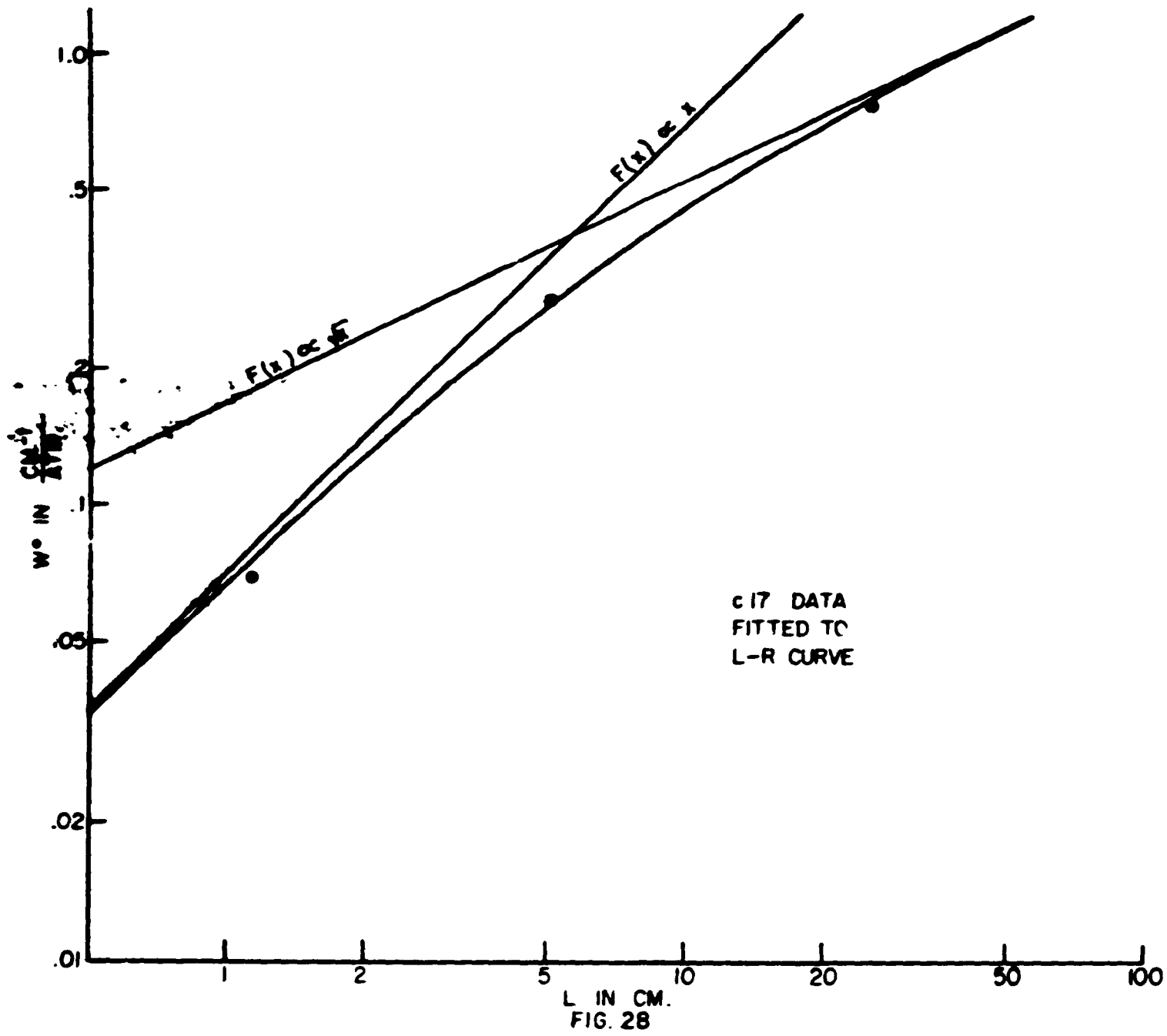

c 17 DATA
FITTED TO
L-R CURVE

FIG. 28

THIS
PAGE
IS
MISSING
IN
ORIGINAL
DOCUMENT

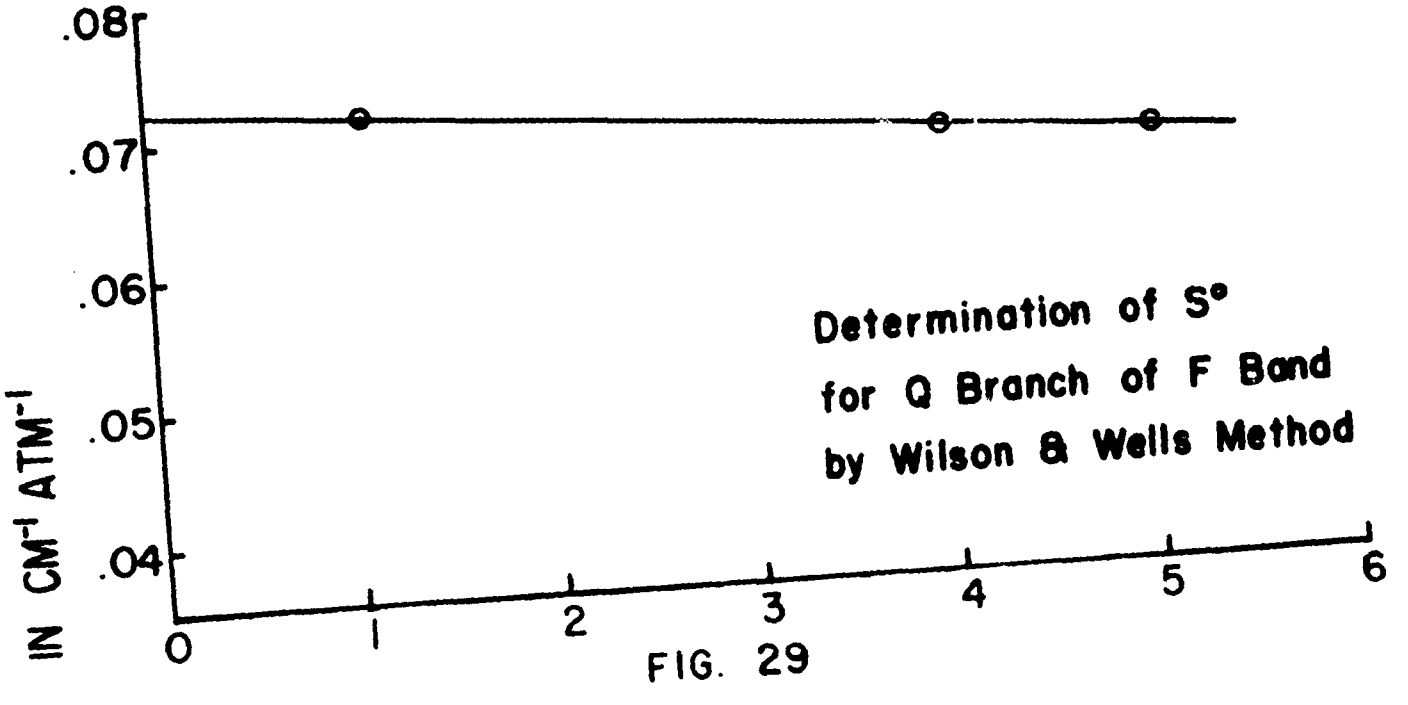
.08
.07
.06
.05
.04
IN CM⁻¹ ATM⁻¹
0
1
2
3
4
5
6
Determination of S°
for Q Branch of F Band
by Wilson & Wells Method

FIG. 29

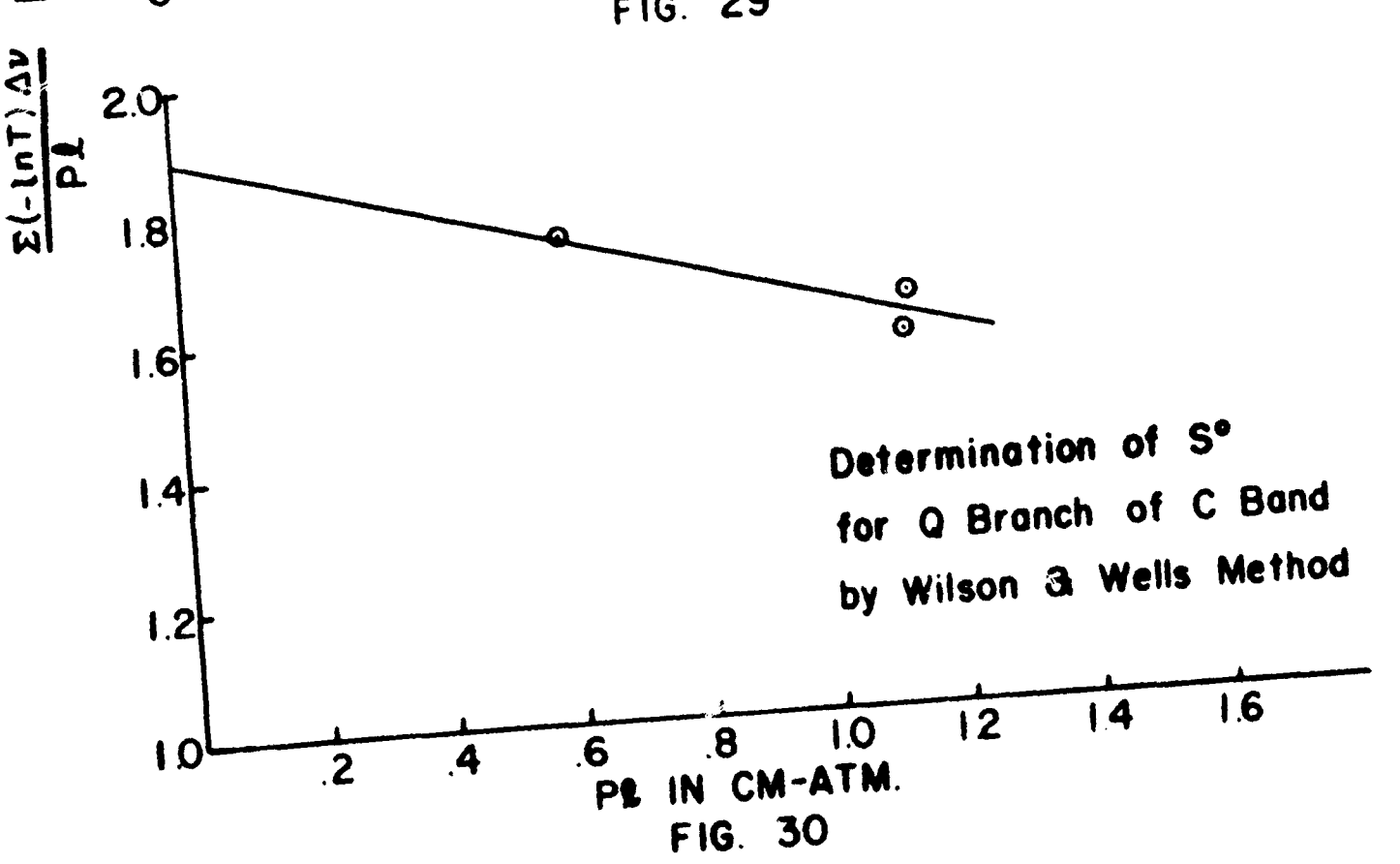
Σ(-lnT)Δν / PL
2.0
1.8
1.6
1.4
1.2
1.0
.2
.4
.6
.8
1.0
1.2
1.4
1.6
PL IN CM-ATM.
Determination of S°
for Q Branch of C Band
by Wilson & Wells Method

FIG. 30

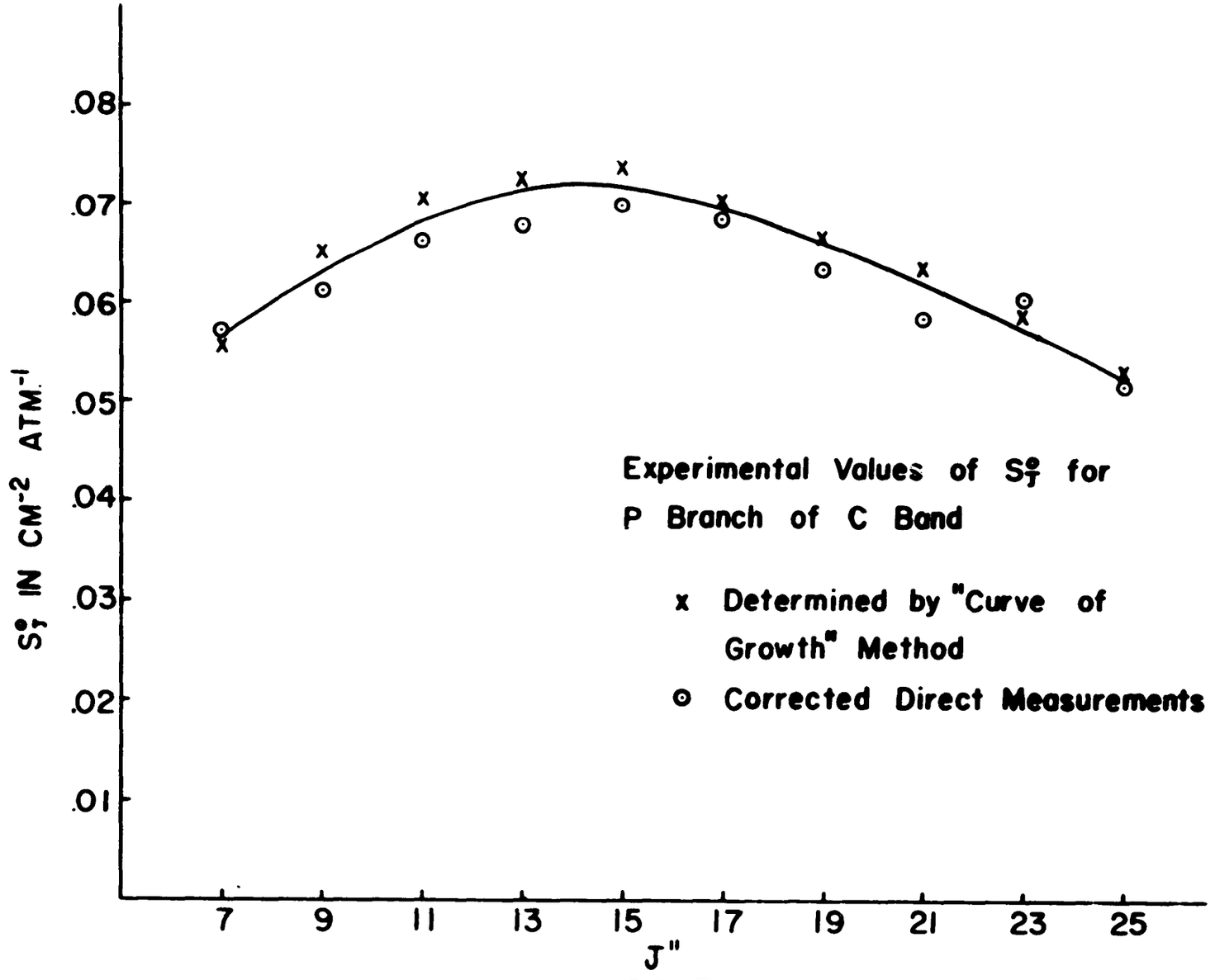
.08
.07
.06
.05
.04
.03
.02
.01
S_J° IN CM^{-2} ATM^{-1}
7
9
11
13
15
17
19
21
23
25
J"
Experimental Values of S_J° for
P Branch of C Band
x Determined by "Curve of Growth" Method
⊙ Corrected Direct Measurements

FIG. 31

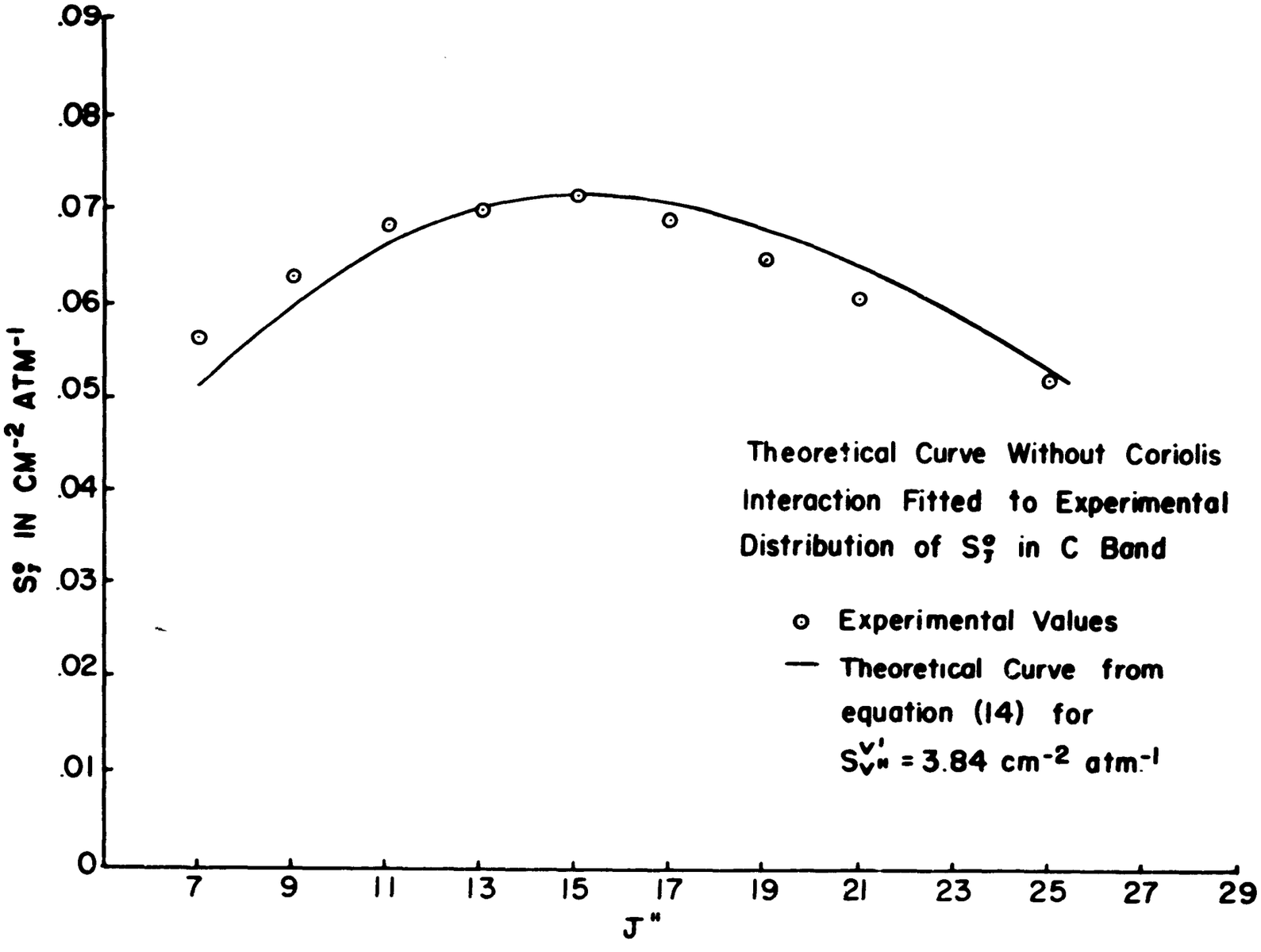
.09
.08
.07
.06
.05
.04
.03
.02
.01
0
S_J^o IN CM^{-2} ATM^{-1}
7
9
11
13
15
17
19
21
23
25
27
29
J"
Theoretical Curve Without Coriolis Interaction Fitted to Experimental Distribution of S_J^o in C Band
⊙ Experimental Values
— Theoretical Curve from equation (14) for $S_{v''}^{v'} = 3.84\ cm^{-2}\ atm^{-1}$

FIG. 32

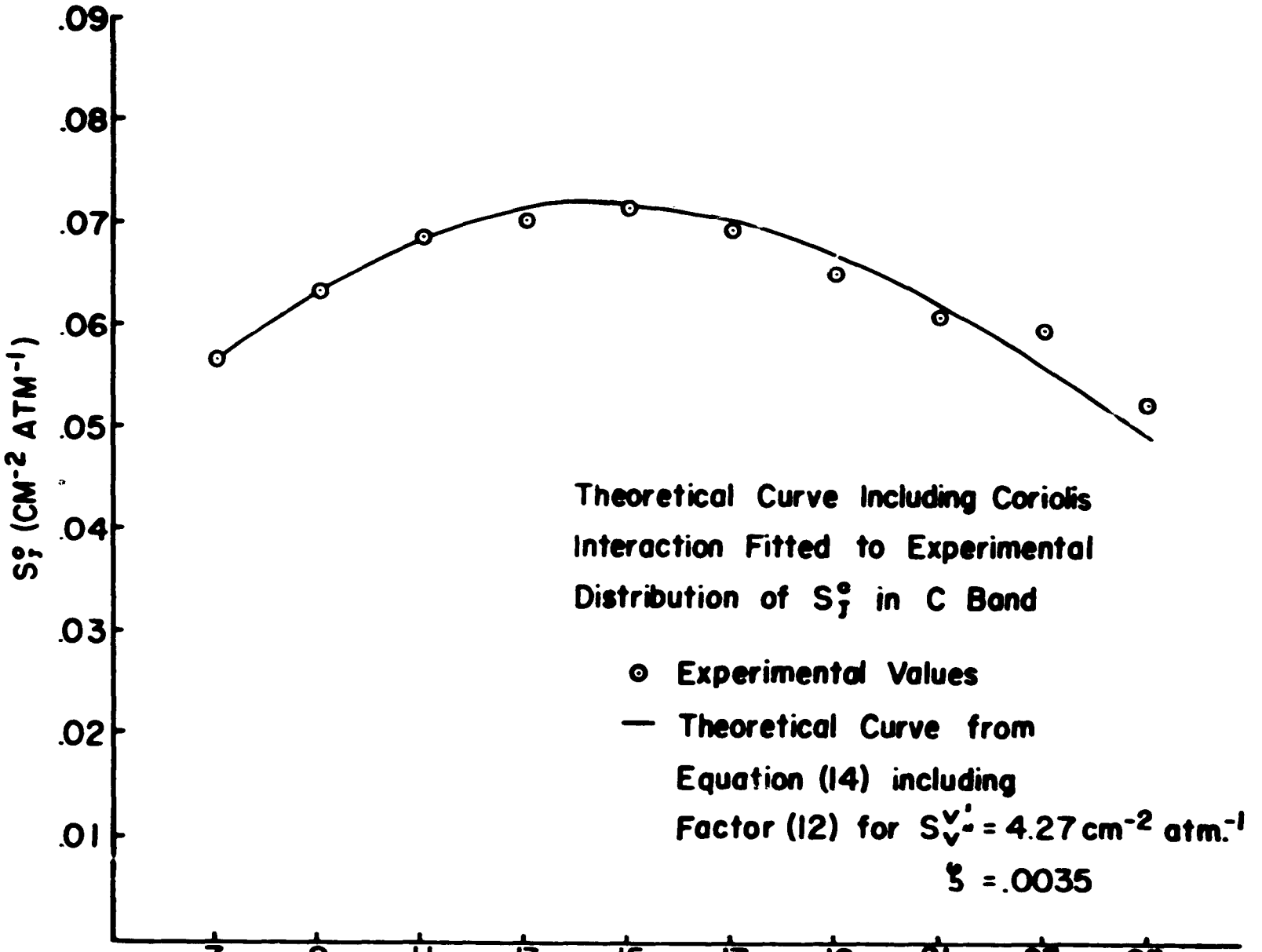
.09
.08
.07
.06
.05
.04
.03
.02
.01
S_J^o (CM^{-2} ATM^{-1})
7
9
11
13
15
17
19
21
23
25
J"
Theoretical Curve Including Coriolis Interaction Fitted to Experimental Distribution of S_J^o in C Band
⊙ Experimental Values
— Theoretical Curve from Equation (14) including Factor (12) for $S_{v''}^{v'} = 4.27\,cm^{-2}\,atm.^{-1}$
$\zeta = .0035$

FIG. 33

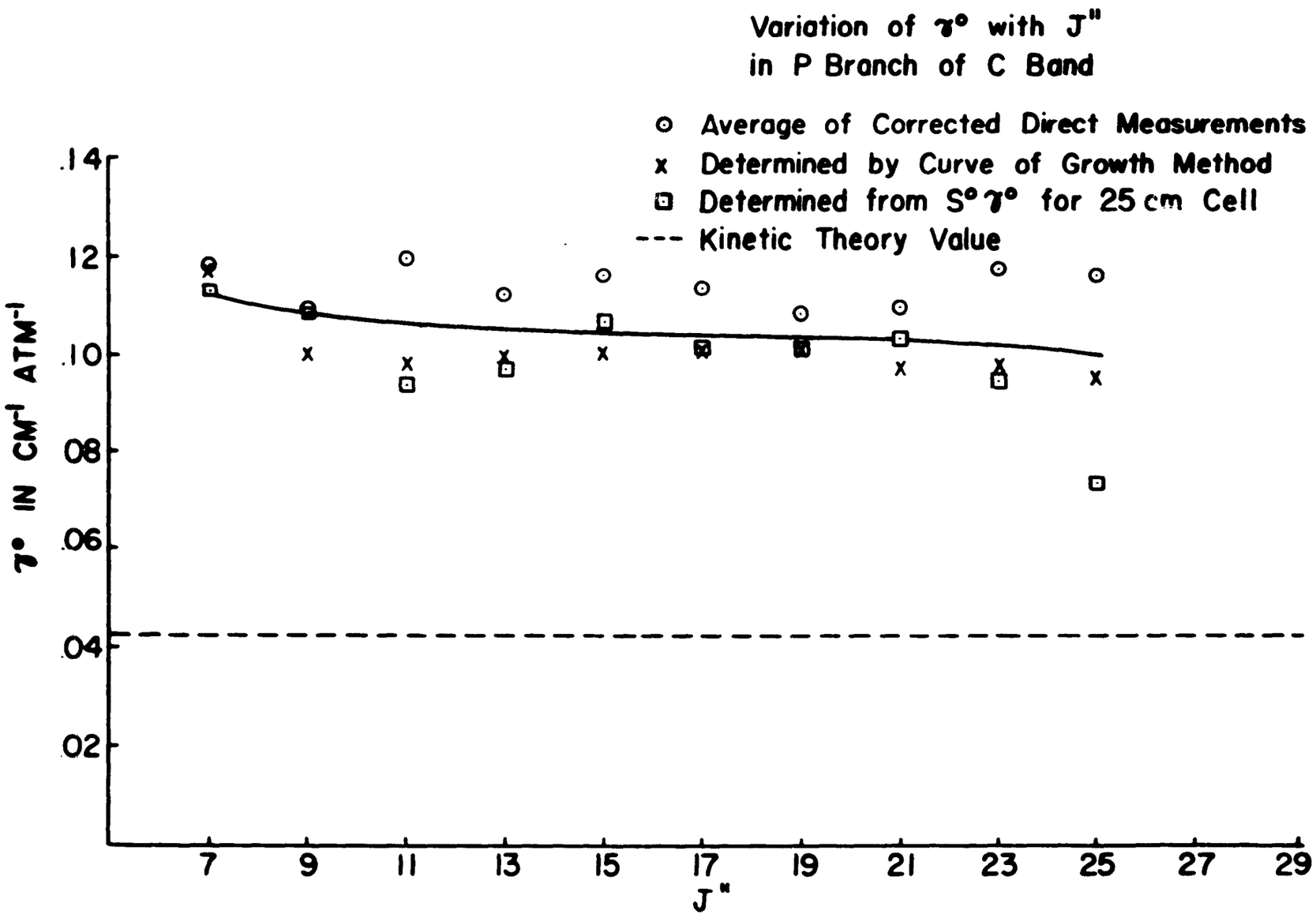
Variation of γ° with J"
in P Branch of C Band
⊙ Average of Corrected Direct Measurements
x Determined by Curve of Growth Method
⊡ Determined from S°γ° for 25 cm Cell
--- Kinetic Theory Value
γ° IN CM⁻¹ ATM⁻¹
.14
12
.10
08
.06
.04
.02
7
9
11
13
15
17
19
21
23
25
27
29
J"

FIG. 34

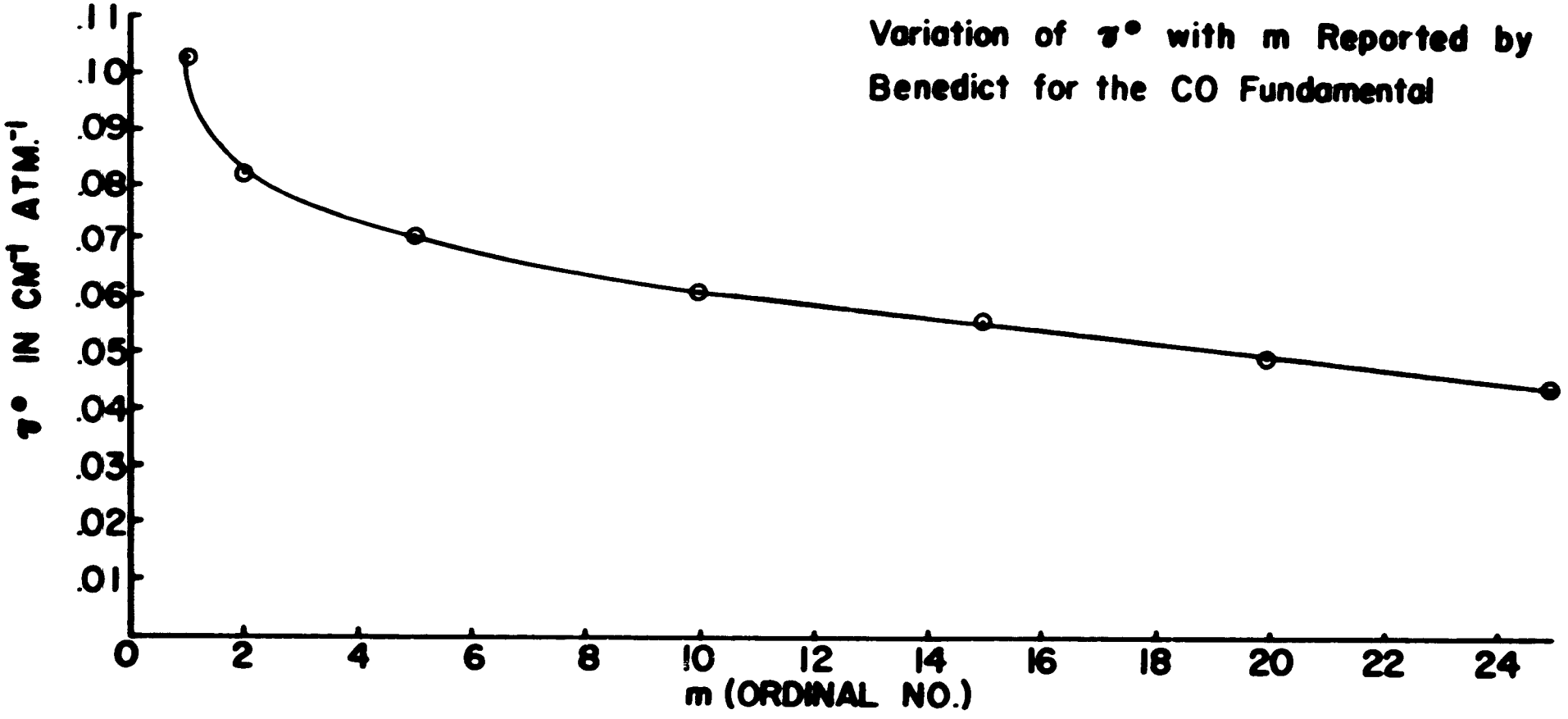
Variation of τ° with m Reported by
Benedict for the CO Fundamental
τ° IN CM⁻¹ ATM.⁻¹
.11
.10
.09
.08
.07
.06
.05
.04
.03
.02
.01
0
2
4
6
8
10
12
14
16
18
20
22
24
m (ORDINAL NO.)

FIG. 35

APPENDIX

Further Details of the Rotation and Drive Mechanisms

Figure A is a sectional drawing of the grating turntable and axis of rotation. Figure B explains the geometry of the cosine drive. An examination of these drawings and of Figures 9 and 10 should make clear the text discussion on pages 21-22.

It will be noted in Figure B that a cosine drive may be obtained even though the drive arm is not normal to the grating. This is made possible by fixing the drive flat at an appropriate angle on the nut.

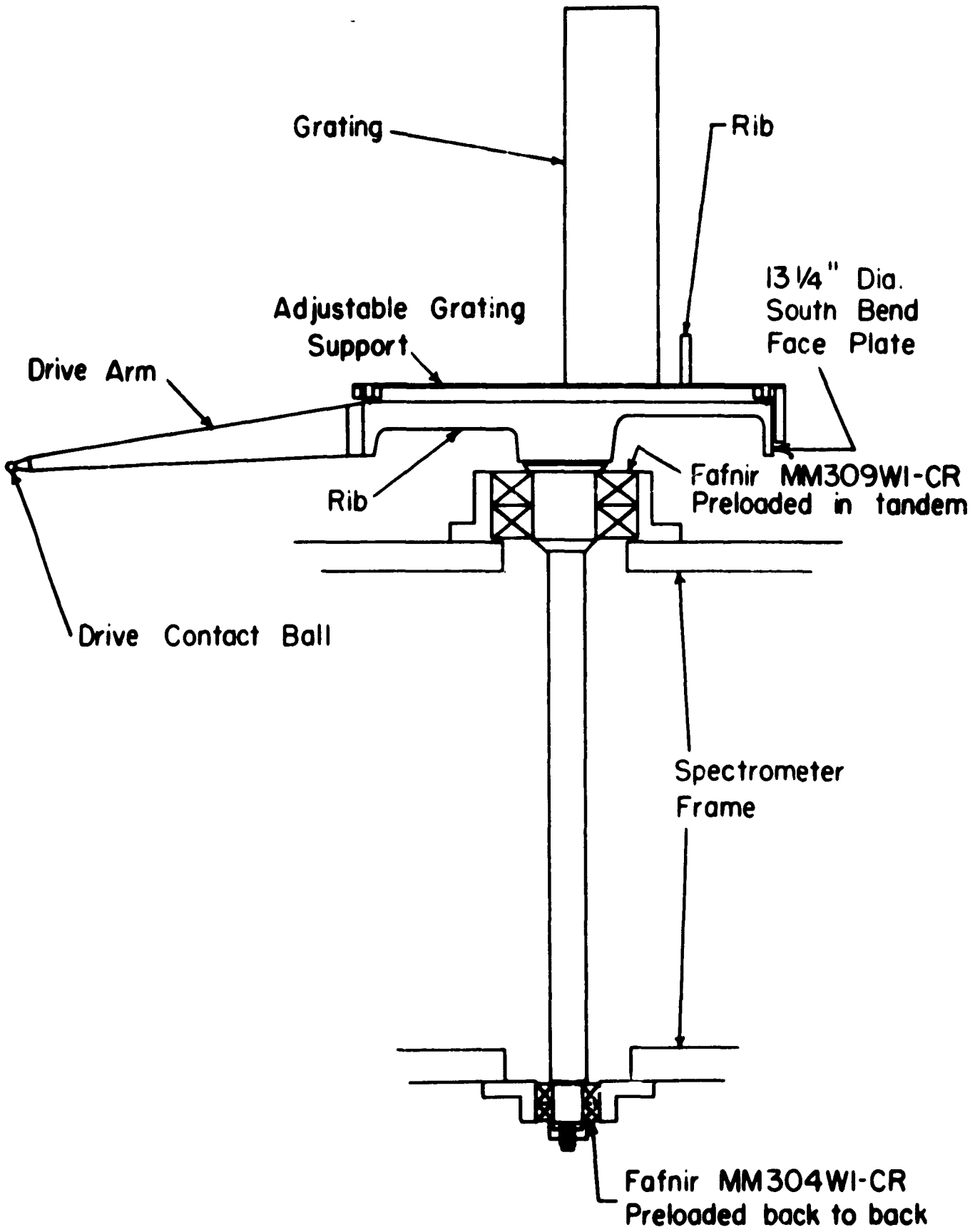

Fig. A DETAILS OF GRATING TURNTABLE
SECTIONAL VIEW

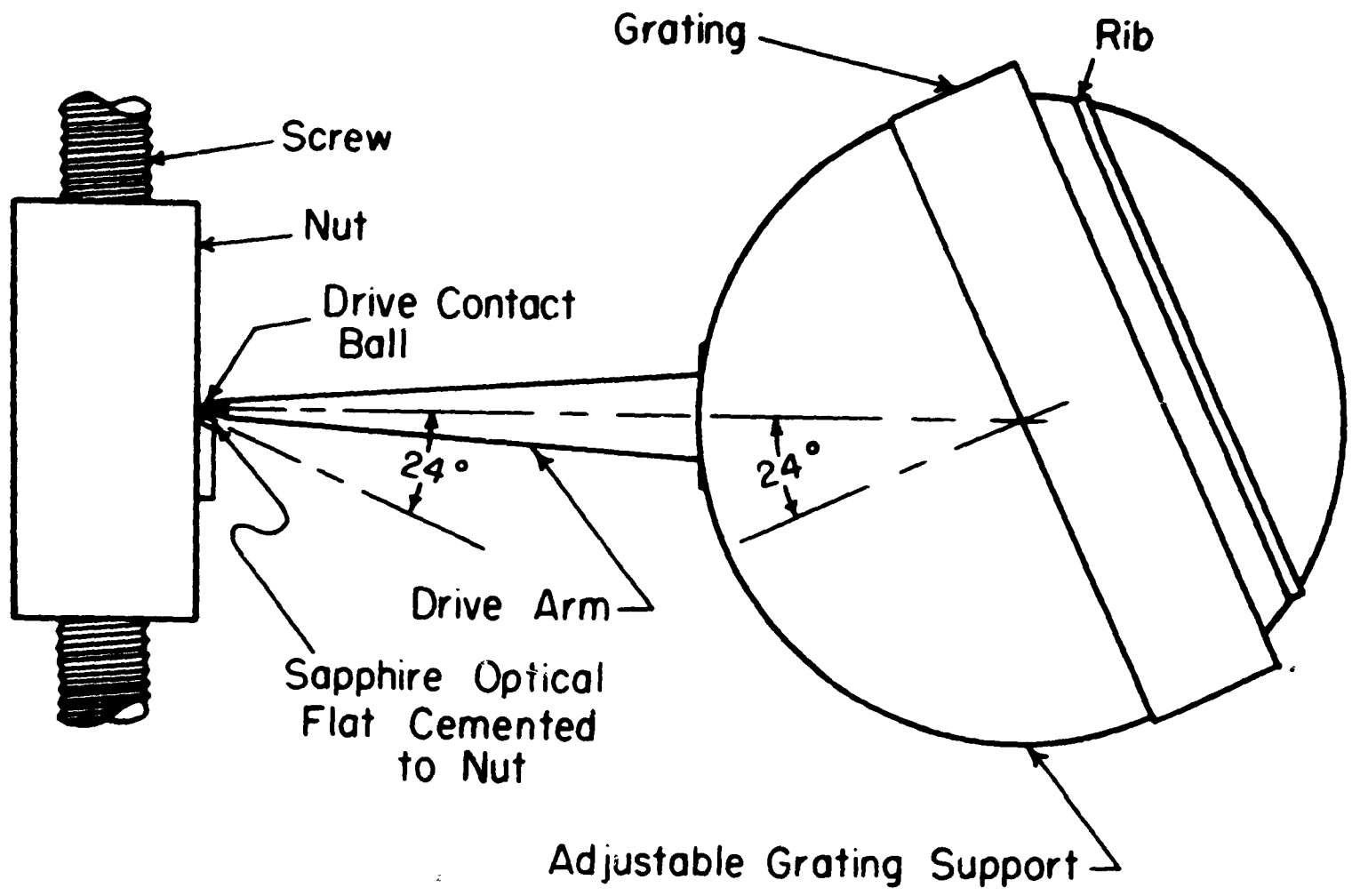

Fig. B GEOMETRY OF GRATING DRIVE